STRUCTURAL AND THERMAL CHARACTERIZATION OF POLYMERS VIA PYROLYSIS MASS SPECTROMETRY

A THESIS SUBMITTED TO
THE GRADUATE SCHOOL OF NATURAL AND APPLIED SCIENCES
OF
MIDDLE EAST TECHNICAL UNIVERSITY

BY

EMİR ARGIN

IN PARTIAL FULFILMENT OF THE REQUIREMENTS
FOR
THE DEGREE OF MASTER OF SCIENCES
IN
CHEMISTRY

AUGUST 2005

Approval of the Graduate School of Natural and Applied Sciences.

_____

Prof. Dr. Canan Özgen
Director

I certify that this thesis satisfies all the requirements as a thesis for the degree of Master of Sciences.

_____

Prof. Dr. Hüseyin İşçi
Head of the Department

This is to certify that we have read this thesis and that in our opinion it is fully adequate, in scope and quality, as a thesis for the degree of Master of Sciences.

_____	_____
Prof. Dr. Zuhal Küçükyavuz	Prof. Dr. Jale Hacaloğlu
Co-Supervisor	Supervisor

Examining Committee Members

Prof.Dr.Ali Usanmaz _____

Prof. Dr. Zuhal Küçükyavuz _____

Prof.Dr.Jale Hacaloğlu _____

Prof.Dr.Ahmet M.Önal _____

Y.Doç.Dr.Hasan N.Testereci _____

I hereby declare that all information in this document has been obtained and presented in accordance with academic rules and ethical conduct. I also declare that, as required by these rules and conduct, I have fully cited and referenced all material and results that are not original to this work.

Name, Last name : Emir Argın

Signature :

ABSTRACT

STRUCTURAL AND THERMAL CHARACTERIZATION OF POLYMERS VIA PYROLYSIS MASS SPECTROMETRY

Argın, Emir

M.Sc., Department of Chemistry

Supervisor: Prof. Dr. Jale Hacaloğlu

Co-Supervisor: Prof. Dr. Zuhal Küçükyavuz

August 2005, 86 pages

In the first part of this study, the structural and thermal characterization of electrochemically and chemically polymerized poly(paraphenylene vinylene), (PPV), have been investigated by direct pyrolysis mass spectrometry. Thermal characteristics, and degradation products of electrochemically prepared poly(paraphenylene vinylene) were compared with those of chemically prepared poly(paraphenylene vinylene). Pyrolysis study indicated that thermal decomposition of PPV occurs at least two steps. The first being due to the loss of supporting electrolyte present and the second being decomposition of the polymer backbone.

In the second part of the study, direct insertion probe pyrolysis mass spectrometry (DIP-MS) technique was used to perform the thermal and the structural characterization of electrochemically synthesized polyaniline, PANI. The effect of dopant used (HCl, HNO_3 and H_2SO_4) and synthesis period have been investigated. For all the samples studied, three main thermal degradation stages have been recorded; evolution of low molecular weight species, evolution of dopant based products and evolution of degradation products of polymer.

Keywords: Conducting polymers, poly(paraphenylene vinylene), polyaniline, direct pyrolysis mass spectrometry

ÖZ

POLİMERLERİN PİROLİZ KÜTLE SPEKTROMETRESİ KULLANILARAK YAPISAL VE ISIL KARAKTERİZASYONU

Argın, Emir
Yüksek Lisans, Kimya Bölümü
Tez Yöneticisi: Prof. Dr. Jale Hacaloğlu
Ortak Tez Yöneticisi: Prof. Dr. Zuhal Küçükyavuz

Ağustos 2005, 86 sayfa

Çalışmanın ilk kısmında, elektrokimyasal ve kimyasal yollarla sentezlenen poli (p-fenilen vinilen)' in yapısal ve ısıl karakterizasyonu direkt piroliz kütle spektrometresi kullanılarak incelendi. Elektrokimyasal ve kimyasal yollarla sentezlenen polimerlerin ısıl karakteristikleri, ısıl parçalanma mekanizmaları ve bozunum ürünleri karşılaştırıldı. Piroliz çalışmaları incelendiğinde, ısıl parçalanmanın katkı bozunumu ve polimer zinciri bozunumu olmak üzere en az iki aşamada gerçekleştiği gözlenmiştir.

Çalışmanın ikinci kısmında ise, HCl, HNO_3 and H_2SO_4 kullanılarak sentezlenen polianilin örnekleri direkt piroliz kütle spektrometresi tekniği kullanılarak incelendi. Üç farklı katkı maddesi (dopant) kullanılarak katkı maddelerinin ve sentezlenme süresinin etkileri araştırıldı. İncelenen tüm örneklerde ısıl bozunumun üç aşamada gerçekleştiği gözlenmiştir. İlk aşamada, düşük molekül ağırlıklı oligomerlerin oluşumu gözlenmiştir. İkinci aşamada elektrokimyasal sentezde kullanılan dopantın ve son aşamada da polimerin bozunumu gerçekleşmektedir.

Anahtar Kelimeler: İletken polimerler, poliparafenilen vinilen , polianilin, direkt piroliz kütle spektrometresi.

DEDICATED TO MY FAMILY

ACKNOWLEDGMENTS

I would like to give my very special thanks to my supervisor Prof. Dr. Jale Hacaloğlu and my co-supervisor Prof. Dr. Zuhal Küçükyavuz for their guidance and encouragement throughout my MSc. studies.

I would like to thank to Mustafa Kenar, Özlem Polat and Feride Tezal for their moral support and help.

I also want to thank to Eczacıbaşı Health Products Co. administiration for their support and help.

I thank to my family for their dedication to support me at every stage of my life.

TABLE OF CONTENTS

LIST OF TABLES

TABLES

LIST OF FIGURES

FIGURES

CHAPTER 1

INTRODUCTION

1.1. Conducting Polymers

Traditionally polymers were thought of as insulators and any electrical conduction in polymers was generally regarded as an undesirable phenomenon. In the last decades an opposite trend has started in as much as examinations directed to the utilization of ionic conductivity of polymeric systems. Also in the 1970s somewhat surprisingly a new class of polymers possessing high electronic conductivity (electronically conducting polymers) in partially oxidized (or less frequently reduced) state has been discovered. Electrochemistry has played a significant role in the preparation and characterization of these novel materials. Electrochemical techniques are especially suitable for controlled synthesis of these compounds and for tuning of a well-defined oxidation state [1].

Polyacetylene (PAc) was known as a black powder until 1974. Later, it was prepared as a film by Shirakawa and co-workers; unfortunately it was not a conductor. In 1977, it was discovered that PAc films can be made conductive when treated with iodine (electron acceptors or p-type dopants), chlorine or bromine vapor, and "doped" form of PAc was found to possess a conductivity of 103 S cm^{-1}[2]. A year later it was discovered that analogous effects may also be induced by electron donors. A more general term "organic metals" is sometimes also used to describe such polymers. Metal-like behavior of the "doped" conjugated polymers has been manifested by their conductance, which may even approach that of metals, and by

anomalies in its temperature dependence [3]. Besides doping, presence of conjugated double bonds in the backbone is required for conducting polymers. In conjugated polymers, bonds between the carbon atoms are alternatingly single and double. Every bond contains a localized sigma bond, which is responsible for holding the polymer together, in addition to less strongly localized π bond which is weaker. These π-bonded unsaturated polymers have small ionization potentials and high electron affinities which provides the ease of oxidation-reduction reactions. In order to provide the conduction, the deficiency or excess π electrons must exist in the polyconjugated chain [4, 5]. Some common conducting polymers are given in Figure 1.1.

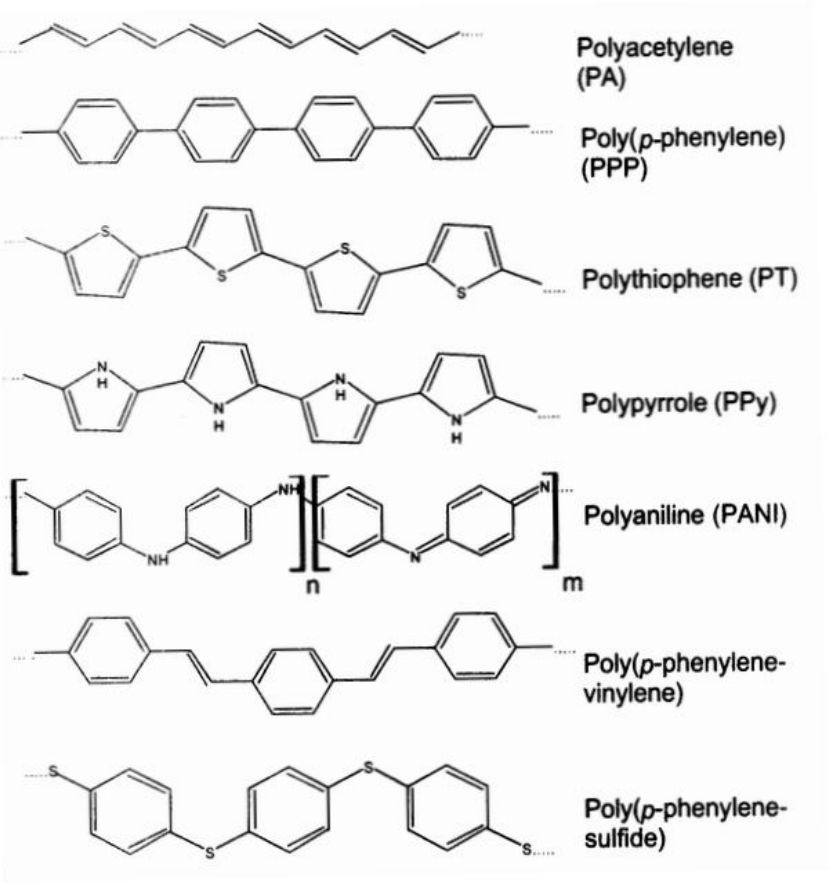

Figure 1.1 Structures of common conducting polymers

The conductive polymers (CP) are of two types. The first type encompasses polymers filled with conductive and semi-conductive materials such as metal flakes, fibers or carbon black. The second type is obtained due to the doping of insulating polymers by electrochemical and galvanic methods. Conducting polymers have a range of conductivity between insulators and metals. Doping can be performed on freestanding polymer films or films deposited on electrodes which remain inert within the range of applied potential.

1.2. Electrical Conduction

The electrical properties of conventional materials depend on the electronic band structure and on the distribution of the available electrons. The energy difference between highest occupied level and the lowest unoccupied level is called the band gap, E_g. The size of this forbidden gap changes significantly depending on material. In a semiconductor, band gap, E_g is narrow and the movement of electrons from the valance band (VB) to the conduction band (CB) provides the conduction.

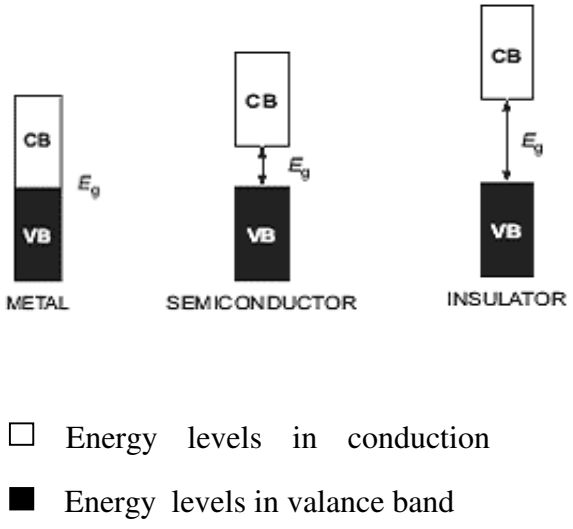

Figure 1.2 Shematic diagram of metals, semiconductors and insulators in terms of their energy diagrams.VB and CB represents the valance and conduction band respectively.

For an insulator, the band gap, E_g is too wide and the electrons cannot be transferred from the valance band to the conduction band. The high conductivity of metals comes from partially occupied valance band or a zero band gap [6]. The three conductivity classes are illustrated schematically in Figure 1.2.

Conductive organic polymers are generally insulator or semi-conductors in their undoped state but they can be made as conductive as metals when they are subjected to a doping process [7,8].

1.3. Electrochemistry of Conducting Polymers

Conducting polymers can be prepared by using chemical or electrochemical methods of polymerization.

1.3.1 Chemical Polymerization

The most useful method for preparing large amounts of conductive polymers is chemical polymerization. Almost all classes of conjugated polymers can be synthesized by this technique (oxidative coupling) the oxidation of monomers yields a cation radical, coupling of these to form dications and polymer is produced by the repetition of this process. In this method, stoichiometric amount of oxidizing agent is used to form polymer that is in its conducting (doped) form. The choice of solvent is limited to one that dissolves both the monomer and the oxidant. The product is usually obtained as a powdery, insoluble precipitate. Since polymerization is very rapid, no film formation is observed, and the product obtained has low conductivity [9,10].

1.3.2 Electrochemical Polymerization

The electrochemical synthesis of conducting polymers is preferred over chemical polymerization because of the simplicity of the technique. Furthermore, frequently

higher polymer conductivity can be obtained. As the electrical potential needed for oxidation of the monomer is significantly higher than that is needed for the doping of the formed polymer, the polymer is directly obtained in its conducting state. In this technique, the oxidation potential at which the system polymerizes is well defined and finely controlled and the properties of the deposited polymer can be controlled. Thus, variety of different conducting polymers can be prepared from the same monomer by simply varying specific electrochemical parameters such as the applied potential, the temperature, the electrolyte and the electrodes used [11].

The electrochemical synthesis of polyheterocyclics can be made with anodic or cathodic coupling. Anodic coupling provides the oxidation of monomer to a polymer with proton elimination whereas the cathodic coupling is based on the reduction of dihalogen-substitued (usually dibromo substituted) monomers to a polymer with halogenide release. Anodic coupling is preferred because it uses the unmodified monomer and the formed polymer, being more easily oxidized (doped), is produced in the conductive state. Therefore, the continuous deposition of the material up to considerable thickness is possible.

Some of the adventages of polymerizations by electrochemical techniques are,
•the simplicity, selectivity and the reproducibility
•the possibility of control of film thickness
•the possibility of carrying out reactions at room temperature
•the homogenity of the films
•the possibility of obtaining smooth polymer films on the conducting substrate
•in-situ characterization (Cyclic Voltametry, FTIR, spectroelectrochemistry)

1.4. Methods of Electrochemical Polymerization

Electrochemical polymerization can be performed at constant potential (potentiostatic method), or constant current (galvanostatic method) .

1.4.1 Potentiostatic method (Constant Potential)

In the potentiostatic method, the potential of the working electrode is adjusted to a desired value and kept constant while current is allowed to vary [12]. In this method, a potential that is low enough to avoid undesirable side reactions but sufficiently high for a reasonable polymerization rate. The applied potential is determined by means of cyclic voltammetry.

1.4.2 Galvanostatic method (Constant Current)

In the galvanostatic method, current is kept constant during the electrolysis and the potential is allowed to vary [12]. In this method the process is forced to occur at a constant rate. The thickness of the film can be easily controlled by controlling the polymerization time. However, the increase in film resistance may cause the potential to rise to a level at which side reactions may occur or the film itself may burn because of the heating effect.

1.5 Dopping

Conjugated organic polymers in their pure (undoped) state are best described as insulators. Due to the relatively large band gaps in conjugated polymers, the concentration of charge carriers at low temperatures is very low. The doping of conducting polymers generates high conductivities primarily by increasing the carrier concentration [13]. Doping is reversible to produce the original polymer with little or no degradation of the polymer backbone. Both doping and undoping processes, involving dopant counterions which stabilize the doped state, may be carried out chemically or electrochemically. By controllably adjusting the doping level, conductivity anywhere between that of the non-doped (insulating or semiconductor) and that of the fully doped (conducting) form of the polymer is easily obtained. In the doped state, the backbone of a conducting polymer consists of a delocalized π system.

The extent of oxidation/reduction is called doping level, which is generally measured as the proportion of dopant ions or molecules incorporated per monomer unit. Increased doping level leads to higher conductivity by the creation of more mobile charges [15].

The maximum doping level depends on characteristics of both conducting polymers and dopant. Doping agents are either strong reducing agents or strong oxidizing agents. The nature of dopants plays an important role in the stability of conductive polymers [15].

1.6. Applications of Conducting Polymers

There have been great excitement about the technological applications of conducting polymers owing to their unique posibility of combination of properties from polymers (processability, chemical stability and flexibility) and metals (electrical conductivity and optical and magnetic properties). Since they offer such a unique combination of properties, they have a wide range of applications.

The recent developments towards the syntheses of new and processable conducting polymers as well as discovery of the broad range of chemical flexibility opens up opportunities for new technological applications. The higher environmental stability, the modified properties and the achieved processibility of the polymers derived from acetylene, pyrrole, thiophene, aniline and their derivatives, polyphenylene, poly(phenylene vinylenes) have resulted in replacement of metals and semiconductors in electrical and electronics industry. Applications with conducting polymers include plastic rechargeable batteries, circuit boards, corrosion protection, sensors, controlled-release applications, radar applications, infrared polarizers, light emitting diodes and electrochromic devices [16,17].

1.7. Properties of Poly(paraphenylene vinylene)

In the field of polyconjugated organic polymers that show large electrical conductivity and optical non linearity, poly(paraphenylene vinylene) (PPV) is becoming the center of interest in basic and applied material science. This material can be easily prepared from a workable precursor which allows preparation of films or stretched samples, has good chemical stability and shows remarkable optical non linearity. In the doped state it shows high electrical conductivity reaching values of $\sigma = 10^3\ \Omega^{-1}\ cm^{-1}$ (H_2SO_4 doping) and $\sigma = 10^2\ \Omega^{-1}\ cm^{-1}$ (AsF_5 doping) for stretch oriented samples.

The chemistry of this class of materials is such that stable oligomers can be prepared allowing a better understanding of the electronic and structural properties of PPV. Oligomers have been initially preprepared by Drefahl et al.and have been found to be not easily soluble making a systematic study of their spectra impossible. These oligomers show relevant photoconducting properties. The problem of solubility has been solved with the synthesis of oligomers capped with t-butyl groups [18].

Poly(paraphenylene vinylene) has been first prepared by means of a direct chemical polymerization reaction. Insoluble powder obtained by this way. Another method to prepare PPV is the sulfonium precursor route which is based on induced polymerization of sulfonium salt monomer in aqueous solution. After the thermal elimination of sulfonium groups PPV films are obtained [19, 20,21].

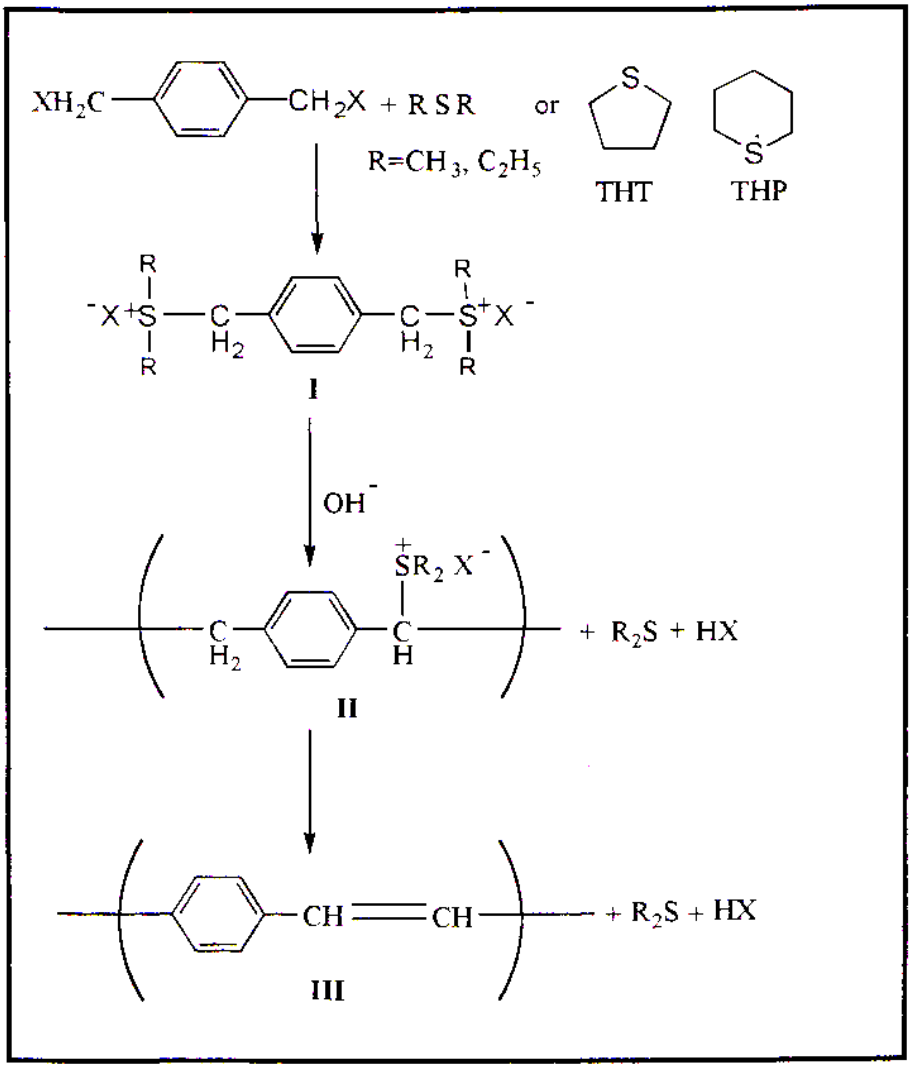

Figure 1.3 Thermal conversion of poly(p-xylene-α-diethysulphonıum chloride) to PPV

1.8. Properties of Polyaniline

Polyaniline, PANI is an enviromentally stable conducting polymer with excellent electrical, magnetic and optical properties [22]. Polyaniline is a typical phenylene-based polymer having a chemically flexible –NH- group in a polymer chain flanked either side by a phenylene ring [23]. Polyaniline is prepared by either chemical or electrochemical oxidation of aniline under acidic conditions [24]. In order to get thin films and better-ordered polymers, electrochemical method is preferred [25].

It has attacted considerable attention over the past 10 years and is generally regarded as one of the conducting polymers with very high potential in commercial applications.The potential applications of polyaniline include secondary batteries , electromagnetic interference shielding, molecular sensors, non-linear optical devices, electrochromic displays and microelectronic devices [26].

Polyaniline film as a typical electroconductive organic polymer has been first prepared by Diaz and Logan by means of anodic oxidation of aniline in aqueous sulfuric acid. They used platinium as the anode and the polymer film was deposited on it [27]. They performed an electrochemical polymerization of aniline in an electrolyte containing aqueous solution of 0.1 M sulfuric acid and growing of free-standing PANI film on a platinum electrode was achieved by continuously sweeping the potential between –0.2 and +0.8 V versus SCE [28].

MacDiarmid et al. suggested four different forms of PANI subunits, two of which are free amine forms, whereas two others are ammonium salt forms, as shown in Figure 1.4. Inter-conversion of these forms can be easily achieved by chemical and electrochemical ways. Furthermore, free amine forms is converted to ammonium salt forms by simply adding acid and the reverse case, similarly, is achieved by treating with a base.

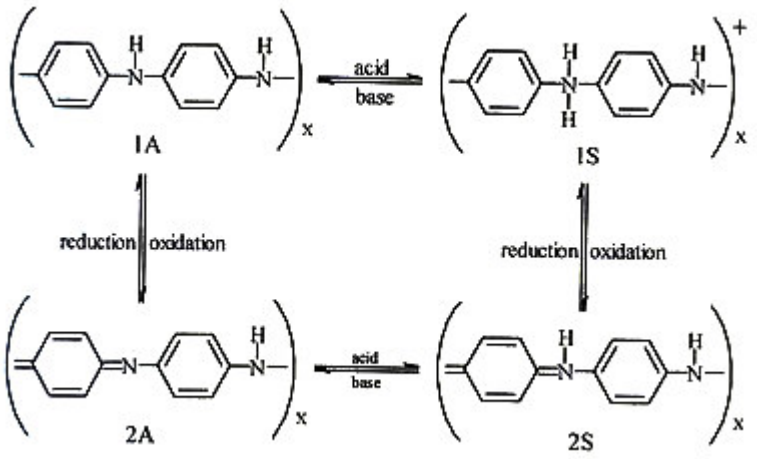

Figure 1.4 Two different free amine forms and ammonium salt forms of polyanilines.

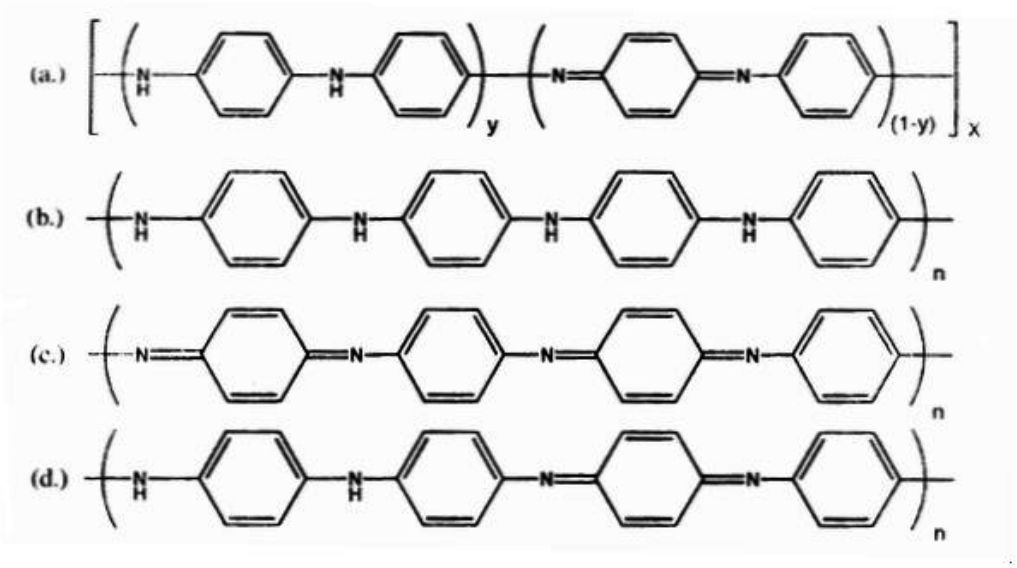

Figure 1.5 Oxidation states of Polyaniline a) general representation of Polyaniline, b) leucomeraldine base, c) pernigraniline base, d) emeralidine base.

In general, the oxidation level of a polyaniline synthesized by either a chemical or electrochemical method can be desciribed by the following molecular formula in the Figure 1.5.a. Here, y= 1, 0.5 and 0, the corresponding polymers are the fully reduced polyaniline (leucoemeraldine), the half oxidized polyaniline (emeraldine), and fully oxidized polyaniline (pernigraniline), respectively [26].

1.9. Characterization of Conducting Polymers

Like most other polymers, conducting polymers can be characterized by a variety of analytical techniques. Many example exist in the literature, some of which include: cyclic voltametry for understanding redox processes in conducting polymers and evaluating potential battery and electrochromic window material candidates;structural and optical characteristics; nuclear magnetic resonance for structure confirmation, chain orientation and molecular motion; gel permeation chromatography for molecular weight; Raman analysis, for vibrational assignments; differential scanning calorimetry and thermogravimetric analysis for evidence of glass and melting transitions and decomposition temperatures; various types of x-ray analysis for understanding the crystal structure [30].

Yet, the structural characterization of the conducting polymers by classical spectrometry techniques is still limited. Because, the highly conjugated backbone causes insolubility of the polymer in all common solvents. During the last decades, it has been shown that pyrolysis techniques offer an alternative way for polymer structure and composition analyses [31,32].

1.10. Pyrolysis Mass Spectrometry

Pyrolysis techniques are the common methods used to analyze high molecular weight substances. In general, pyrolysis techniques applied not only to investigate thermal stability but also to determine thermal decomposition products. Mass spectrometry (MS), Gas Chromatography (GC), GC/MS and Infrared spectroscopy can identify

pyrolysis products. The most common pyrolysis techniques coupled with mass spectrometers are indirect , direct, flash, Curie point and laser pyrolysis techniques [33,34]. Each technique has its own advantages and limitations. In general, indirect, flash, curie point and laser pyrolysis analysis, heating process occurs in high vacuum conditions of the mass spectrometers. A mass spectrometer produces ions from the substance under investigation and seperates them according to their mass-to-charge ratio (m/z), and records the relative abundance of each ionic species present.

1.11. Pyrolysis Techniques With Mass Spectrometry System

For the pyrolysis analysis with mass spectrometry Curie point, laser, indirect (evolved gas), direct and flash (rapid) pyrolysis techniques are used. Using these techniques, the total ion chromatograms and mass spectra of the decomposition products can be analyzed by recording mass spectra continuously during pyrolysis [35].

1.11.1. Indirect (Evolved Gas) Pyrolysis Technique

The nature and amount of evolved gaseous products from a sample heated using a controlled temperature program can be determined by evolved gas analysis. In this technique, as heating occurs in a closed chamber connected to the MS. Only gaseous volatile and low molecular weight products enter into MS system and can then be analyzed [36, 37].

1.11.2. Flash (Rapid) Pyrolysis Technique

Reaching a constant temperature rapidly is the aim of flash pyrolysis. Low molecular weight volatile products and high mass fragments can be analyzed within a very short time period. With the help of rapid heating system, degradation is carried out in a short time and pyrolysis products obtained are again primary products like incase of direct pyrolysis.

1.11.3. Direct Pyrolysis Technique

Pyrolysis is achieved inside the Mass Spectrometer (MS) under high vacuum conditions of the MS. Both low molecular weight products and relatively high MW fragments can be detected as condensation is prevented. Since pyrolysis mass spectrometry techniques are carried out under high vacuum conditions, the possibility of secondary reactions is minimized. For this reason, possibility of the secondary reactions is prevented and primarily thermal degradation products can be analyzed. The temperature is increased gradually and the degradation products as a function of temperature can be detected continuously during the process.

1.12. Aim of The Study

The objectives of this study are

- To synthesize poly(paraphenylene vinylene) both by using chemical and electrochemical polymerization techniques,

- To characterize the monomer and polymers by using direct pyrolysis mass spectrometry

- To determine the thermal behavior, decomposition products and degradation mechanism of poly(paraphenylene vinylene)

- To study the structural and thermal characterization of polyanilines by using direct pyrolysis mass spectrometry.

- To investigate the effect of doping and the experimental conditions on electrochemically prepared polyaniline by pyrolysis mass spectrometry.

CHAPTER 2

EXPERIMENTAL

2.1. Materials

Acetonitrile (Merck) , diethylsulfide (Merck) , methanol (Merck) , acetone (Merck) α,α-dichloro-p-xylene (Aldrich) were used without further purification. Tetrabuthylamonium tetrafluoroborate (Aldrich) was dried under vacuum for 24 hours at 25°C before use. HNO_3 (Merck), H_2SO_4 (Merck), HCl (Merck) and NaOH (Merck) were used without any purification. Reagent quality Methanol (Merck) and Acetone (Merck) were used without any purification. Reagent quality aniline (Merck) was used without purification

2.2. Instrumentation

2.2.1. Potentiostat

Electrolysis was performed by Potentioscan MODEL PS 95D potentiostat. This device was used for the supply of a constant potential in the electrochemical polymerization. Electrochemical polymerization is carried out in a three electrode system containing working electrode (WE), reference electrode (RE) and counter electrode (CE). Electrochemical reactions studied occur at the working electrode. The reference electrode is used in measuring the working electrode potential. A reference electrode should have a constant electrochemical potential as long as no

current flows through it. Potentiostat can achieve to maintain the voltage difference between the working and reference electrodes at a constant desired value during the electrolysis.

2.2.3 Electrolysis Cell

A three compartments electrolysis cell was used. These were working electrode part, counter electrode part and reference electrode part. The two main parts the working electrode (anode) and counter electrode (cathode) were separated from each other by a sintered glass. Platinum plate (1.5 cm^2) was used as working and counter electrodes and Ag wire was used as the reference electrode. The cell had suitable inlets for passing N_2 gas through or above the solution as shown in Figure 2.1.

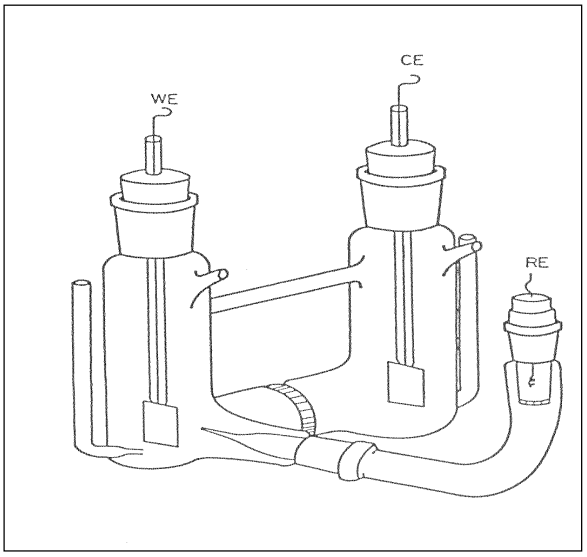

Figure 2.1 The H-shaped electrolysis cell

2.3. Mass Spectrometer

In this work 5973 HP quadruple mass spectrometry system coupled to a JHP SIS direct insertion probe pyrolysis system was used. The instrument consist of three major components: an ion source for producing gaseous ions from the substance being studied , an analyzer for resolving ions into their characteristic mass components according to mass-to-charge ratios, and a detector system for detecting the ions and recording the relative abundance of each of the resolved ionic species. In addition, a sample introduction system is necessary to admit the samples to be studied to the ion source while maintaining the high vacuum requirements (~10^{-6} to 10^{-8} mm of mercury) of the technique; and a computer is required to control the instrument, acquire and manipulate data, and compare spectra to reference libraries. Figure 2.2 shows that, the major components of mass spectrometer.

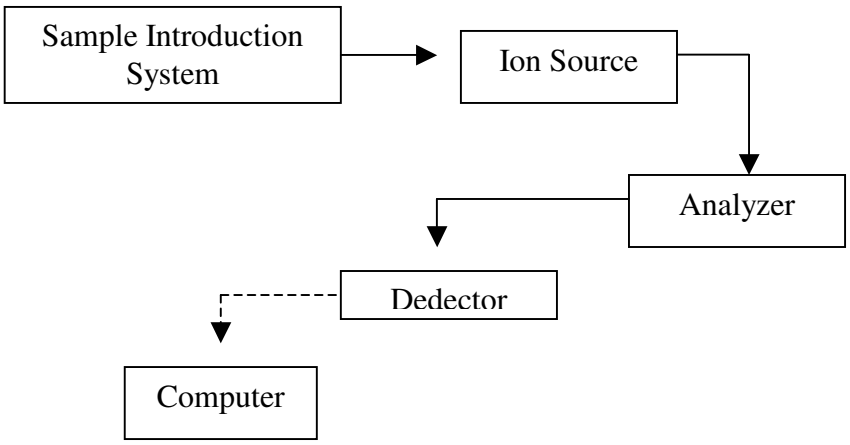

Figure 2.2 Block diagram of mass spectrometer

2.3.1 Sample Introduction

In general, samples are introduced either as a gas to be ionized in the ion source, or by enjection of charged molecular species from a solid surface or solution. In some

cases sample introduction and ionization take place in a single process, making a distinction between them somewhat artificial. For volatilizable solids, the most frequently used method of sample introduction is the direct insertion probe. Here, the sample is placed in a small crucible at the tip of the probe, which is heated under high vacuum in close proximity to the ion source. In this work JHP SIS direct insertion probe pyrolysis system was used.

2.3.2 Ion Source

In the ion source, ionization and the fragmentation of the molecules are occurred. Among the several ion source electron impact (EI) is the most common one. In electron impact ionization, the sample molecules are bombarded with high energy electrons, and then positive ions are produced. Provided the energy of electron beam is greater than the ionization potential of the sample, the sample is ionized and/or fragmented, as represented by the following equation:

$$e^- + M \rightarrow M^+ \bullet + 2\, e^-$$

In the present study, electron impact ion source was used. The experiments were carried out using 70 and 19 eV electrons to control and minimize dissociation of thermal decomposition products.

2.3.3 Analyzer

Mass analyzers separate the charged species in the ionized sample according to their mass-to-charge ratios (m/z), thus permitting the mass and abundance of each species to be determined. Four commonly used analyzers are the magnetic sector; the quadrupole, the time-of-flight, and the fourier transform analyzers. The quadrupole analyzer is a mass filter because it separates ions in the basis of their m/z ratio. . The main advantages of quadrupole mass analyzer are fast scanning, good reproducibility and self-tuning of the experimental parameters.

At a given time, only ions of a selected mass to charge ratio can pass through the filter to the detector. The 5973 HP system used works with a quadrupole mass analyzer. Mass range is determined by the analyzer. For the present system mass range is 1.6-800 amu (atomic mass units).

2.3.4. Detector

The detector in the MSD is a high energy conversion dynode (HED) coupled to an electron multiplier (EM). The detector is located at the exit end of the quadrupole mass filter. It receives the ions that have passed through the mass filter.

2.4. Procedure

2.4.1 Electrochemical polymerization of Poly(p-phenylene vinylene)

2.4.1.1 Synthesis of p-xylene-bis(diethylsulphonium chloride) monomer

0,75 M α,α-dichloro-p-xylene was reacted with excess diethyl sulphide at 50 °C in a methanol: water (80:20) solution for 24h to obtain p-xylene-bis(diethylsulphonium chloride) monomer. After the solution concentrated by heating, the product was precipitated in cold acetone (0 °C). Filtration and vacuum drying were performed.

2.4.1.2 Chemical polymerization of PPV

Equal volumes of 0.5 M aqueous solution of monomer and 0.5 M aqueous solution of NaOH were mixed at 0 °C under nitrogen with stirring. A white precipitate was obtained after one hour. The solution was neutralized with 1M HCl and dried at 30 °C under vacuum. The latter polymer obtained by the thermal elimination of water, organic sulfides and HCl at 245 °C vacuum drying for 6 h.

2.4.1.3 Electrochemical polymerization of PPV

PPV has been prepared from p-xylene-bis (diethylsulphonium chloride) in acetonitrile-tetrabutylammonium tetrafluoroborate solvent-electrolyte couple via electrochemical polymerization. The electrochemical polymerization was carried in a three electrode system. Platinum plate was used as working and counter electrodes and Ag wire was used as the reference electrode under N_2 atmosphere. 0.003 mole PXBDC monomer, 0.006 mole supporting electrolyte (TBAFB) and 0.2 % water were dissolved in 60ml acetonitrile. The polymerization reaction was carried out by current with fixed voltage (-2.3V) at room temperature. The polymer was peeled of the electrode surface and vacuum drying were performed at 245 °C for 6h. The polymer obtained from the electrode surface was converted to PPV by the thermal elimination of diethyl sulfide, ethyl sulfide and hydrochloric acid.

2.4.2 Electrochemical polymerization of Aniline

2.4.2.1 Sulfuric Acid as supporting electrolyte

The experiment was performed at +0.8 V by using 1 M aqueous H_2SO_4 as supporting electrolyte and 0.01 M pure aniline as monomer. Nitrogen gas was purged from the system prior to the electrolysis. However, polyaniline could not be obtained in the form of freestanding films. It could not be peeled off from the electrode. Electrode were washed with distilled water to remove the supporting electrolyte after the synthesis and dried at 80 °C for 1h [28,38].

2.4.2.2 Hydrochloric Acid as supporting electrolyte

The experiment was performed at +0.7 V by using 2 M aqueous HCl as supporting electrolyte and 0.5 M pure aniline as monomer. Nitrogen gas was purged from the system prior to the electrolysis. Films were washed with distilled water to remove the supporting electrolyte after the synthesis and dried at 80 °C for 1h [39].

2.4.2.3 Nitric Acid as supporting electrolyte

The experiment was performed at +0.7 V by using 2 M aqueous HNO_3 as supporting electrolyte and 0.5 M pure aniline as monomer. Nitrogen gas was purged from the system prior to the electrolysis. Films were washed with distilled water to remove the supporting electrolyte after the synthesis and dried at 80 °C for 1h.

CHAPTER 3

RESULTS AND DISCUSSION

Conducting polymers gained great interest during the last decades but the use of common spectroscopic techniques for structural analyses is limited due to their network structure. Direct insertion probe pyrolysis mass spectrometry (DIP-MS) technique can be used to perform the thermal and the structural characterization of these polymers. Yet, the interpretation of the mass spectral data is difficult, as the complex multicomponent mixtures produced by thermal degradation of the polymer further dissociate during the ionization processes in MS. In this study, in order to investigate structural and thermal characteristics of conducting polymers, poly(paraphenylene vinylene), PPV and polyaniline, PANI, DIP-MS technique is applied.

PART A. Polyparaphenylene vinylene

For thermal and structural characterization of polyparaphenylene vinylene, PPV firstly, mass spectrum of its monomer is investigated. In Figure 3.1 the mass spectrum of the monomer is given. A careful analysis of the mass spectrum indicated presence of starting materials also. Peaks at m/z=104 Da due to C_8H_8 and at m/z=90 Da due to $S(C_2H_5)_2$ confirm presence of unreacted reactants that can not be removed. The fragmentation pattern determined with the use of the mass spectrum is inaccordance with the expected fragmentation routes and summarized in Table 3.1.

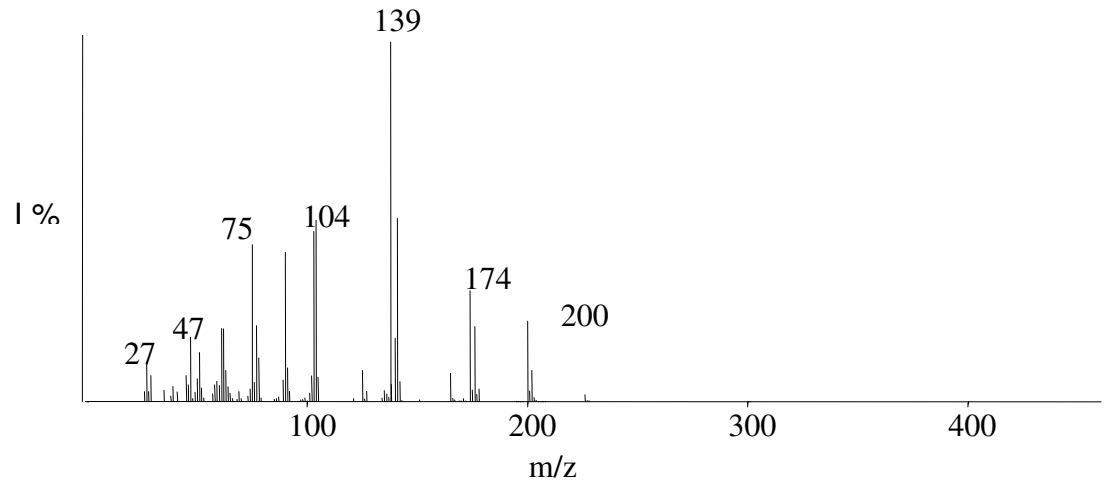

Figure 3.1 Mass spectrum of the monomer

Table 3.1 The characteristics and/or intense peaks present in the pyrolysis mass spectrum of the monomer PPV.

m/z	% I	Assignment
35	29	Cl
47	187	CHCl, $HSCH_2$
62	215	$HSCH_2CH_3$
75	428	$CH_2SC_2H_5$
90	411	S $(C_2H_5)_2$, $C_6H_4CH_2$
104	488	$C_6H_4CH_2CH_2$
121	171	$C_6H_3CH_2S$
139	1000	$C_8H_8{}^{35}Cl$, $CH_2C_6H_4CH_2Cl$
141	464	$C_8H_8{}^{37}Cl$
174	292	$C_8H_8{}^{35}Cl_2$
176	195	$C_8H_8{}^{35}Cl^{37}Cl$
178	33	$C_8H_8{}^{37}Cl_2$
200	106	$ClCH_2C_6H_6CH_2S(C_2H_5)$
226	5	$(C_2H_5)SCH_2C_6H_6CH_2S(C_2H_5)$

3.A.1. Electrochemically prepared PPV

In order to investigate the polymerization processes taking place pyrolysis mass spectrometry analysis of samples polymerized electrochemically at –2,3 V and a)dried at 30 ^{0}C for two hours (EPPV1), b) heated further to 245 ^{0}C for 3 hours (EPPV2), c). heated further at 245 ^{0}C for 3 more hours (EPPV3) were performed.

3.A.1.1. EPPV1

The total ion current curve, (the variation of total ion-yield as a function of temperature) of the sample EPPV1, is given in Figure 3.2. The mass spectra recorded at the TIC maxima are also included in the figure and the mass spectral data are summarized in Table 3.2.

The total ion current (TIC) curve of a polymer (summation of 4800 mass spectra recorded) is usually similar to its TGA curve. Yet, peak intensities may change as intensities of the peaks not only depend on amounts of products but also on their ionization efficiencies. Thermal degradation products can be identified by analyzing the mass spectra recorded at the peaks present in the TIC curve. However, pyrolysis mass spectra of polymers are usually very complex as the thermal degradation products further dissociate in the mass spectrometer during ionization. Furthermore, as not only the fragments that are structural isomers, but also various products involving different combinations of C, H, O, having the same m/z value, all have contributions to the intensity of the same m/z peak in the mass spectrum.

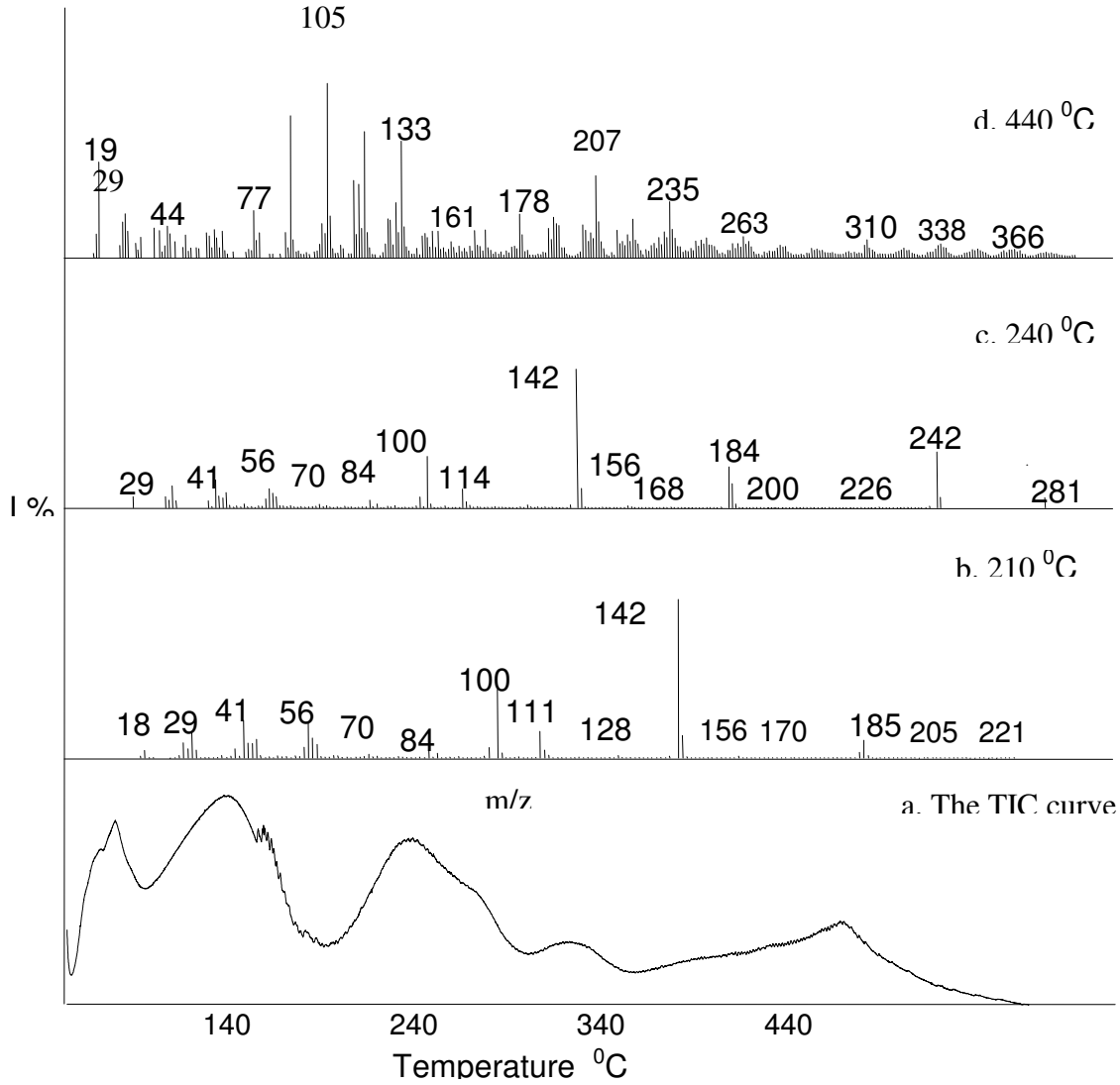

Figure 3.2 Total ion current curve of EPPV1 and the mass spectra recorded at b.210 ^{0}C, c.240 ^{0}C, d.440 ^{0}C.

Table 3.2 The characteristics and/or intense peaks present in the pyrolysis mass spectra at the maxima of the TIC curves of EPPV1.

m/z	Relative Yield					Assigment
	60 ^{0}C	110 ^{0}C	215 ^{0}C	300 ^{0}C	445 ^{0}C	
19				185	556	F
20			2	140	479	HF
29	29	14	136	98	254	CH_3CH_2
34	1		2	8	122	H_2S
35	6	3	5	67	217	Cl
61	20	3	6	45	56	SCH_2CH_3
64	11	2	4	24	61	CH_3CH_2Cl
68	5	5	6	16	142	BF_3
75	31	2	4	15	125	$CH_2SCH_2CH_3$
77	81	51	9	24	269	C_6H_5
91	73	4	9	48	837	$C_6H_4CH_3$, $HS(C_2H_5)_2$
102	7		1	9	87	$C_6H_4CH{=}CH$
104	68	4	4	14	138	$C_6H_4CH_2CH_2$
105	66	5	7	41	1000	$C_6H_4CH_2CH_3$
110	1000	1000	149	96	82	C_6H_5SH
139	102	3	2	4	57	$CH_2C_6H_4CH_2Cl$
142	10	14	1000	1000	144	$N(C_4H_9)_2\,CH_2$
164	5		1	3	43	$CH_2C_6H_4CH_2SCH_2CH_2$
174	11		1	3	35	$CH_2\ C_6H_4\ CH_2Cl_2$
204	2		1	3	43	$(C_6H_4CH{=}CH)_2$
208	2		1	2	43	$(C_6H_4CH_2CH_2)_2$
306	1			1	26	$(C_6H_4CH{=}CH)_3$
312	4	4		1	26	$(C_6H_4CH_2CH_2)_3$
330					17	$(CH_2C_6H_4CH_2SCH_2CH_3)_2$

Thus, what is important in pyrolysis MS analysis is not the detection of a peak but the variation of its intensity as a function of temperature. The trends in these curves (single ion pyrograms, or evolution profiles) can be used to determine the source of the product, or the mechanism of thermal degradation.

For polymer analyses, another problem is the contamination. Actually, before each experiment, the system is heated, pumped and background spectrum is recorded for background subtraction. Still, the contamination can complicate the spectra and in most cases the experiments have to be repeated. Background subtraction may affect the fragmentation pattern, and may not be applicable if identical peaks are also present in the background spectrum as in this case.

In general, a TIC curve involving several peaks and shoulders points a complex nature for the polymer sample. In general, the low temperature peaks below 100 ^{0}C can directly be attributed to desorption of unreacted monomer, solvent or any other low molecular weight species adsorbed on the polymer film. However, presence of more than one peak or a broad peak with several shoulders in the moderate and elevated temperature ranges can be associated either with a multi-step thermal degradation process, as in the case of polymers having labile side groups, or with presence of more than one compound or segments with different thermal stabilities. For electrochemically prepared polymers, thermal decomposition involves at least two steps, the first being due to the loss of supporting electrolyte present and the second due to the degradation of polymer backbone.

The TIC curve for EPPV1 shows several peaks. Analysis of the pyrolysis mass spectra recorded at the maxima of the peaks present in the TIC curve, and the trends in the evolution profiles indicated presence of several molecules such as unreacted $CH_2ClC_6H_4CH_2Cl$ (m/z=174, 139, 91, and 77 Da), $ClCH_2C_6H_4CH_2S(CH_2CH_3)_2$ (m/z=330, 295, 164, 139, 91, and 77 Da), C_6H_5SH (m/z=110, 84, 77, 66, 51 Da), and $S(CH_2CH_3)_2$ (m/z=90, 75, and 62 Da) (Figure 3.2.a). These species were evolved below 200 ^{0}C. The peaks recorded in the single ion pyrograms of these fragments at

temperatures above 200 ^{0}C are mainly due to the contributions of high molecular weight species yielding products with the same m/z values during the degradation of the polymer.

Products related to supporting electrolyte were detected at moderate temperatures. Evolution of $N(C_4H_7)_4^+$ (m/z=242, 185, 142,100, and 57 Da), $N(C_4H_7)_3$ (m/z=185, 142, 100, and 57 Da) , BF_3 (m/z=68,49,30 and 19 Da) and HF (m/z=20 Da) were recorded in the temperature range of 200-350 ^{0}C (Figure 3.2.b).

In the temperature region 280-400 ^{0}C, fragments that can be attributed to CH_3CH_2Cl, (m/z=64, 35, and 29Da) and $ClSCH_2CH_3$ (m/z=96, 75, 61, 35 Da) were observed (Figure 3.2.c). Taking into account the low molecular weight of these molecules it can be concluded that they were generated during the thermal degradation of high molecular weight compounds. In the final stage of pyrolysis, at elevated temperatures above 380^{0}C products that can be attributed to high molecular weight polymeric species were recorded such as $–(CH_2C_6H_4CH_2SCH_2CH_3)_x–$ (m/z=165, 330, 495, 660 Da for x=1,2,3 and 4 respectively), $–(C_6H_4CH_2CH_2)_x–$ (m/z=104, 208, 312, 416, 520, and 625 Da where x=1, 2, 3, 4 5 and 6 respectively), $–(C_6H_4CH=CH)_x–$ (m/z=102, 204, 306, 408 and 510 Da for x=1, 2, 3, 4 5 and 6 respectively) and —$(C_6H_4CH_2CH_2)_x(C_6H_4CH=CH)_y$— (m/z=306, 308, 412, and 416 Da where x, y=1, 2, respectively) (Figure 3.2.d).

It may be thought that the thermal degradation of $–(CH_2C_6H_4CH(S(CH_2CH_3)_2^+Cl^-))_x$ – occurs in two steps, the first being due to the loss of CH_3CH_2Cl, and $ClSCH_2CH_3$ and the second being due to the decomposition of the polymer backbone yielding segments having the structures $–(CH_2C_6H_4CH_2SCH_2CH_3)x–$, $–(C_6H_4CH_2CH_2)_x–$ – $(C_6H_4CH=CH)_x–$ and —$(C_6H_4CH_2CH_2)_x(C_6H_4CH=CH)_y$— .

Present results indicated that polymerization of the monomer during the electrochemical reduction started. Yet, the reactions were not completed and several structures were detected.

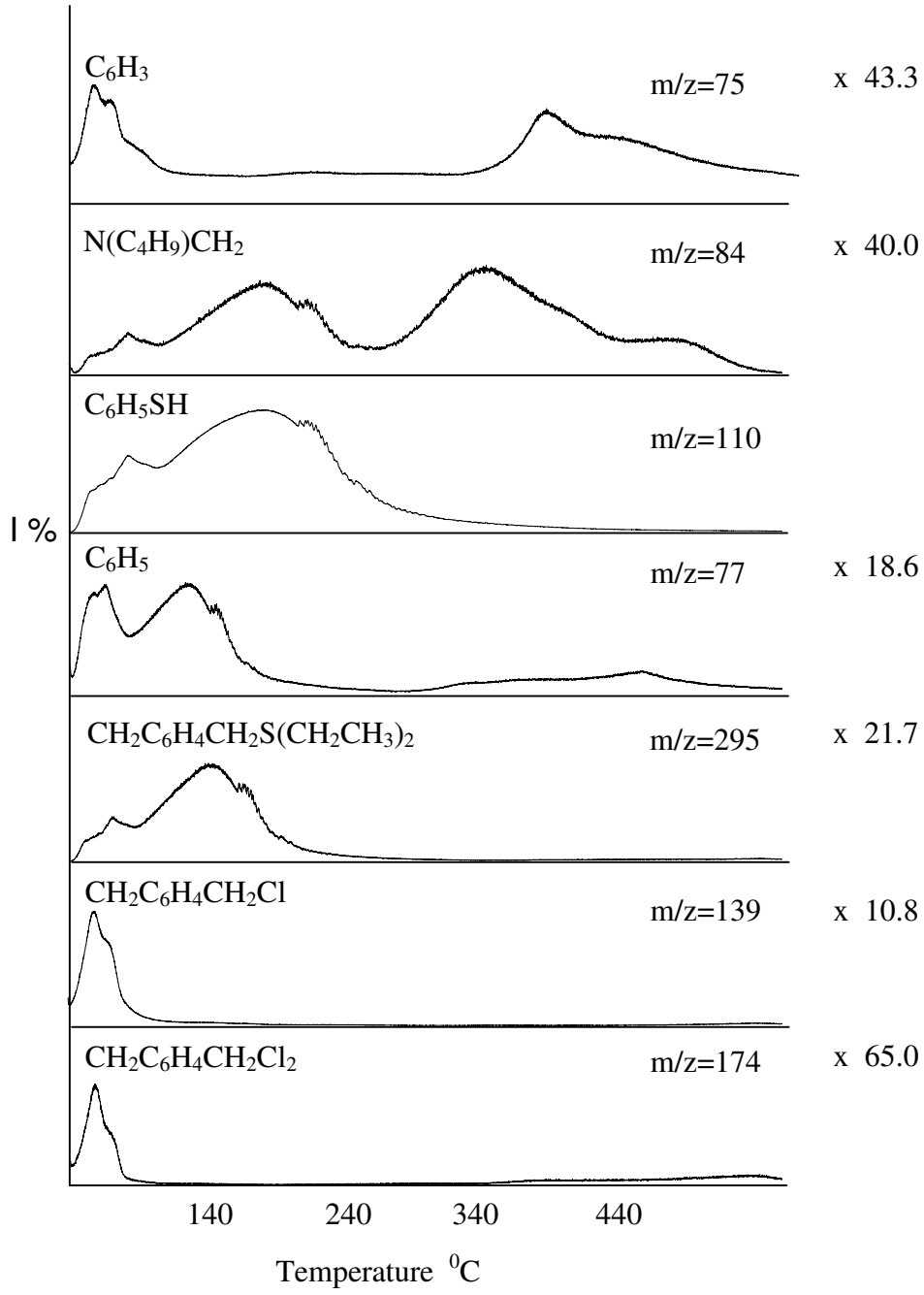

Figure 3.2.a Single ion pyrograms of the ions at m/z 75, 84, 110, 77, 295, 139, 174 Da recorded during pyrolysis of EPPV1.

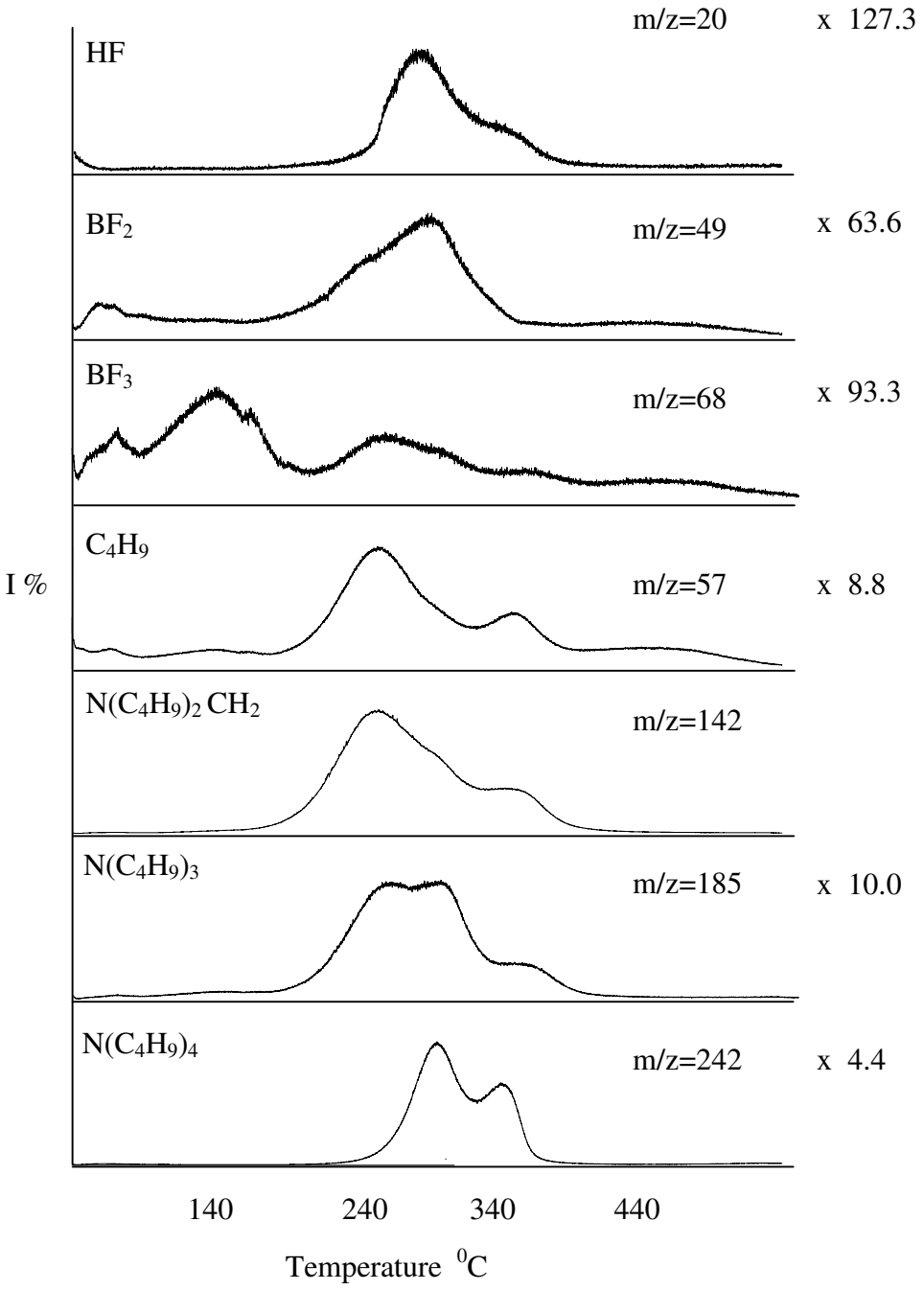

Figure 3.2.b Single ion pyrograms of the ions at m/z 20, 49, 68, 57, 142, 185 and 242 Da recorded during pyrolysis of EPPV1.

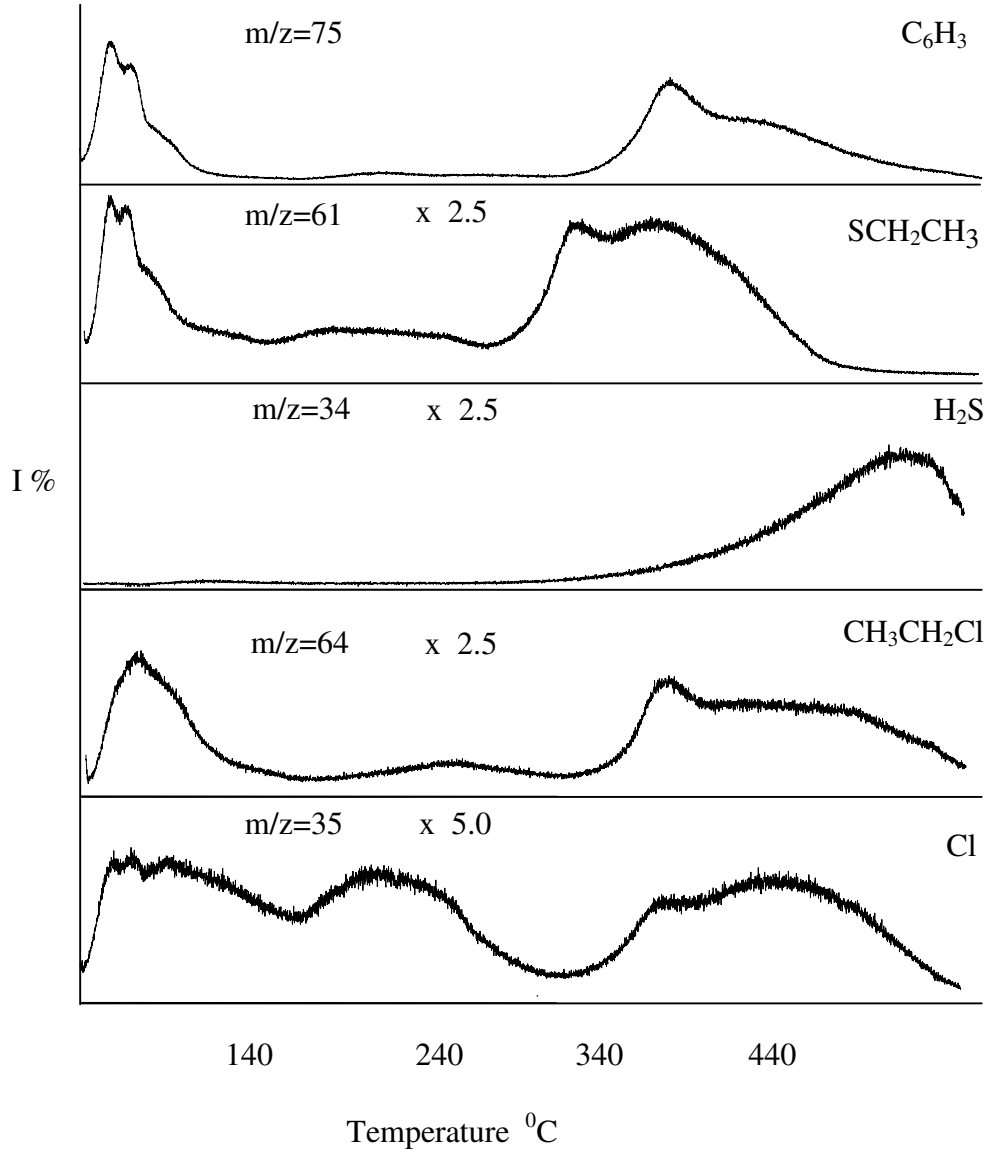

Figure 3.2.c Single ion pyrograms of the ions at m/z 75, 61, 34, 64, 35 Da recorded during pyrolysis of EPPV1.

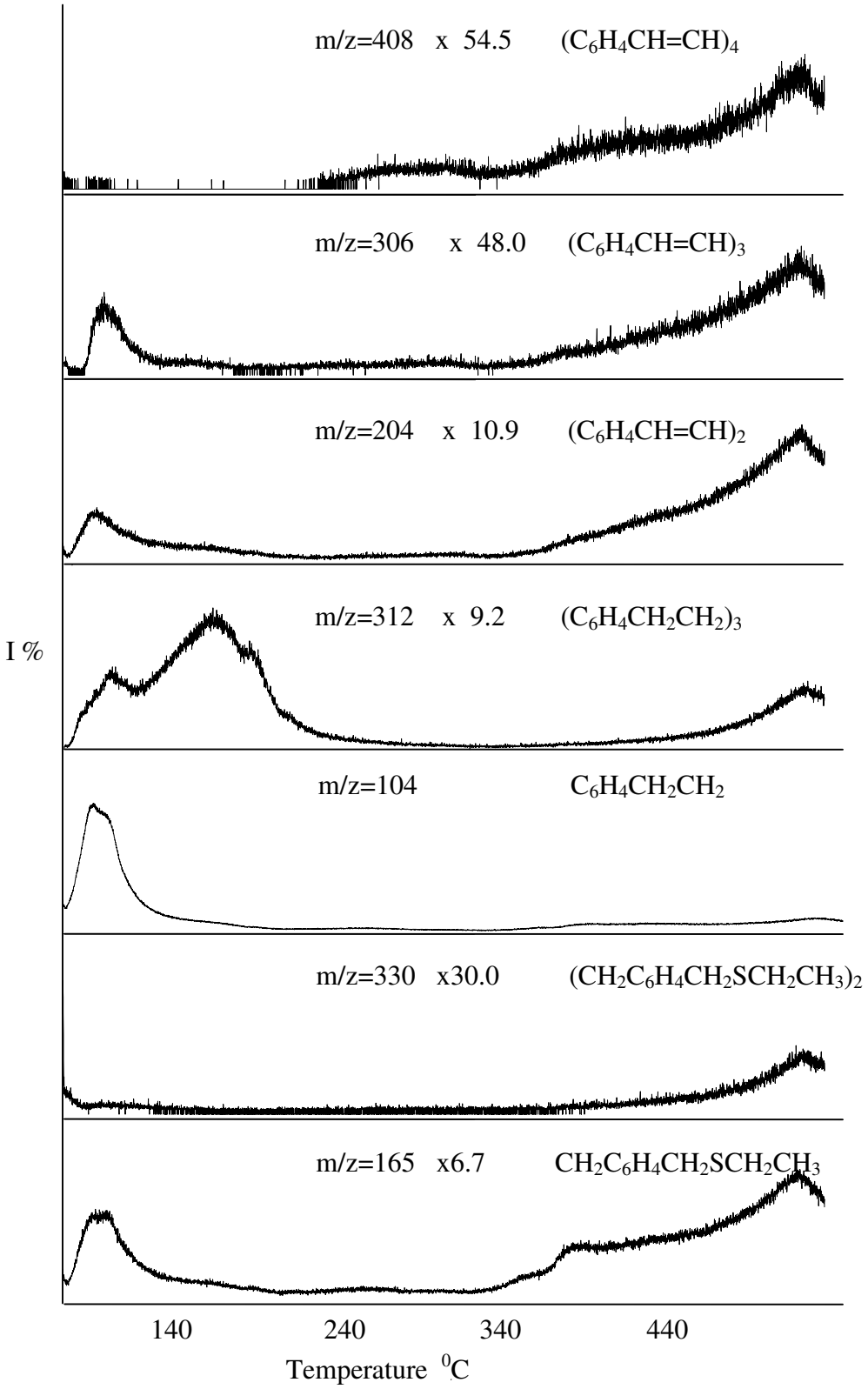

Figure 3.2.d Single ion pyrograms of the ions at m/z 408, 306, 204, 312, 104, 330 and 165 Da recorded during pyrolysis of EPPV1.

3.A.1.2. EPPV2

The total ion current curve, (the variation of total ion-yield as a function of temperature) of the sample EPPV2, is given in Figure 3.3. The mass spectra recorded at the TIC maxima are also included in the figure. The mass spectral data are summarized in Table 3.3.

Table 3.3 The characteristics and/or intense peaks present in the pyrolysis mass spectra at the maxima of the TIC curves of EPPV2.

m/z	Relative Yield			Assigment
	45 ^{0}C	90 ^{0}C	445 ^{0}C	
68	5	5	21	BF_3
77	37	42	352	C_6H_5
84	16	17	29	$N(C_4H_9)$ CH
91	3	2	1000	$C_6H_4CH_3$
102	1		102	C_6H_4CH=CH
104	3	2	143	$C_6H_4CH_2CH_2$
105	3	2	839	$C_6H_4CH_2CH_3$
110	1000	1000	70	C_6H_5SH
142	1	1	66	$N(C_4H_9)_2$ CH_2
165	1	1	193	$CH_2C_6H_4CH_2SCH_2CH_3$
204			92	$(C_6H_4CH=CH)_2$
208			139	$(C_6H_4CH_2CH_2)_2$
242			36	$N(C_4H_9)_4$
295	30	39	35	$CH_2C_6H_4CH_2S(C_3H_5)_2$
306			34	$(C_6H_4CH=CH)_3$
312	3	4	43	$(C_6H_4CH_2CH_2)_3$
330			19	$(CH_2C_6H_4CH_2SCH_2CH_3)_2$
408			18	$(C_6H_4CH=CH)_4$
510			7	$(C_6H_4CH=CH)_5$

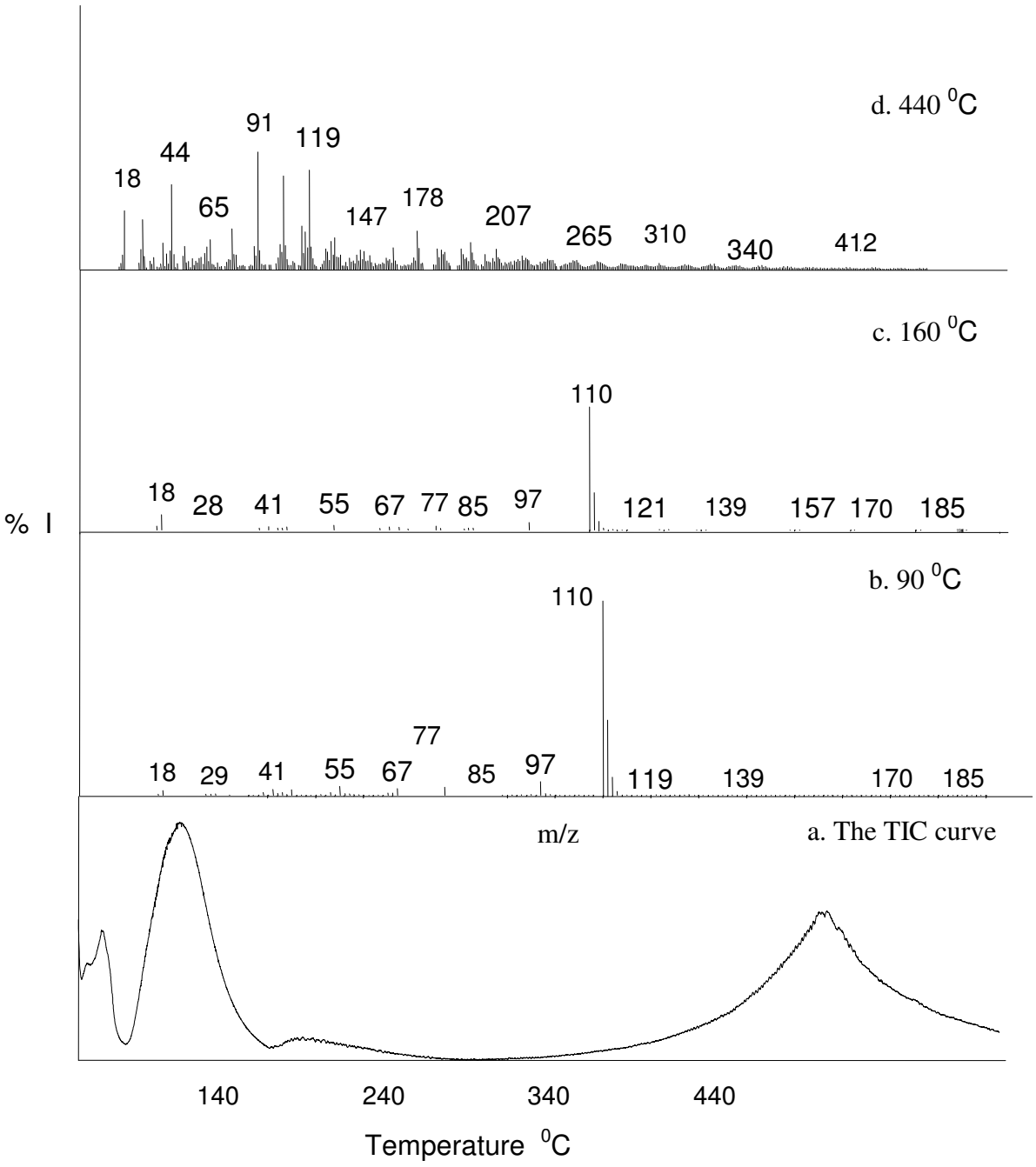

Figure 3.3 Total ion current curve of EPPV2 and the mass spectra recorded at b.90 ^{0}C, c.160 ^{0}C, d.440 ^{0}C

It is clear that some of the low molecular weight molecules adsorbed on the sample were evolved during the heating process at 245 ^{0}C. In Figure 3.3.a evolution profiles of some selected products, namely $CH_2C_6H_4CH_2S(CH_2CH_3)_2$ (m/z= 295 Da), C_6H_5SH (m/z=110 Da), and C_6H_5 (m/z=77 Da), are shown. It is clear that the sample still contained significant amount of $CH_2C_6H_4CH_2S(CH_2CH_3)_2$ (m/z=295, 110, 97, and 77 Da), and C_6H_5SH (m/z=110, 84, 77, 66, 51 Da).

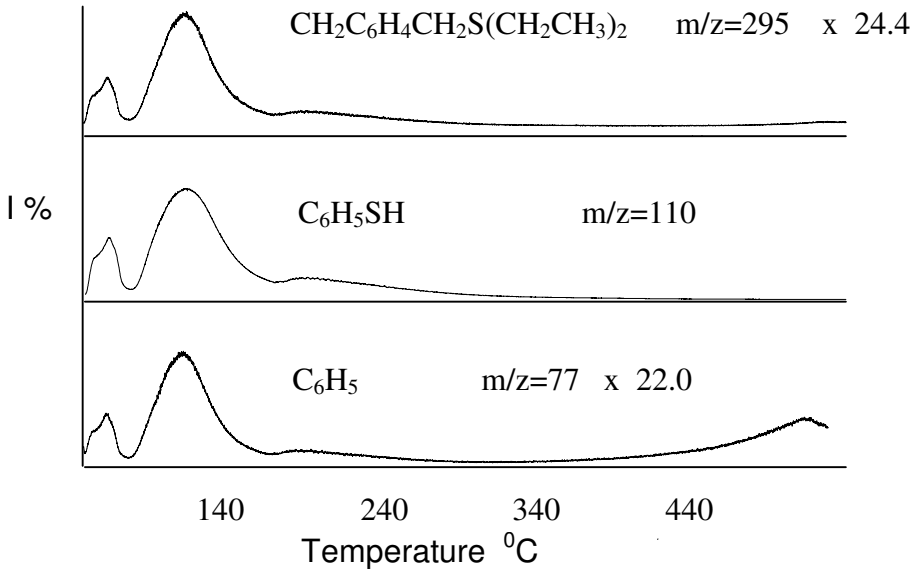

Figure 3.3.a Single ion pyrograms of the ions at m/z 77, 110, 295 Da recorded during pyrolysis of EPPV2.

The dopant based products were absent in the pyrolysis mass spectra, as TBATFB itself dissociates and evolves around 240 ^{0}C readily. Thus, adsorption of $CH_3C_6H_4CH_2S(CH_2CH_3)_2$ and C_6H_5SH (m/z=110, 84, 77, 66, 51 Da) was quite efficient. In Figure 3.3.b, the evolution profiles of H_2S (m/z=34 Da) C_7H_7 (m/z= 91 Da), $C_6H_4CH_2CH_3$ (m/z= 105 Da), $CH_2CH_2C_6H_4CH_2$ S CH_2CH_2 (m/z= 178 Da), $(CH_2C_6H_4CH_2SCH_2CH_3)_2$, (m/z= 330 Da) $CH_2CHC_6H_4C_6H_4CH_2CH_2$ decomposition of polymeric molecules present were recorded above 380 ^{0}C and showed similar trends as can be noted in Figure 3.3.a.

Thus, it can be concluded that during the heating process at 245^0C, not only evolution of low molecular weight species, unreacted reactants and dopant occured but also the polymerization processes proceeded yielding a polymer that had thermally more uniform structure.

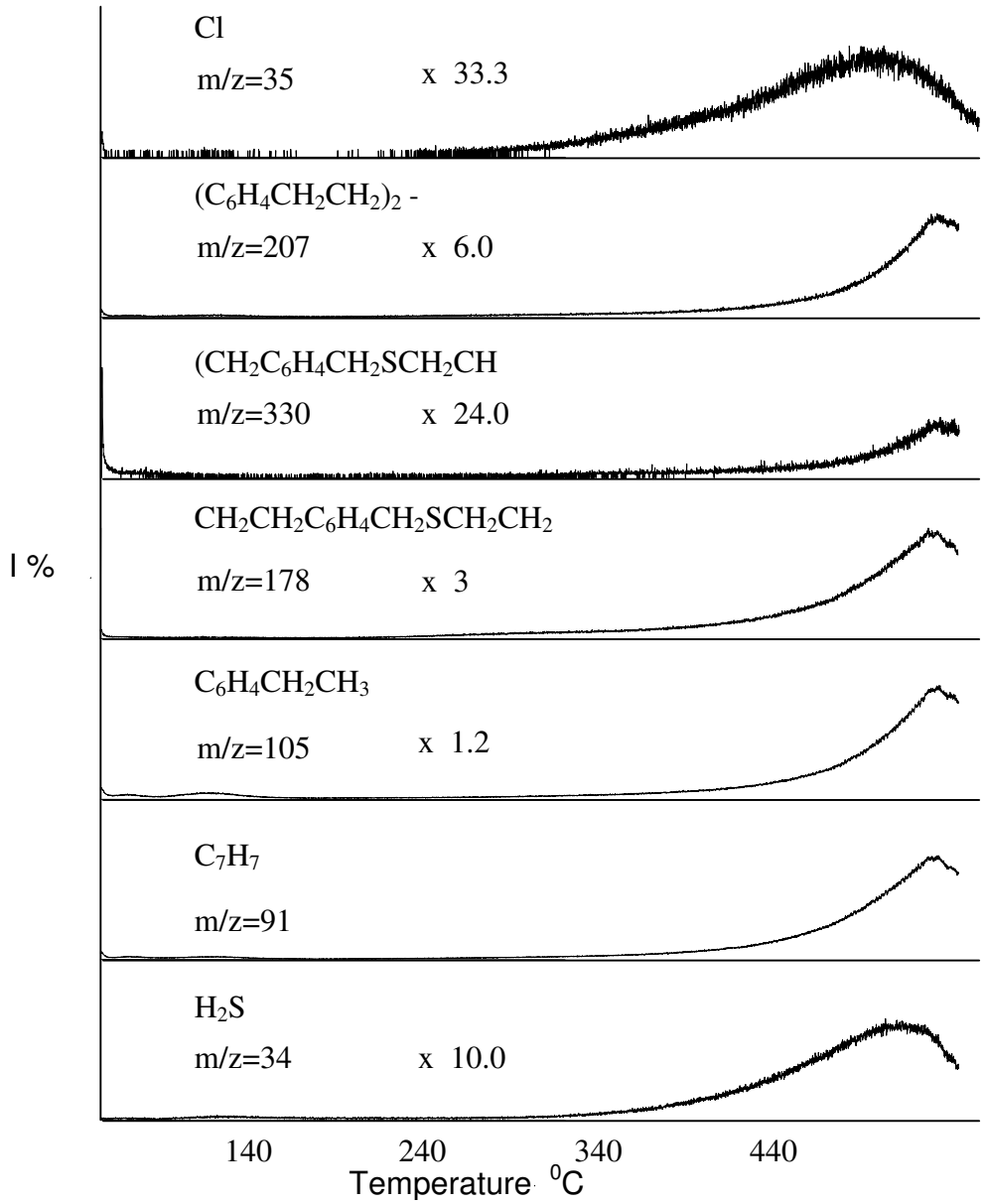

Figure 3.3.b Single ion pyrograms of the ions at m/z 35, 207, 330, 178, 105, 91, 34 Da recorded during pyrolysis of EPPV2.

3.A.1.2. EPPV3

The total ion current curve, (the variation of total ion-yield as a function of temperature) of the sample EPPV3, is given in Figure 3.4. At initial stages intense H_2O evolution was recorded. The mass spectra recorded at the TIC maxima are also included in the figure. When background subtraction was applied a weak peak with two shoulders appeared. The mass spectral data are summarized in Table 3.4.

Table 3.4 The characteristics and/or intense peaks present in the pyrolysis mass spectra at the maxima of the TIC curves of EPPV3.

m/z	Relative Yield				Assigment
	50 ^{0}C	75 ^{0}C	170 ^{0}C	445 ^{0}C	
76	41	44	44	123	C_6H_4, $CHSC_2H_5$
91	7	2	6	1000	$C_6H_4CH_3$
102	2	1	1	111	$C_6H_4CH{=}CH$
104	65	64	66	164	$C_6H_4CH_2CH_2$
105	13	8	10	766	$C_6H_4CH_2CH_3$
110	1000	1000	1000	123	C_6H_5SH
139	21	3	4	61	$CH_2C_6H_4CH_2Cl$
149	136	140	133	245	$CH_2CHC_6H_4CH_2S$
165	1		2	210	$CH_2C_6H_4CH_2SCH_2CH_3$
178	1			301	$CH_2CHC_6H_4CH_2SCH_2CH_3$
204	1			70	$(C_6H_4CH{=}CH)_2$
208				95	$(C_6H_4CH_2CH_2)_2$
259	84	96	83	34	$(C_6H_4CH{=}CH)_2C_4H_3$
306				22	$(C_6H_4CH{=}CH)_3$
330				15	$(CH_2C_6H_4CH_2SCH_2CH_3)_2$
408				13	$(C_6H_4CH{=}CH)_4$

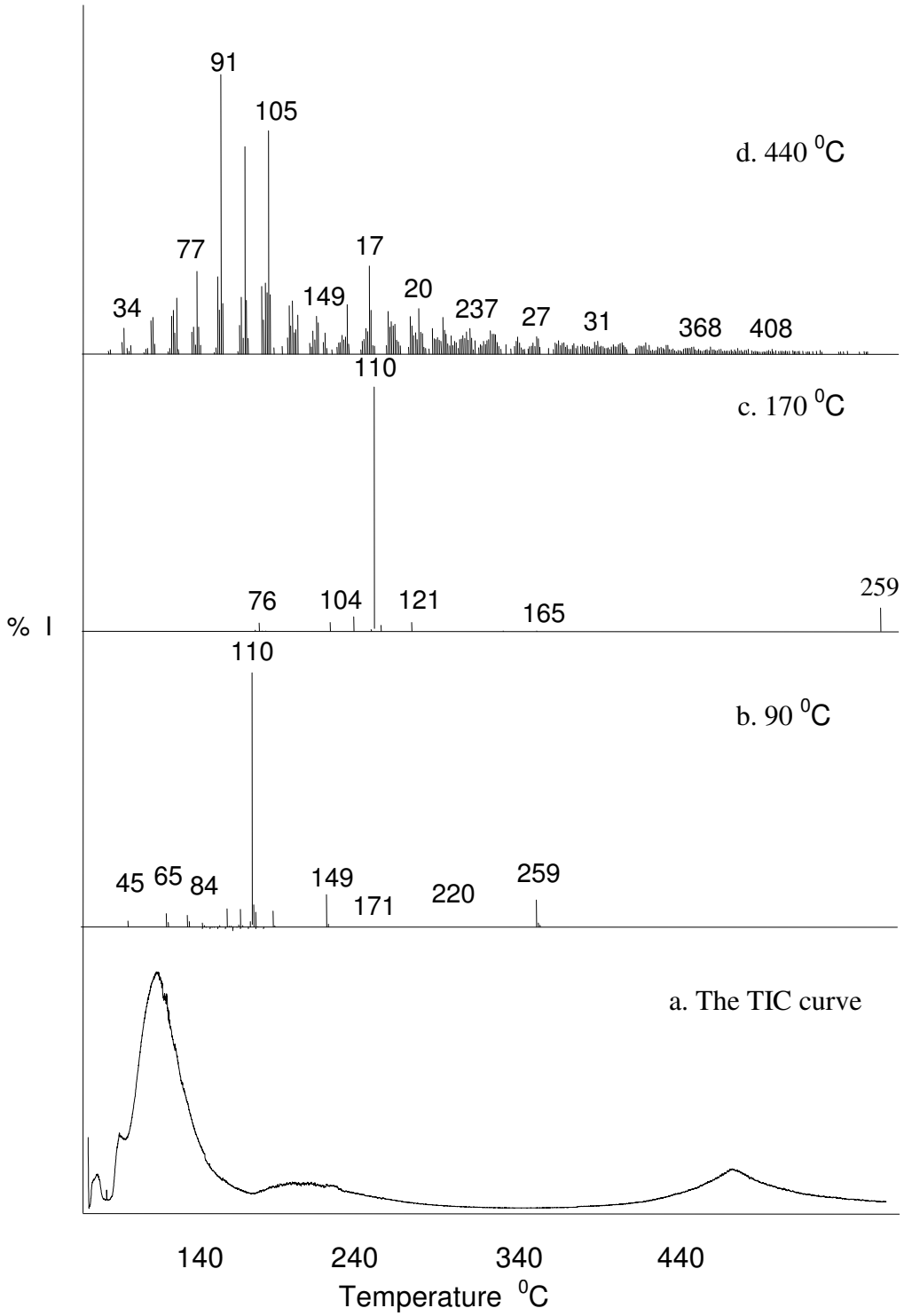

Figure 3.4 Total ion current curve of EPPV3 and the mass spectra recorded at b.90 ^{0}C, c.170 ^{0}C, d.440 ^{0}C

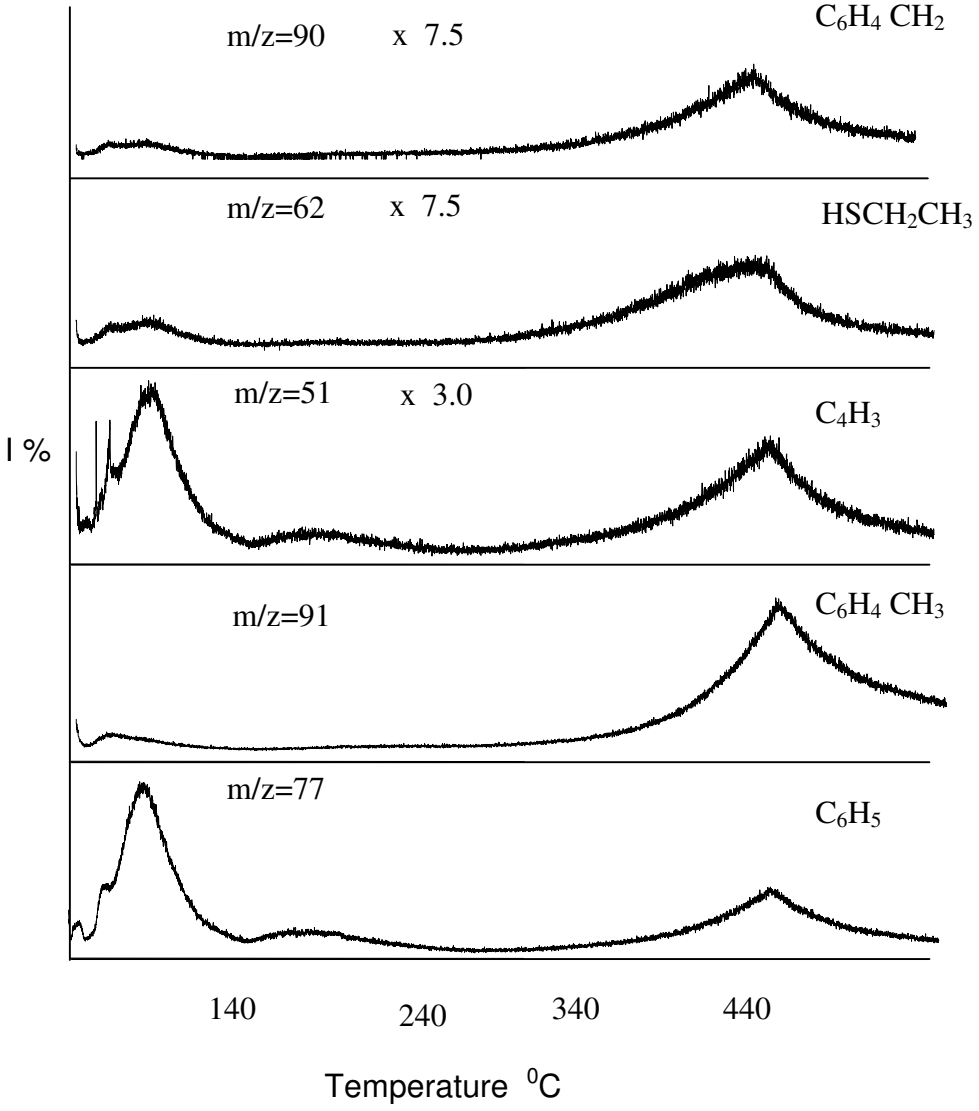

Figure 3.4.a Single ion pyrograms of the ions at m/z 90, 62, 51, 91, 77 Da recorded during pyrolysis of EPPV3.

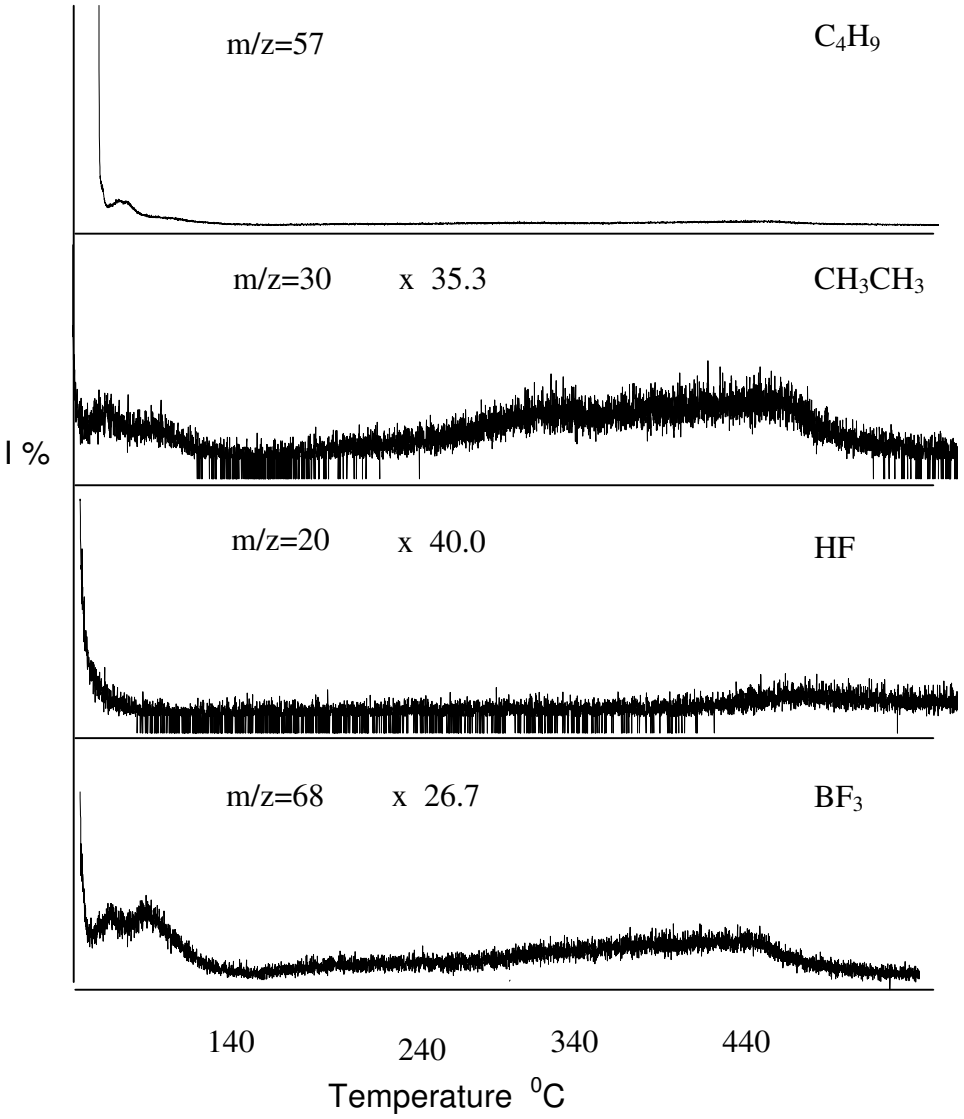

Figure 3.4.b Single ion pyrograms of the ions at m/z 57, 30, 20, 68 Da recorded during pyrolysis of EPPV3.

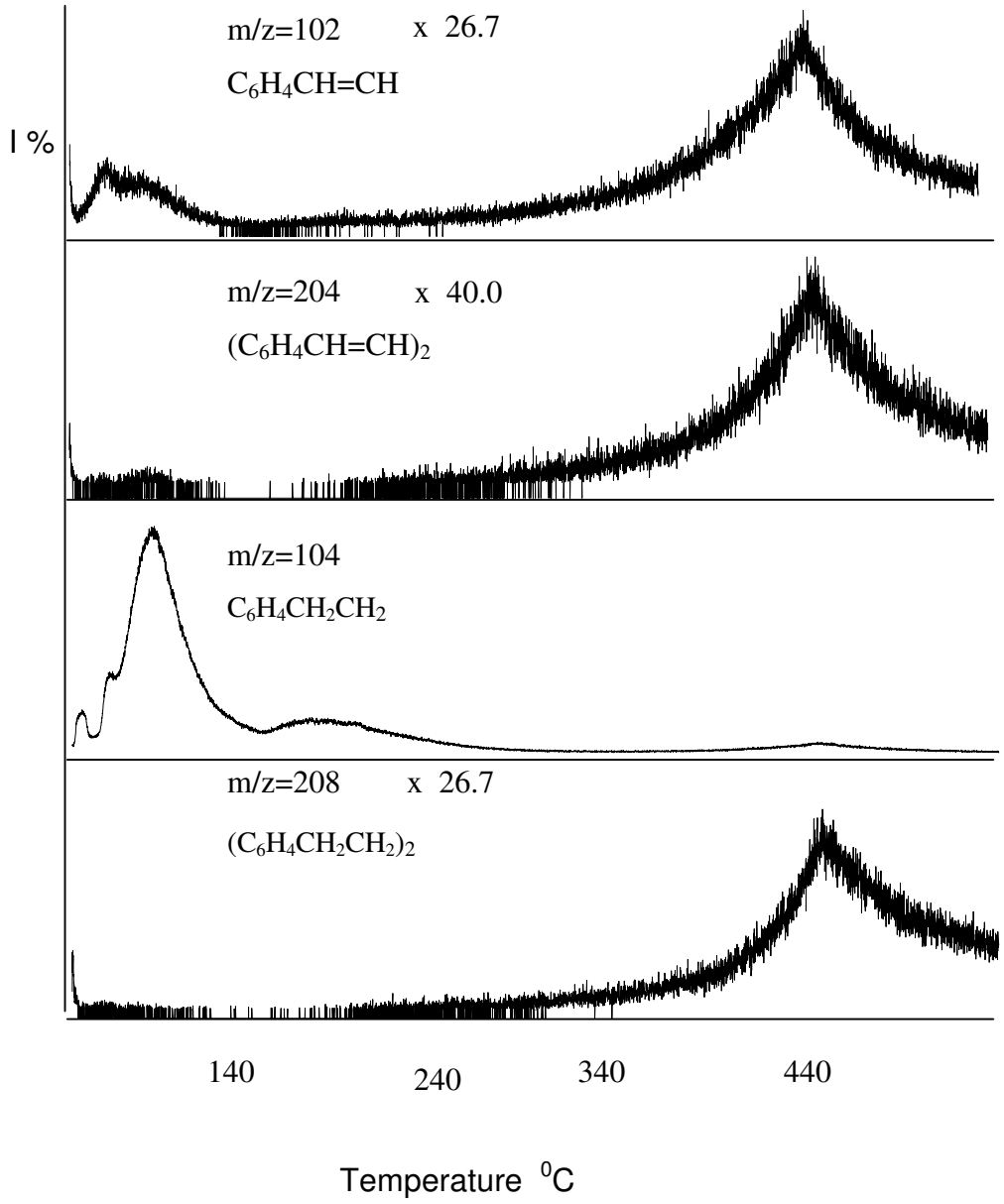

Figure 3.4.c Single ion pyrograms of the ions at m/z 102, 204, 104, 208 Da recorded during pyrolysis of EPPV3.

In Figure 3.4.a , single ion pyrograms of the ions namely $C_6H_4CH_2$ (m/z=90 Da), SCH_3CH_3 (m/z=62 Da), C_4H_3 (m/z=51 Da), $C_6H_4CH_3$ (m/z=91 Da) and C_6H_5 (m/z=77 Da) are given. It is clear that all the low molecular species were removed from the sample after heating for three more hours. Especially dopant based products nearly disappeared. Yet, still fragments involving SC_2H_5 groups were detecting In Figure 3.4.a

Figure 3.4.b , shows that single ion pyrograms of the ions at (m/z 57 Da) due to C_4H_9, (m/z 30 Da) due to C_2H_6, (m/z 20 Da) due to HF and (m/z 68 Da) due to BF_3 recorded during pyrolysis of EPPV3.

In Figure 3.4.c, single ion pyrograms of the ions namely $C_6H_4CH=CH$ (m/z=102Da), $(C_6H_4CH=CH)_2$ (m/z=204Da), $C_6H_4CH_2CH$ (m/z=104Da), $(C_6H_4CH_2CH_2)_2$ (m/z=208Da) are given

The peaks attributed to high molecular weight species were mainly recorded at high temperature. Although they contain different structures, their thermal degradation behavior was quite similar. Thus, it may be thought that polymer chain contains different units randomly. However, doublecate measurements showed significant differences. i.e. for some samples presence of dopant and reactants were detected even after heating at 245 ^{0}C for six hours .

3.A.2. Chemically prepared PPV

Similarly, pyrolysis mass spectrometry analysis of chemically polymerized polyparaphenylene vinylene were also repeated for samples
i.dried at 30 ^{0}C for two hours (CPPV1),
ii.heated further to 245 ^{0}C for 3 hours (CPPV2)
ii heated further at 245 ^{0}C for 3 more hours (CPPV3).
for a better understanding of polymerization routes

3.A.2.1. CPPV1

The total ion current curve, (the variation of total ion-yield as a function of temperature) of the sample CPPV1, is given in Figure 3.5. The TIC curve involves a broad peak with maxima at 50 ^{0}C and a long tail at high temperature region with two shoulders at 250 and 440 ^{0}C. The mass spectra recorded at the maxima of the TIC curve are also included in the figure, and the mass spectral data are summarized in Table 3.5

In order to get a better understanding of thermal degradation processes, single ion pyrograms, the variation of intensity of a product peak as a function of temperature, have been studied. Figure 3.5.a shows the single ion pyrograms of the ions; $C_8H_8Cl_2$ (m/z=174 Da), $CH_2C_6H_4CH_2Cl$ (m/z=139 Da), $C_6H_4CH_2$ (m/z=90 Da), $CH_2C_6H_4CH_2SCH_2CH_2$ (m/z=164 Da), C_6H_5SH (m/z=110 Da), C_4H_3 (m/z=51 Da), $CH_2SC_2H_5$ (m/z=75 Da) and SCH_3CH_3 (m/z=62 Da) recorded during pyrolysis of CPPV1.

In Figure 3.5.b, the single ion pyrograms of the ions namely $N(C_4H_9)_3$ (m/z=185 Da), $N(C_4H_9)_2\,CH_2$ (m/z=142 Da), C_4H_9 (m/z=57 Da), BF_3 (m/z=68 Da) and CH_3CH_3 or BF (m/z=30 Da) are given. Evolution of these species at early stages of pyrolysis indicated contamination of mass spectrometer. In Figure 3.5.c, single ion pyrograms of the ions, namely C_5H_5 (m/z=65 Da), Cl (m/z=35 Da), CH_3CH_2 (m/z=29 Da), $CH_2SC_2H_5$ (m/z=75 Da) and SCH_3CH_2 (m/z=61 Da) are given.

In Figure 3.5.d, single ion pyrograms of the ions namely, $C_6H_4CH{=}CH$ (m/z=102 Da), $CH_2C_6H_4CH_2SCH_2CH_3$ (m/z=165 Da), $C_6H_4CH_2CH_2$ (m/z=104 Da), $(C_6H_4CH{=}CH)_3$ (m/z=306 Da) and $(C_6H_4CH{=}CH)_2$ (m/z=204 Da) are given. Inspection of single ion pyrograms indicated that, all the thermal degradation products show similar trends. Thus, it may be proposed that, they were generated through the same degradation mechanisms.

Table 3.5 The characteristics and/or intense peaks present in the pyrolysis mass spectra at the maxima of the TIC curves of CPPV1.

m/z	Relative Yield				Assigment
	45 ^{0}C	55 ^{0}C	175 ^{0}C	350 ^{0}C	
36	47	13	1000	85	HCl
47	585	206	14	53	CCl
51	190	252	19	37	C_4H_3
61	565	212	16	35	SCH_2CH_3
75	1000	420	22	17	$CH_2SC_2H_5$
78	117	156	29	42	C_6H_6
90	947	369	46	44	$C_6H_4CH_2$, S $(C_2H_5)_2$
91	242	195	168	247	$C_6H_4CH_3$, $HS(C_2H_5)_2$
103	424	523	45	59	$C_6H_4CH_2CH$
104	445	584	77	102	$C_6H_4CH_2CH_2$
121	194	154	59	70	$CH_2C_6H_5CH_2CH_2$
139	962	1000	54	47	$CH_2C_6H_4CH_2Cl$
140	147	188	13	14	$CH_3C_6H_4CH_2Cl$
174	240	292	4	6	$C_8H_8Cl_2$
176	157	196	19	33	C_8H_8 ^{35}Cl ^{37}Cl
204	1	2	126	186	$(C_6H_4CH=CH)_2$
237	2	3	254	352	$(C_6H_4CH=CH)C_6H_4SCH_2CH_3$
306			144	187	$(C_6H_4CH=CH)_3$
369	1	2	826	1000	$(C_6H_4CH=CH)_3SCHCH_2$
370		1	269	464	$(C_6H_4CH=CH)_3SCH_2CH_2$
430	1	2	635	738	$(C_6H_4CH_2CH_2)_3(SCHCH_2)_2$
431		1	195	239	$(C_6H_4CH_2CH_2)_3(SCHCH_2)_2H$

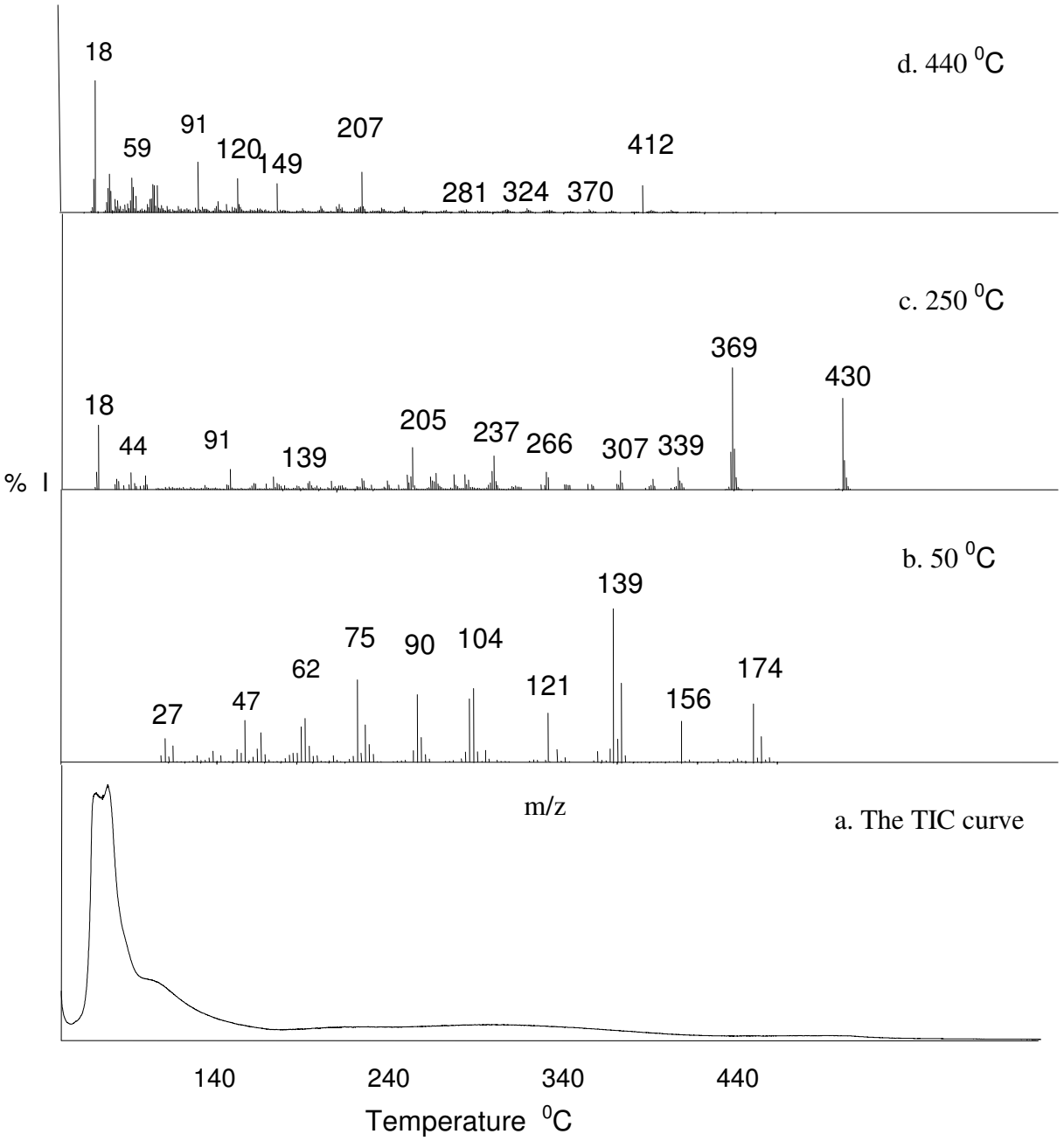

Figure 3.5 Total ion current curve of CPPV1 and the mass spectra recorded at b.50 ^{0}C, c.250 ^{0}C, d.440 ^{0}C.

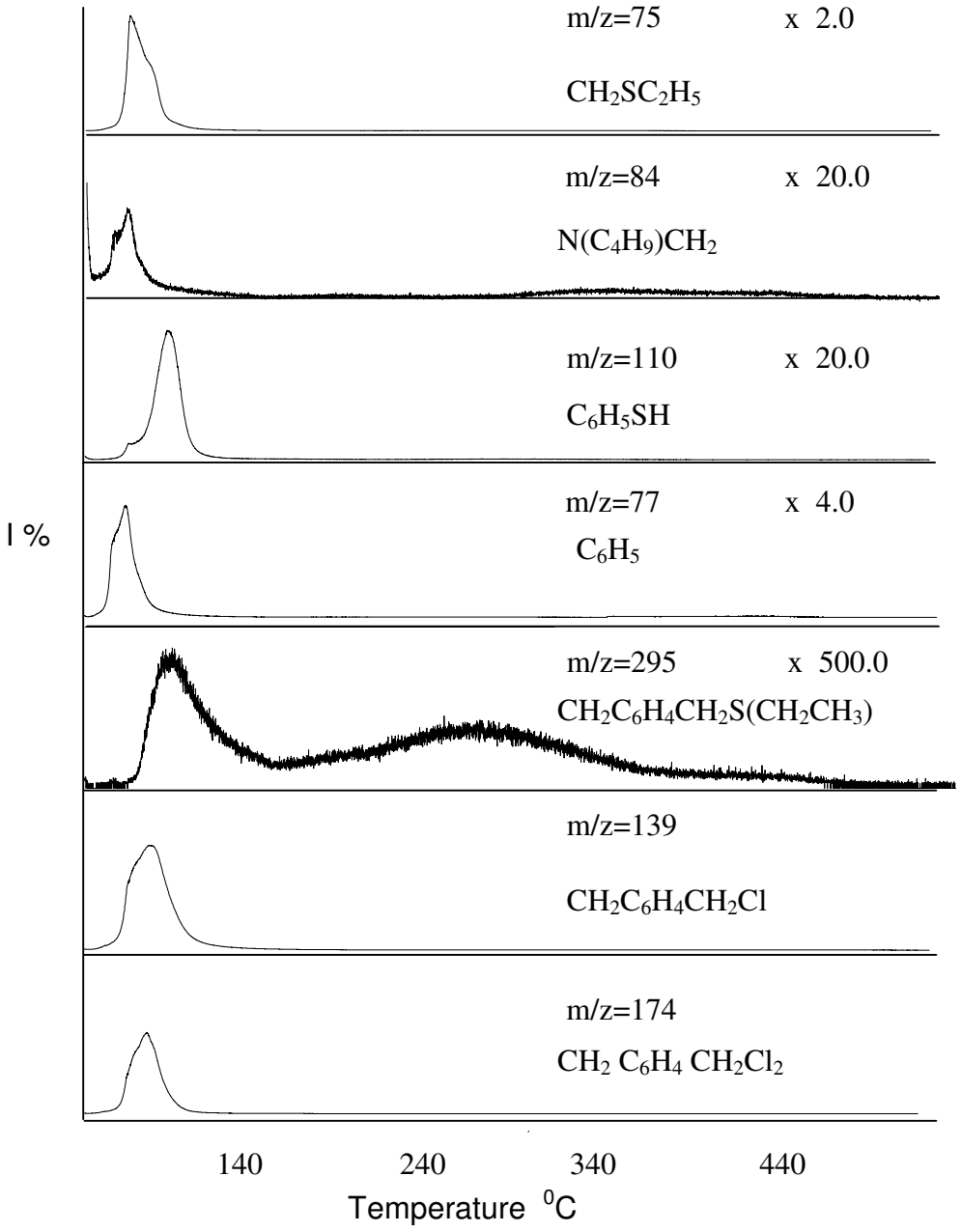

Figure 3.5.a Single ion pyrograms of the ions at m/z 75, 84, 110, 77, 295, 139, 174 Da recorded during pyrolysis of CPPV1.

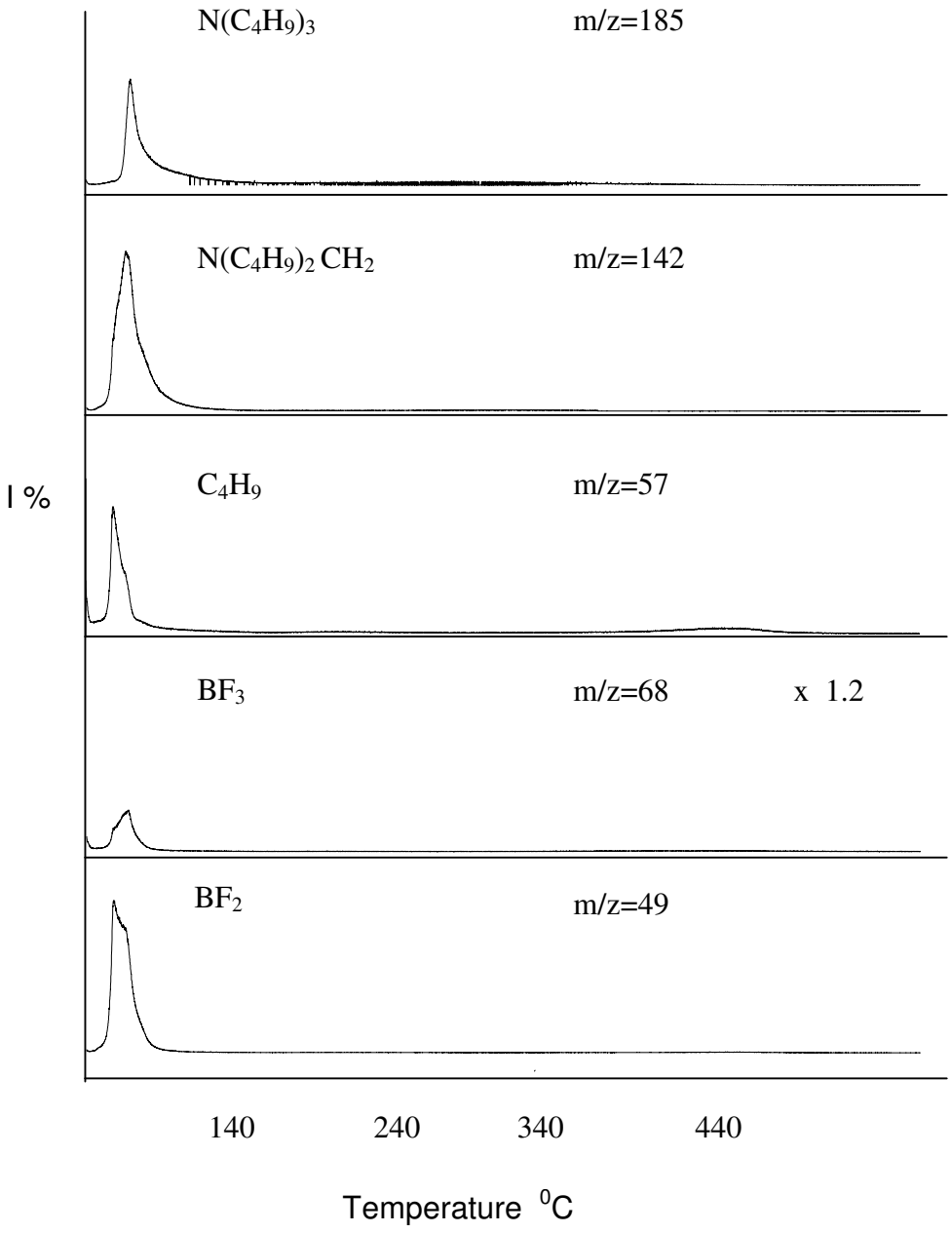

Figure 3.5.b Single ion pyrograms of the ions at m/z 185, 142, 57, 68, 49 Da recorded during pyrolysis of CPPV1.

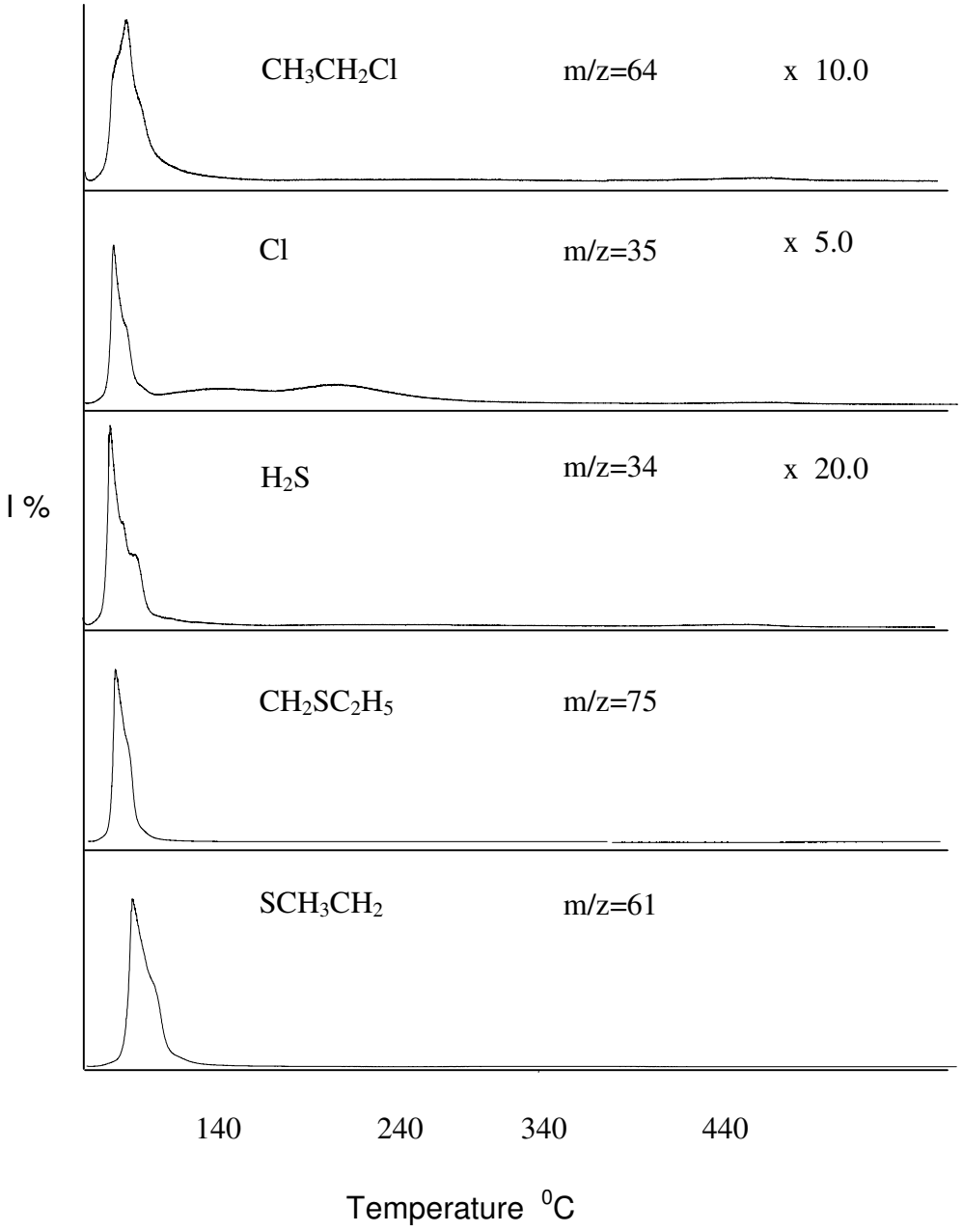

Figure 3.5.c Single ion pyrograms of the ions at m/z 64, 35, 34, 75, 61 Da recorded during pyrolysis of CPPV1.

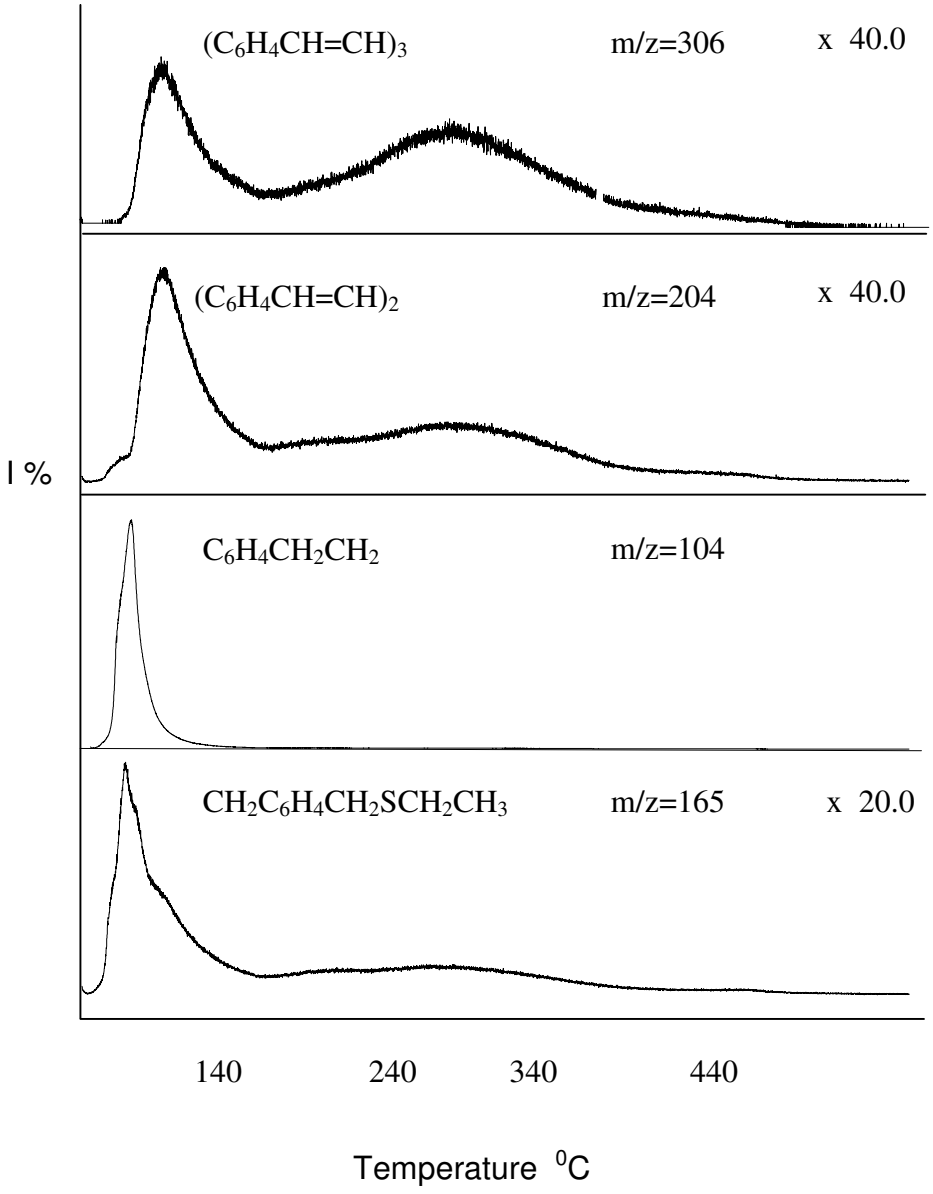

Figure 3.5.d Single ion pyrograms of the ions at m/z 306, 204, 104, 165 Da recorded during pyrolysis of CPPV1.

It is clear that the amount of high molecular weight species generated is quite low compared to the electrochemically prepared sample at this stage.It may be concluded that polymerization proceeded during electrochemical synthesis before the heating step.

3.A.2.2. CPPV2

Pyrolysis mass spectrometry analysis of CPPV2, chemically polymerized polyparaphenylene vinylene dried at 30 ^{0}C for two hours and heated further to 245 ^{0}C for 3 hours, has also been performed. In Table.3.6 the related mass spectral data is summarized at 55, 140, 325 and 360 ^{0}C.

Table 3.6 The characteristics and/or intense peaks present in the pyrolysis mass spectra at the maxima of the TIC curves of CPPV2.

m/z	Relatıve Yield				Assigment
	55 ^{0}C	140 ^{0}C	325 ^{0}C	360 ^{0}C	
41	797	783	405	216	C_3H_5
55	787	777	362	198	C_4H_7
57	1000	777	204	149	C_4H_9
60	572	177	157	81	S CH_2CH_2
68	684	591	255	118	BF_3
71	620	365	154	73	C_3H_2SH
83	496	422	173	92	C_4H_3SH
91	123	157	181	160	$C_6H_4CH_3$
96	380	276	122	69	ClS CH_2CH_3
111	665	1000	292	154	$C_6H_5SH_2$
204			62	64	$(C_6H_4CH=CH)_2$
205	39		94	138	$(C_6H_4CH=CH)_2H$
207		64		187	$C_6H_4CH_2CH_2$ $C_6H_4CH_2CH$
208	31		66	61	$(C_6H_4CH_2CH_2)_2$
306			79	93	$(C_6H_4CH=CH)_3$
324			120	154	$(C_6H_4C_2H_2)_3CH_2$
368	407		1000	1000	$(C_6H_4C_2H_2)_2C_6H_4C_2H_4(SCH_2CH_2)$

The TIC curve of CPPV2 is given Figure 3.6. The pyrolysis mass spectra recorded at 40, 360, 440 ^{0}C are also included in Figure.3.6.

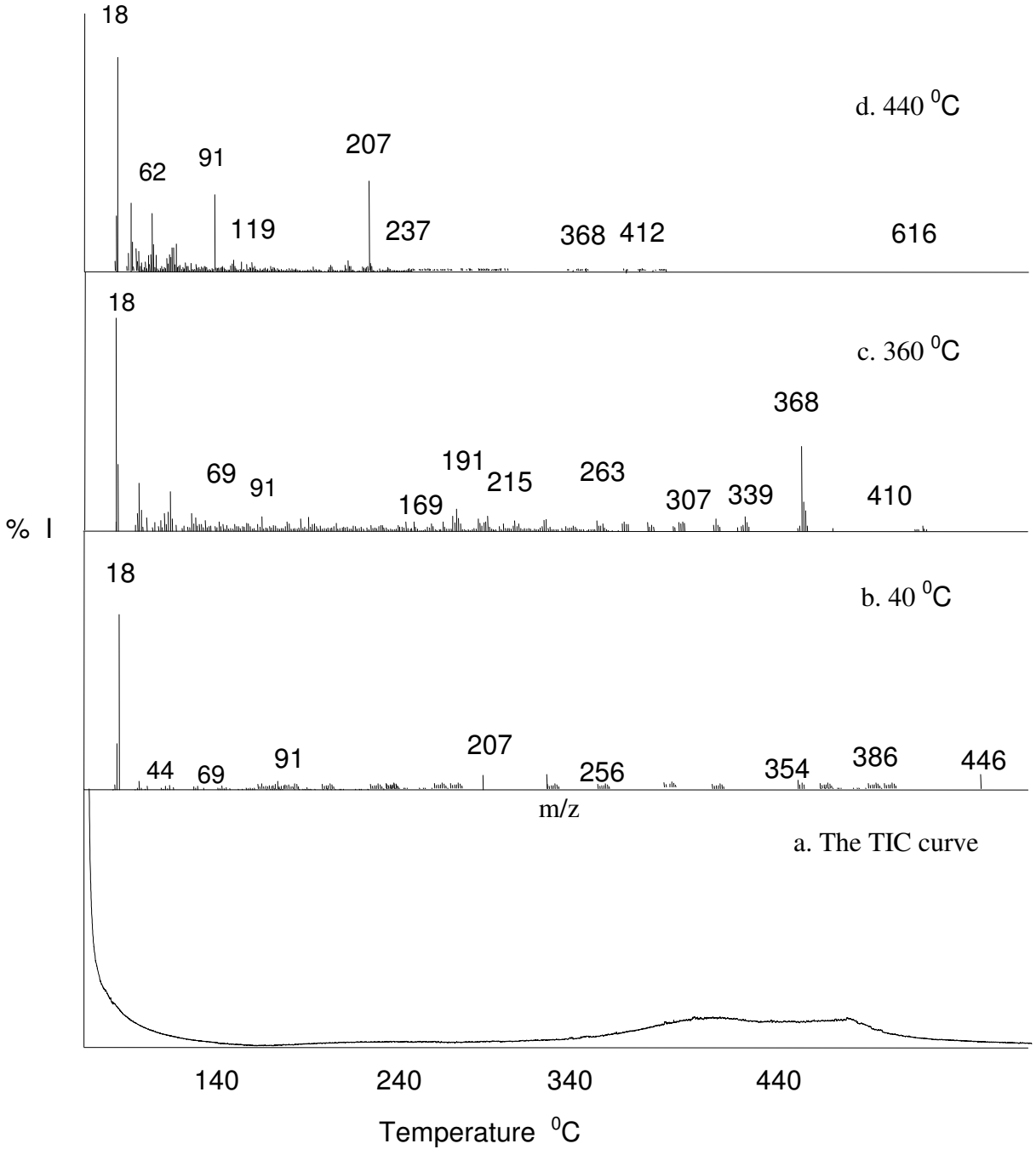

Figure 3.6 Total ion current curve of CPPV2 and the mass spectra recorded at b.40 ^{0}C, c.360 ^{0}C, d.440 ^{0}C

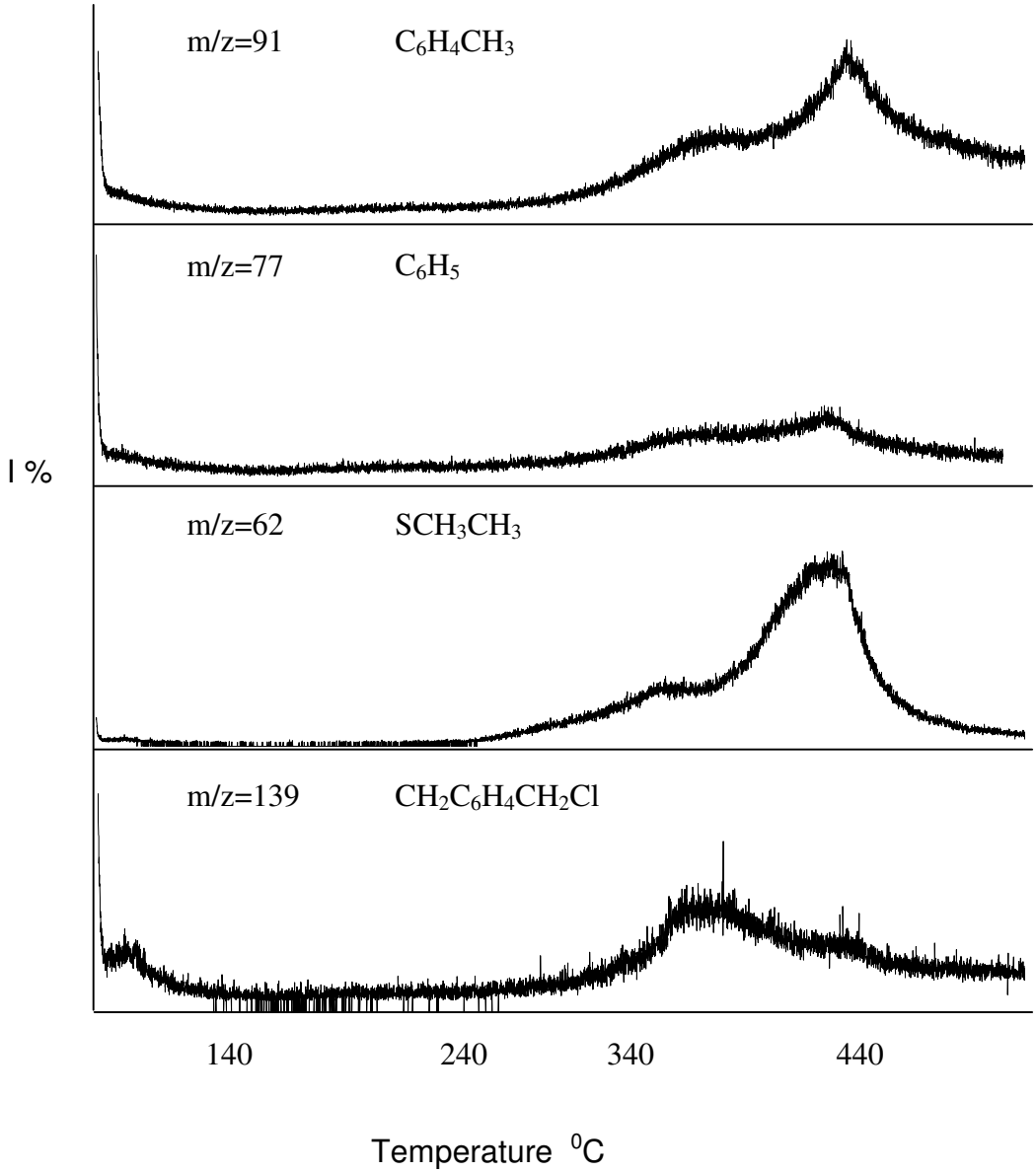

Figure 3.6.a Single ion pyrograms of the ions at m/z 91, 77, 62, 139 Da recorded during pyrolysis of CPPV2

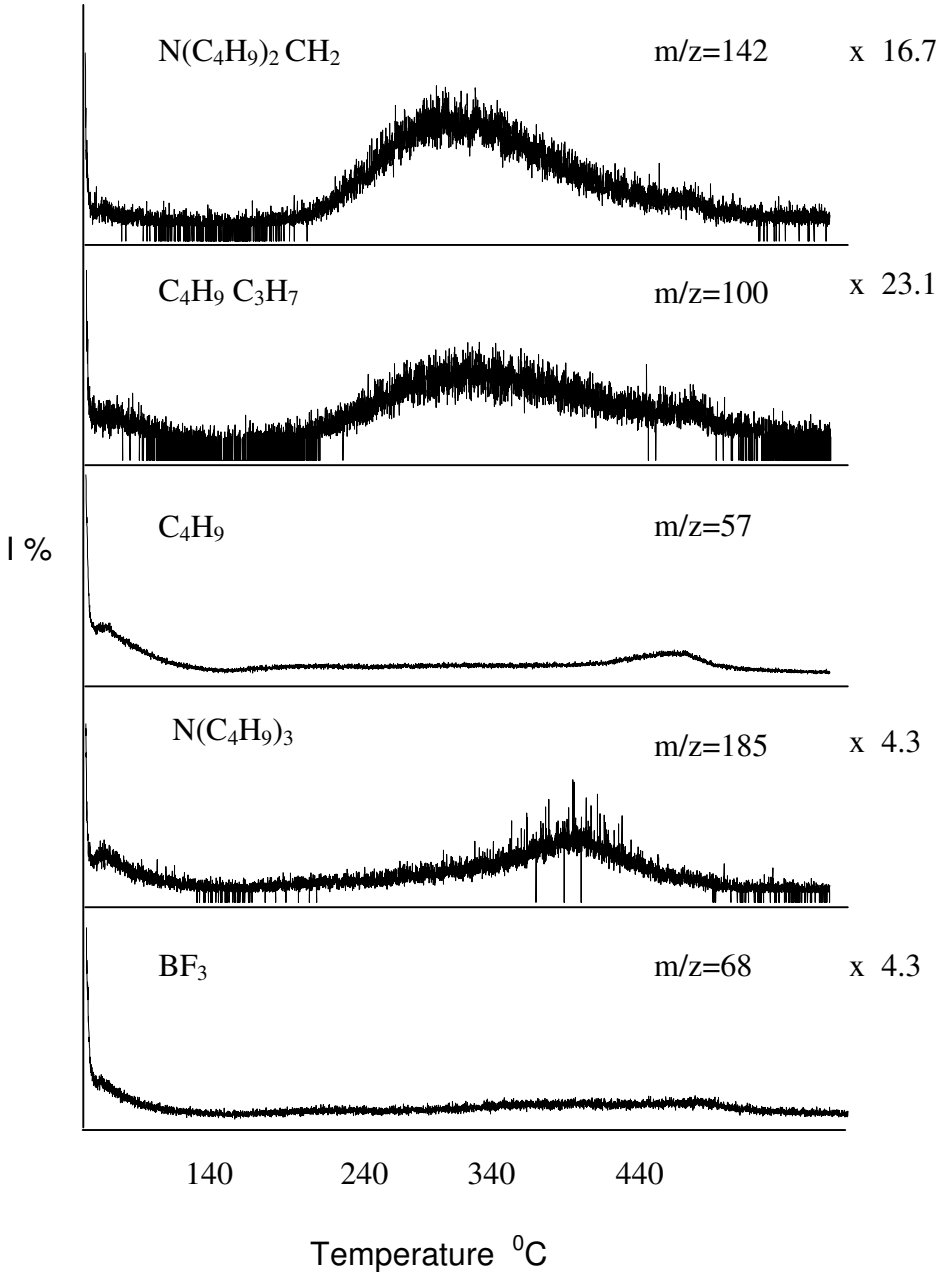

Figure 3.6.b Single ion pyrograms of the ions at m/z 142, 100, 57, 185, 68 Da recorded during pyrolysis of CPPV2

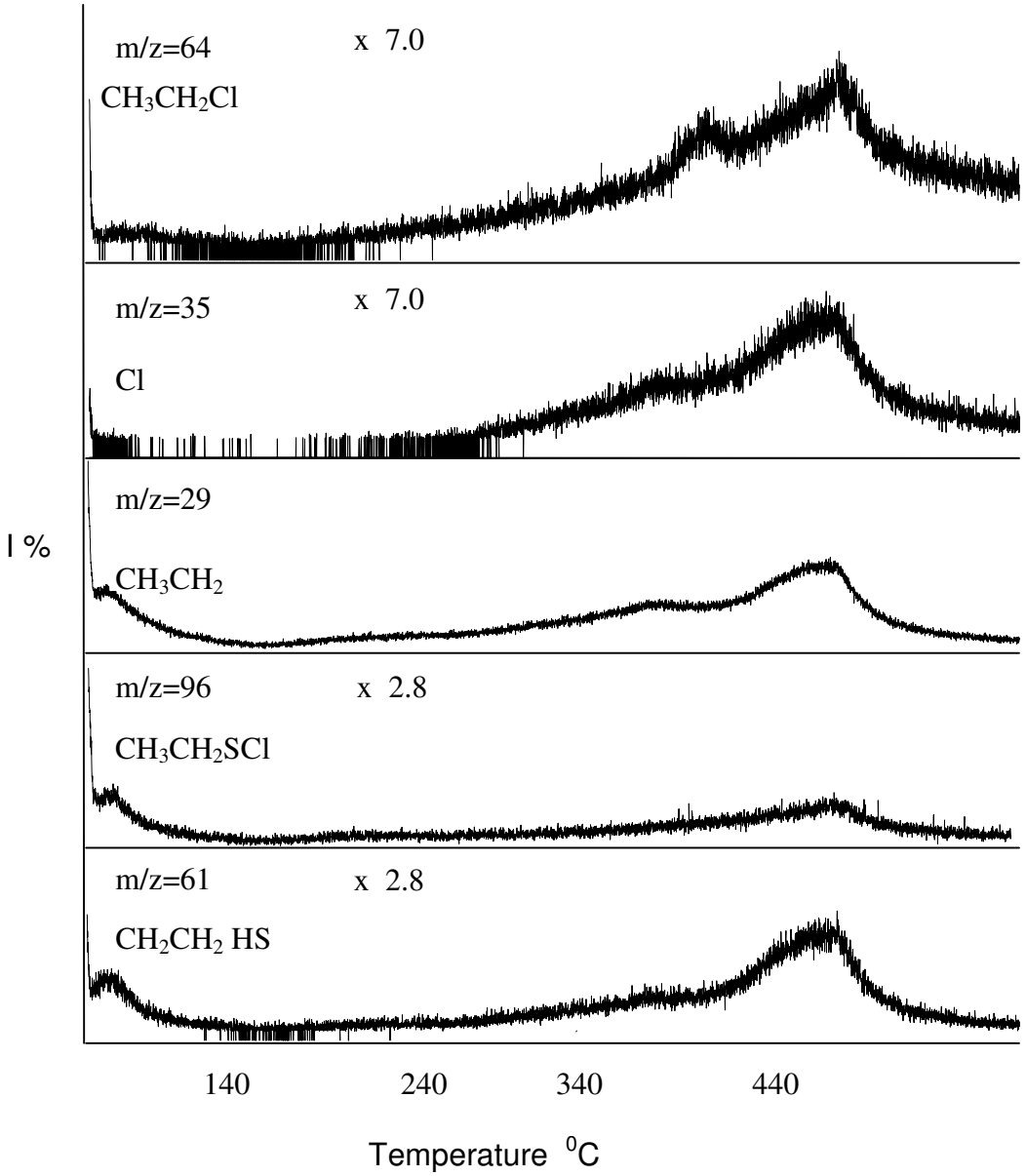

Figure 3.6.c Single ion pyrograms of the ions at m/z 64, 35, 29, 96, 61 Da recorded during pyrolysis of CPPV2

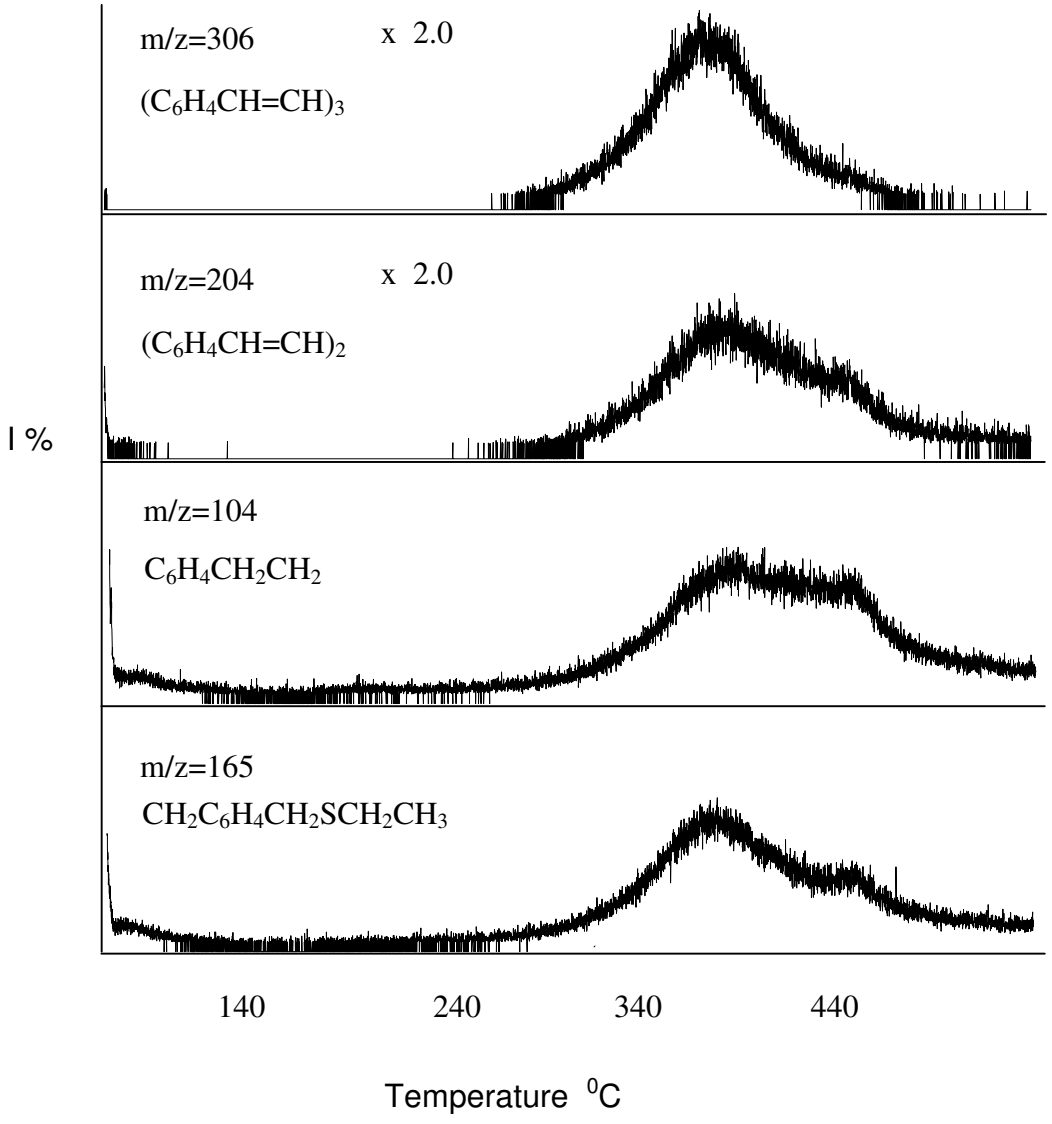

Figure 3.6.d Single ion pyrograms of the ions at m/z 306, 204, 104 and 165 Da recorded during pyrolysis of CPPV2

In Figure 3.6.a, single ion pyrograms of unreacted species C_7H_7 (m/z=91 Da), C_6H_5 (m/z=77 Da), $HSCH_2CH_3$ (m/z=62 Da), $CH_2C_6H_4CH_2Cl$ (m/z=139 Da) gave two maxima around 350 ^{0}C and 440 ^{0}C.

In Figure 3.6.b, evolution profiles of some characteristic species related to supporting electrolyte at m/z 142, 100, 57, 185, 68 Da are shown. Figure 3.6.c single ion pyrograms of some selected ions namely CH_3CH_2Cl indicating , still some contamination inside mass spectrometer. Also, m/z=64 Da due to S_2, m/z=35 Da due to Cl, m/z=29 Da due to CH_3CH_2, m/z=96 Da due to CH_3CH_2SCl, m/z=61 Da due to $HSCH_2CH_2$ are given. These ions generated from the thermal degradation of high molecular weight species.

It can be observed from Figure 3.6.d that evolution profiles of high molecular weight polymeric species such as $(C_6H_4CH=CH)_2$ (m/z=204 Da), $(C_6H_4CH=CH)_3$ (m/z=306 Da), $CH_2C_6H_4CH_2SCH_2CH_3$ (m/z=165 Da) and $C_6H_4CH_2CH_2$ (m/z=104 Da) showes different trends indicating presence of different chains with different thermal stabilities.Inspection of single ion pyrograms indicated that the sample contains various reactants and products with various thermal stabilities. Thus, it can be concluded polymerization reactions continued and relative yield of high molecular weight species increased.

3.A.2.3. CPPV3

Pyrolysis of CPPV3 yielded a total ion curve (TIC), that also indicated a multi-step degradation mechanism. It can be noted from Figure 3.7 that, actually, the evolution of pyrolysis products started at initial stages of pyrolysis and continued throughout the process. Besides the two intense peaks at 350 and 440 ^{0}C, weak peaks with maxima at 270 ^{0}C, were present in the TIC curve. The mass spectrum recorded at the maxima of the TIC curve are also included in the figure. Relative intensities of some of the characteristic and/or intense peaks recorded at 55, 100, 200, 380 ^{0}C and their assignments are collected in Table 3.7.To get a better insight, in Figure 3.7.a, single ion pyrograms of some selected ions, namely $C_6H_4CH_2$ (m/z=90 Da), SCH_3CH_3 (m/z=62 Da), C_4H_3 (m/z=51 Da), $C_6H_4CH_3$ (m/z=91 Da) and C_6H_5 (m/z=77 Da) are shown.

In Figure 3.7.b, single ion pyrograms of some selected ions, namely $C_6H_4CH=CH$ (m/z=102 Da), $(C_6H_4CH=CH)_2$ (m/z=204 Da), $C_6H_4CH_2CH_2$ (m/z=104 Da), and $(C_6H_4CH_2CH_2)_2$ (m/z=208 Da) are shown

Table 3.7 The characteristics and/or intense peaks present in the pyrolysis mass spectra at the maxima of the TIC curves of CPPV3.

m/z	Relatıve Yield				Assigment
	55 ^{0}C	100 ^{0}C	200 ^{0}C	380 ^{0}C	
39	413	355	297	544	C_3H_3
41	599	542	403	726	C_3H_5
55	512	408	328	481	C_4H_7
57	914	518	412	501	C_4H_9
71	569	213	149	167	C_3H_2SH
77	11	143	432	293	C_6H_5
83	346	277	258	273	C_4H_3SH
85	446	189	109	181	C_4H_5SH
96	282	177	134	257	$ClS\ CH_2CH_3$
102				79	$C_6H_4CH=CH$
105	103	99	125	304	$C_6H_4CH_2CH_3$
111	1000	1000	1000	1000	$C_6H_5SH_2$
121	237	312	240	397	$C_6H_3CH_2S$
128	229	135	98	213	$C_6H_7\ CH_2Cl$
149	219	137	172	320	$CH_2CHC_6H_4CH_2S$
178		93	127	370	$C_8H_8{}^{37}Cl_2$
204				100	$(C_6H_4CH=CH)_2$
236			163	83	$(C_6H_4CH_2=CH_2)_2C_2\ H_4$

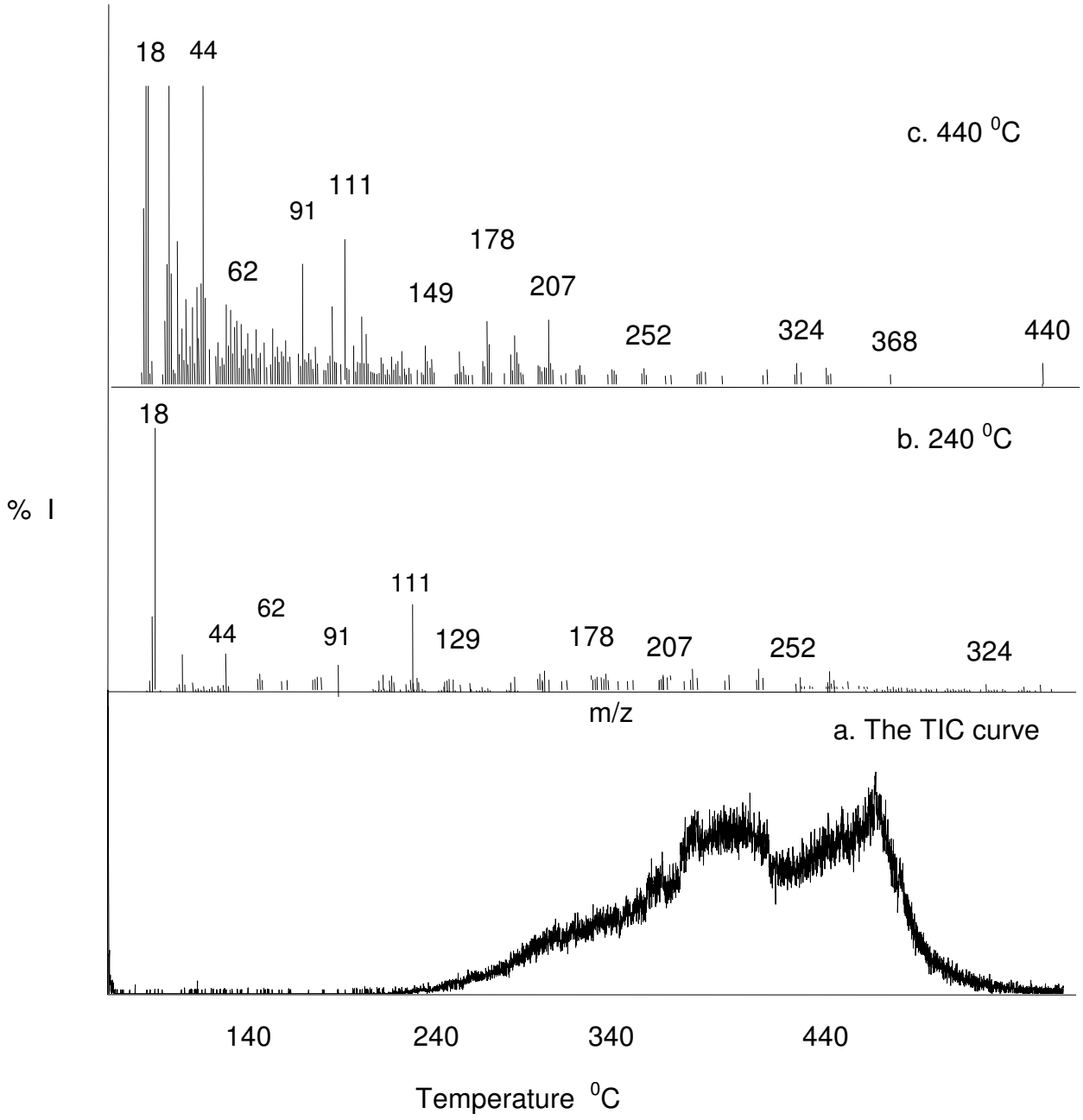

Figure 3.7 Total ion current curve of CPPV3 and the mass spectra recorded at b.240 ^{0}C, c.440 ^{0}C

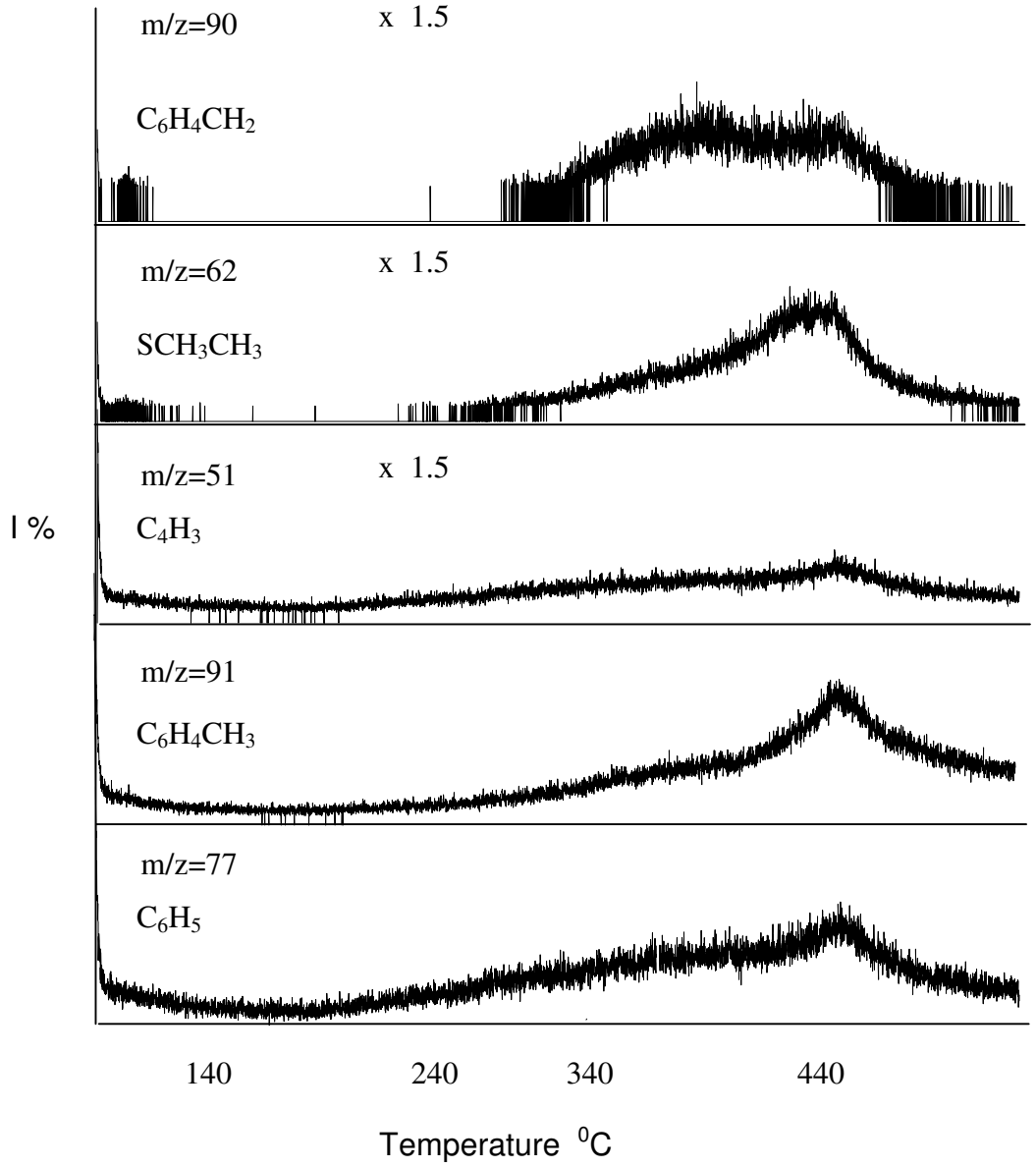

Figure 3.7.a Single ion pyrograms of the ions at m/z 90, 62, 51, 91, 77 Da recorded during pyrolysis of CPPV3.

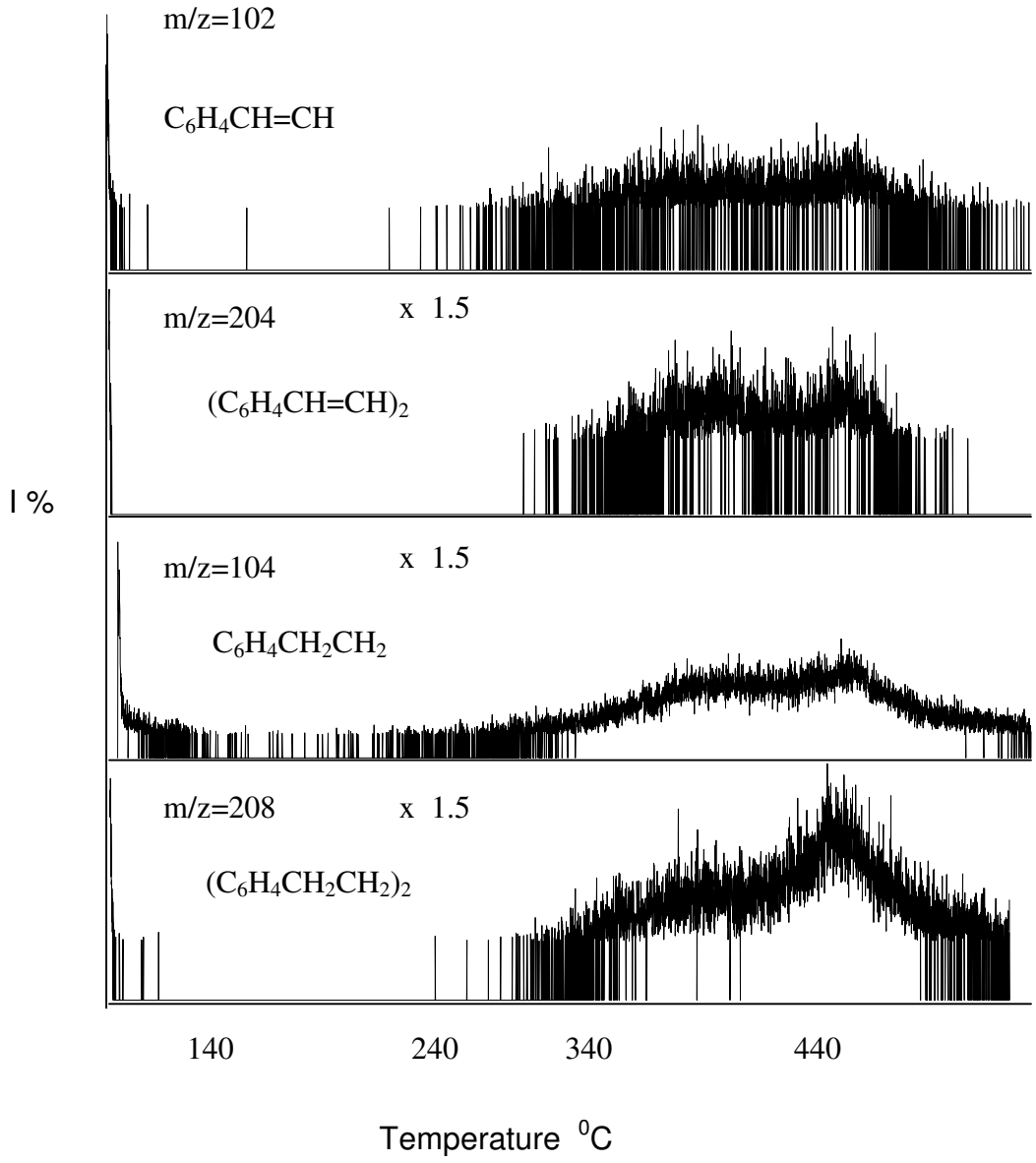

Figure 3.7.b Single ion pyrograms of the ions at m/z 102, 204, 104, 208 Da recorded during pyrolysis of CPPV3.

The TIC curve recorded at the pyrolysis of the CPPV3 is significantly different than those of CPPV2 and CPPV1. Clearly seen in the Figure 3.7 that there is no intense peak below 240 ^{0}C. During pyrolysis of CPPV3 the most abundant fragment has a value of m/z 111Da may readily be attributed to $C_6H_5SH_2$.

Inspection of single ion pyrograms revealed that both high molecular weight polymeric species and low molecular weight degradation products were mainly detected above 240 ^{0}C. Yet, it is clear that their intensities were quite weak.

The TGA data showed that PPV degrades above 550 ^{0}C. Thus, it may be thought that lack of intense peak in the pyrolysis mass spectra was mainly due to high stability of the sample as the maximum attainable only 445 ^{0}C with the present system more than 110 ^{0}C lower than the decomposition temperature of CPPV [40].

PART B. Polyaniline

3.B. Electrochemically Prepared Polyaniline

Thermal degradation of polyaniline has been studied extensively. TGA thermogram of polyaniline revealed three weight losses; at 89 ^{0}C due to the solvent removal and evolution of low molecular weight species, at 146 ^{0}C due to dopant based species, as the main weight loss at 230 ^{0}C.

In this section the thermal degradation behavior of polyaniline (PANI), the effect of dopant namely Cl^-, NO_3^- and SO_4^{2-} and electrochemical synthesis period on structural and thermal characteristics have been studied and discussed. For all the samples studied, three main thermal degradation stages have been recorded. Evolution of low molecular weight species around 50-60 ^{0}C, just above 100 ^{0}C, evolution of dopant based products and at moderate and elevated temperatures evolution of degradation products of the polymer have been occured. In Figure 3.8 the total ion current, TIC, curves of HCl, HNO_3 and H_2SO_4 doped PANI prepared by passing current for 15 minutes are shown. Although all the samples showed mainly three degradation stages, the trends observed in the TIC curves above 100 ^{0}C are significantly different.

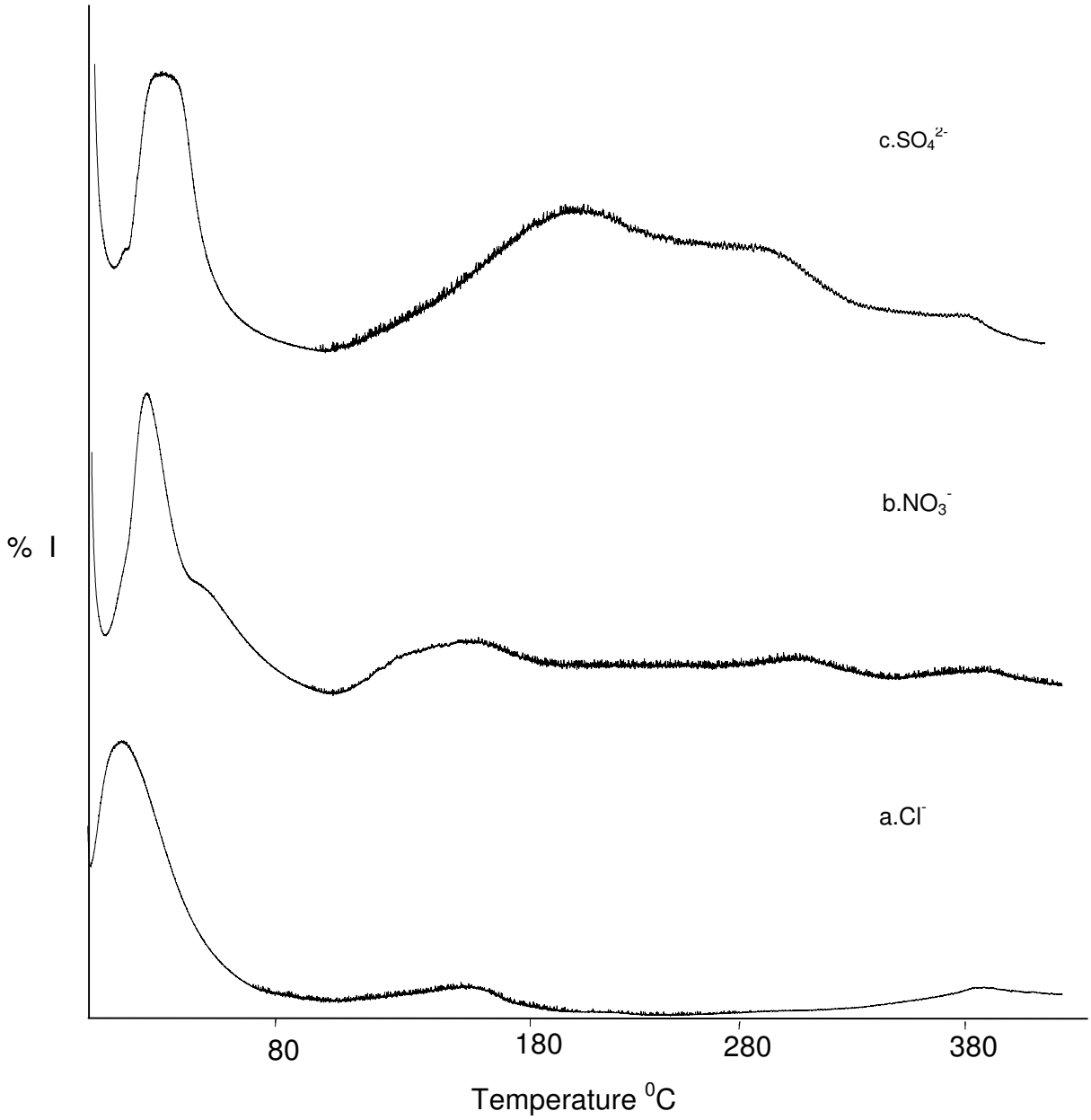

Figure 3.8 Total ion current curve of a. HCl doped polyaniline b. HNO_3 doped polyailine c. H_2SO_4 doped polyaniline.

3.B.1. Hydrochloric Acid Doped PANI

The pyrolysis mass spectra recorded at the peak maxima of the TIC curve of HCl doped PANI is shown in Figure 3.9 and the relative intensities of characteristic peaks in these samples are collected in Table 3.8.

It is clear that the low temperature evolutions are mainly due to the adsorbed dopant HCl yielding peaks at m/z= 35, 36, 37 and 38 Da due to ^{35}Cl, $H^{35}Cl$, ^{37}Cl, $H^{37}Cl$ respectively and peaks at m/z= 93, 77, 66 and 51 Da due to $C_6H_5NH_2$, the monomer, C_6H_5, C_5H_6 or C_4H_3NH, and C_4H_3 respectively and at m/z=18, and 17 due to H_2O, and OH respectively. The monomer based peaks at low temperatures were more abundant indicating presence of unreacted monomer. The mass spectrum of aniline shows only few peaks due to the stability of the aromatic structure. The base peak is the molecular ion at m/z= 93 Da. There are only three other peaks that have more than 10% relative abundance, namely, the peaks at m/z= 66 (RI=32%) due to C_4H_3NH, 65 Da (RI=16%) due to C_5H_5 and 39 Da (RI=13%) due to C_3H_3 respectively. For the HCl doped PANI, as the relative abundances of peaks at m/z= 93 and 66 Da are quite similar to that of pure aniline, it can be concluded that at early stages of pyrolysis evolution of unreacted aniline has occured. Around 200 ^0C the yield of dopant increased significantly. Furthermore, in the pyrolysis mass spectra recorded around this temperature, the relative intensity of the peak at m/z= 77 Da due to C_6H_5 increased three fold although that of the monomer decreased significantly. Thus, it is clear that peak at m/z= 77 Da was not only due to anilline but also due to some other subtances yielding C_6H_5 fragment during thermal degradation and/or ionization inside the mass spectrometer. Such a trend can be associated with degredation of high molecular weight species yielding phenyl ring. Thus, it can be concluded that low molecular weight oligomers also decomposed at this temperature range. In the final stage of pyrolysis presence of oligomer peaks indicated decomposition of the polymer itself.

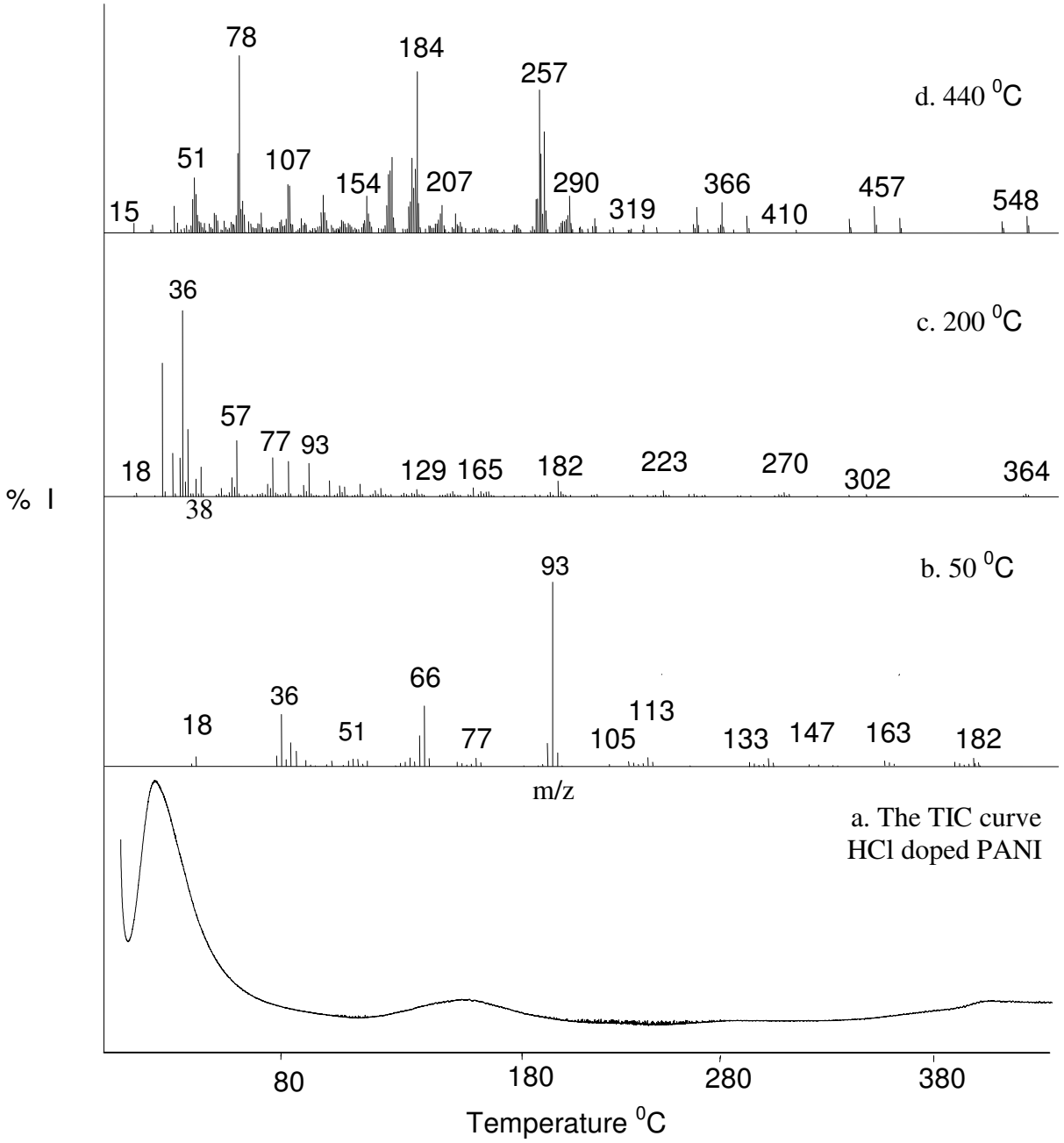

Figure 3.9 Total ion current curve of a. HCl doped polyaniline and the mass spectra recorded at b.50 ^{0}C, c.200 ^{0}C, d.440 ^{0}C.

Table 3.8 The characteristics and/or intense peaks present in the pyrolysis mass spectra at the maxima of the TIC curves of HCl doped polyaniline .

m/z	Relative Yield			Assigment
	50 ^{0}C	200 ^{0}C	440 ^{0}C	
35	54	196		^{35}Cl
36	291	1000		$H^{35}Cl$
38	130	344		$H^{37}Cl$
39	89		163	C_3H_3
66	321			C_4H_4N
77	50	192	480	C_6H_5
78	50		1000	C_6H_6
91		7	113	C_6H_5N
92		13	35	C_6H_5NH
93	1000	73		monomer
108			287	$H_2NC_6H_4NH_2$
128			231	$C_6H_5C_4H_3$
154			229	$C_6H_5C_6H_5$
169			447	$C_6H_5NHC_6H_5$
181			419	$C_6H_4NC_6H_4NH$
184		7	886	dimer
257			740	$C_6H_5NC_6H_4NC_6H_4$
275			261	trimer
351			138	tetramer-NH
366			176	tetramer
457			180	pentamer
548			129	hexamer

.

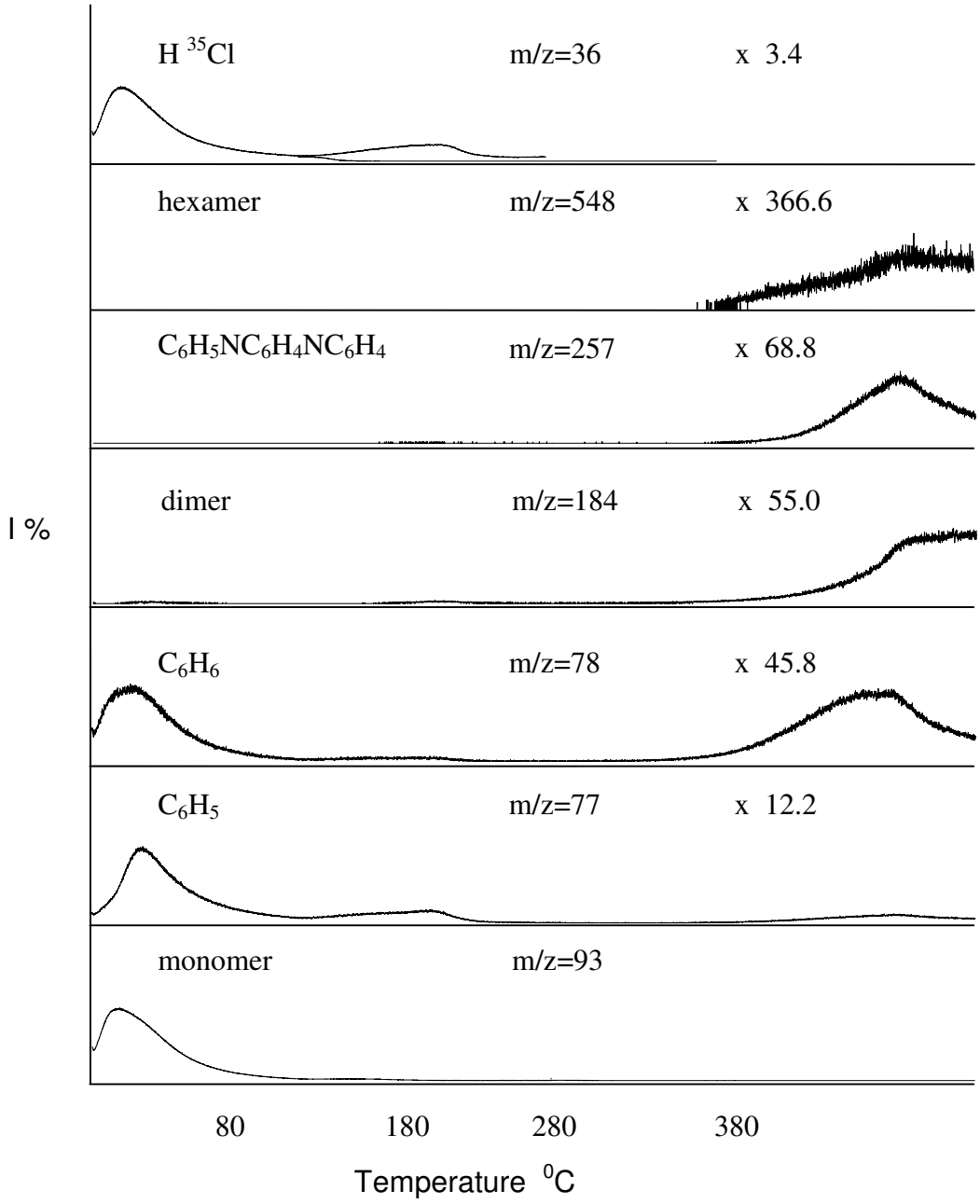

Figure 3.9.a Single ion pyrograms of the ions at m/z 36, 548, 257, 184, 78, 77, 93 Da recorded during pyrolysis of HCl doped polyaniline .

The single ion pyrograms of some selected products namely H ^{35}Cl (m/z=36 Da), hexamer (m/z=548 Da), $C_6H_5NC_6H_4NC_6H_4$ (m/z=257 Da), dimer (m/z=184 Da), C_6H_6 (m/z=78 Da), C_6H_5 (m/z=77 Da), monomer (m/z=93 Da) are shown in Figure 3.9.a. It can be observed from the evolution profiles that aniline and dopant evolution occured at the first two degradation stages whereas, degradation of the polymer yielding mainly oligomers occured in the final stage of pyrolysis. It can also be observed from the single ion pyrograms that C_6H_6 (m/z= 78 Da) and $C_6H_5NC_6H_4NC_6H_4$ (m/z= 257 Da) fragments showed identical trends. Then, it may be thought that during the pyrolysis hydrogen transfer from NH group to the phenyl generates benzene.

3.B.1.1.The Effect of Reaction Period

The samples prepared by electrolysis for 30 and 75 minutes showed quite similar pyrolysis behavior. In Figure 3.10 the TIC curve and the pyrolysis mass spectra recorded at the maxima of the peaks present in the TIC curve of the sample obtained by electrolysis for 75 minutes are shown. The only difference that can be noticed was the increase in the amount of characteristic peaks of aniline around 200 ^{0}C. This temperature range was too high for evolution of monomer adsorbed on the polymer sample. Thus, it can be concluded that as the film thickness increases the amount of unreacted monomer adsorbed in the bulk of the polymer also increases. The single ion pyrograms of the products for these samples also showed identical behaviors with those of the sample prepared by electrolysis for 15 minutes.

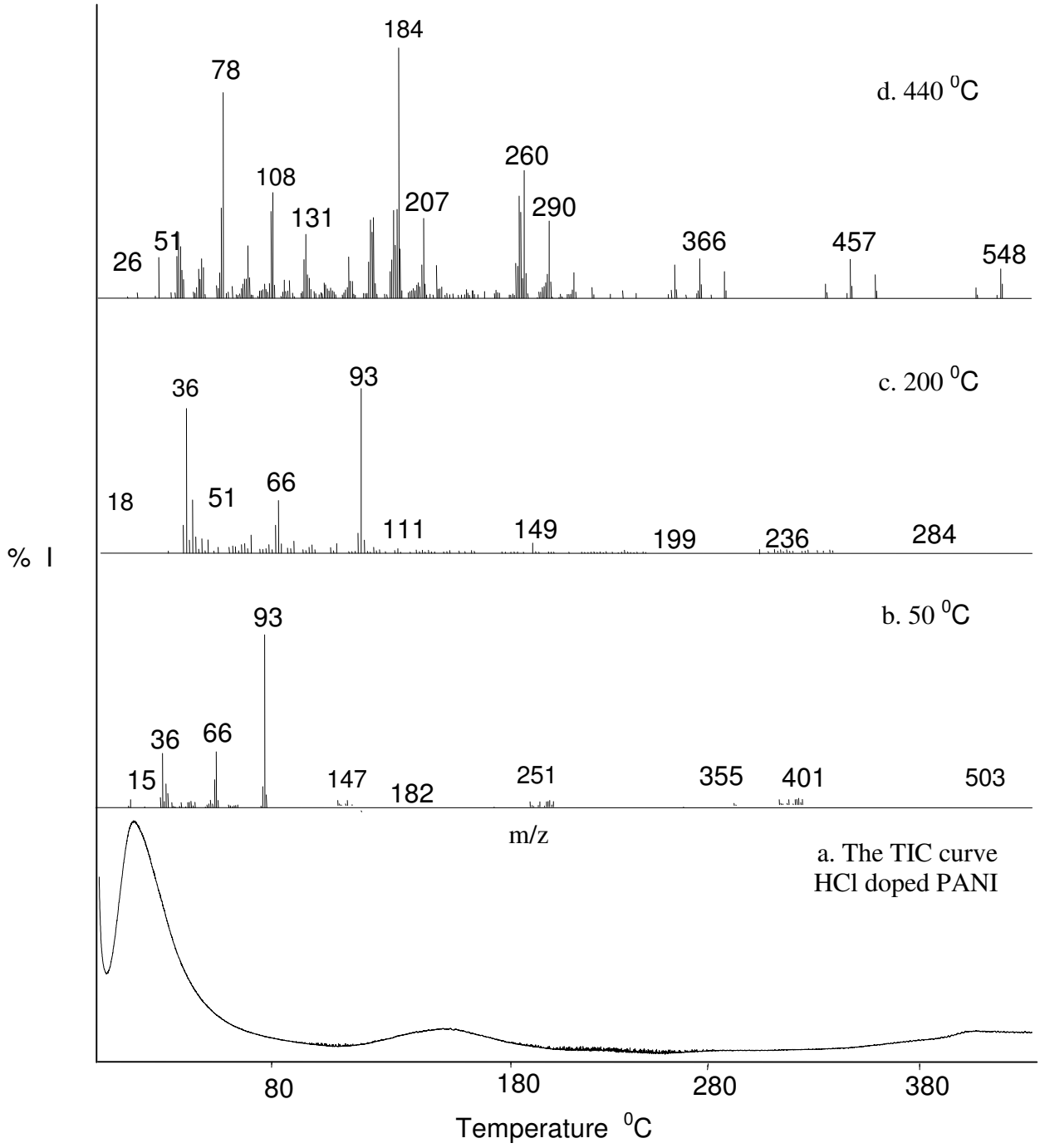

Figure 3.10 Total ion current curve of a. HCl doped polyaniline prepared by 75 minutes electrolysis and the mass spectra recorded at b.50 ^{0}C, c.200 ^{0}C, d.440 ^{0}C.

3.B.2.Nitric Acid Doped PANI

The TIC curve of HNO_3 doped PANI is given Figure.3.11. The pyrolysis mass spectra recorded at 50, 200, 440 ^{0}C are also included in Figure.3.11.

In Figure 3.11.a. the evolution profiles (single ion pyrograms) of some characteristic and intense products namely hexamer (m/z=548 Da), $C_6H_5NC_6H_4NC_6H_4$ (m/z=257 Da), dimer (m/z=184 Da), $C_5H_5NO_2$ (m/z=111 Da), C_6H_6 (m/z=78 Da), C_6H_5 (m/z=77 Da), monomer (m/z=93 Da), NO_2 (m/z=46 Da) from NO_3^- doped PANI are shown. The products attributed to $C_6H_5NC_6H_4NC_6H_4$ (m/z=257 Da), dimer (m/z =184 Da) and C_6H_5 (m/z=77 Da) showed similar trends as can be noted from Figure 3.11.a.

For HNO_3 doped PANI, at initial and moderate stages of pyrolysis, intense peaks at m/z=111 and 139 Da may be attributed to formation of nitroaniline. Fragments involving NO_3 and NO_2 groups degraded around 200 ^{0}C. Furthermore presence of intense CO_2 peak at elevated temperatures indicated oxidation of phenyl ring.

The trends observed in the single ion pyrograms of oligomer peaks are identical to those recorded from HCl doped PANI. Yet, the relative intensities of oligomer based peaks decreased significantly at elevated temperatures. Thus, it may be proposed that upon NO_2 substitution and oxidation of phenyl ring polymerization reactions were poisened.

Relative intensities of some of the characteristic and/or intense peaks recorded at 50, 200, 440 ^{0}C and their assignments are also given in Table 3.9.

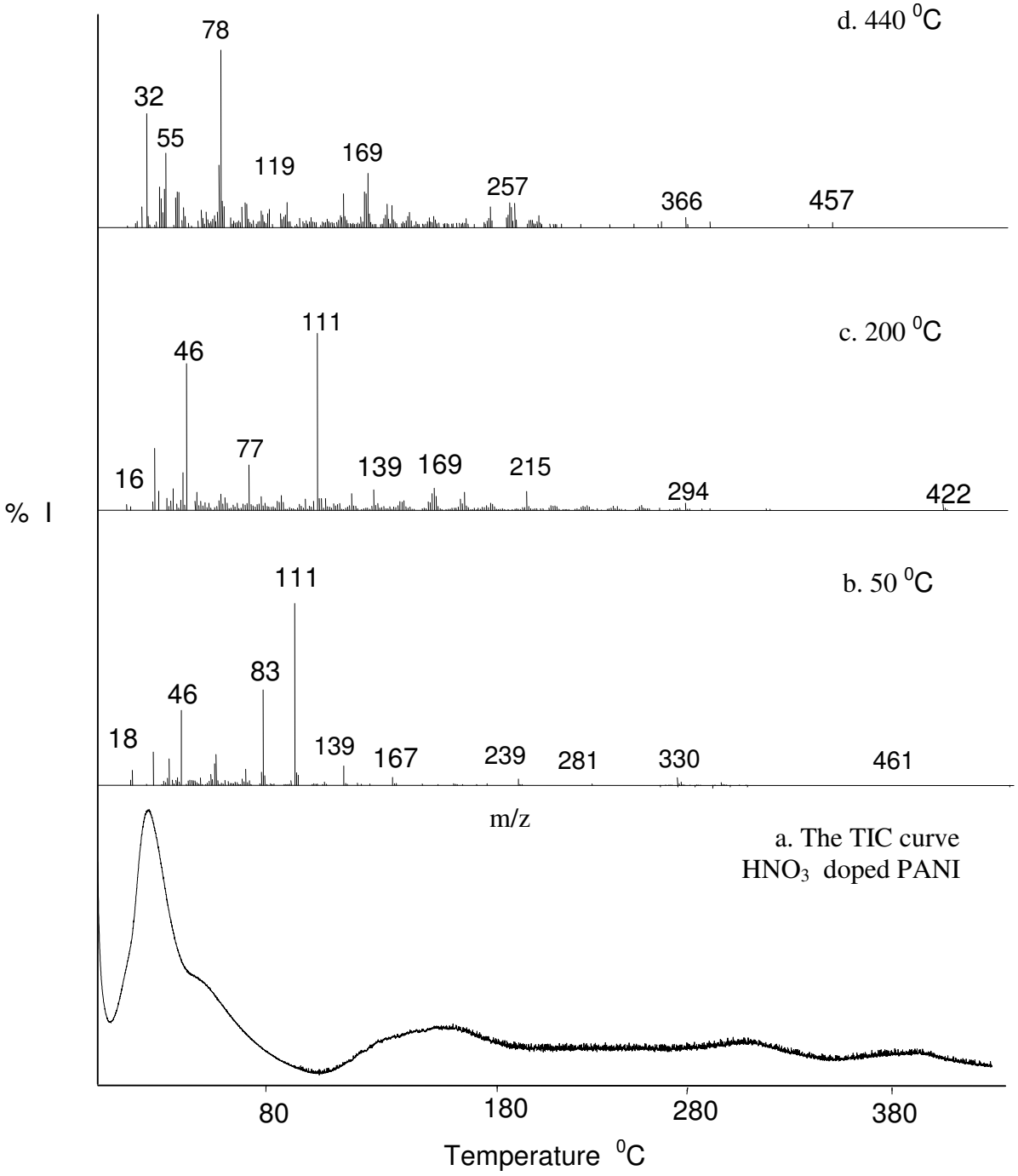

Figure 3.11 Total ion current curve of a. HNO_3 doped PANI prepared by 15 minutes electrolysis and the mass spectra recorded at b.50 ^{0}C, c.200 ^{0}C, d.440 ^{0}C.

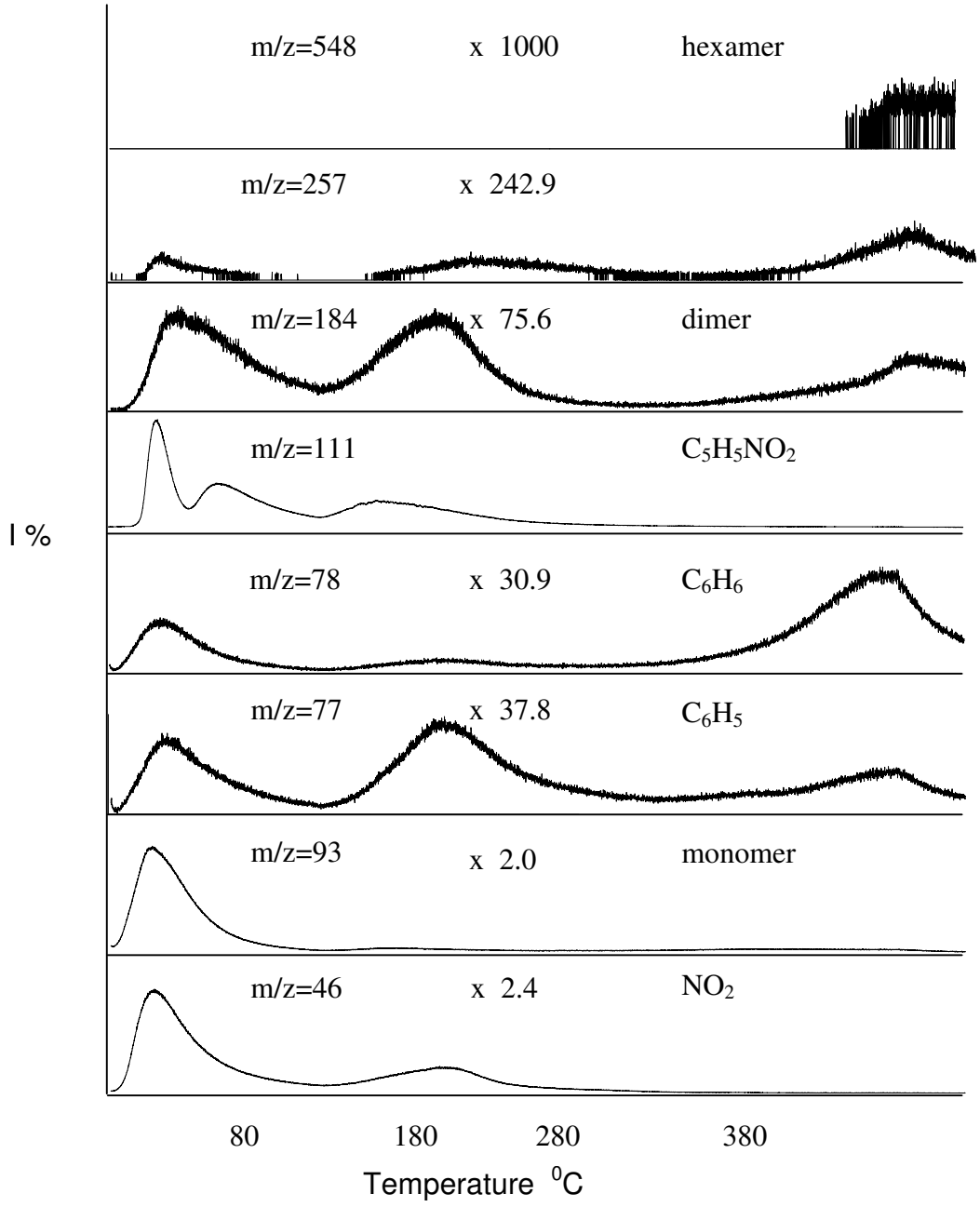

Figure 3.11.a Single ion pyrograms of the ions at m/z 548, 257, 184, 111, 78, 77, 93, 46 Da recorded during pyrolysis of HNO_3 doped polyaniline .

Table 3.9 The characteristics and/or intense peaks present in the pyrolysis mass spectra at the maxima of the TIC curves of HNO_3 doped polyaniline .

m/z	Relative Yield			Assigment
	50 ^{0}C	200 ^{0}C	440 ^{0}C	
28			464	N_2, CO
32			566	O_2
30	185	411		NO
44		259	512	CO_2
46	412	1000		NO_2
66	168		139	C_4H_4N
78	17	33	1000	C_6H_6
91	10	51	156	C_7H_7, C_6H_5NH
92	73	75	11	C_6H_5NH
93	523	92	163	monomer $C_6H_5NH_2$
108		18	109	$H_2NC_6H_4NH_2$, C_6H_5NOH
111	1000	881		$C_5H_5NO_2$
128		78	22	$C_6H_5C_4H_3$
139	111	87	15	$C_6H_5NO_3$, $HOC_6H_4NO_2$
167	41	70	191	$C_6H_4NHC_6H_4$
169		130	418	$C_6H_5NHC_6H_5$
181		23	134	$C_6H_4NC_6H_4NH$
184		122	121	dimer
199		6	54	$(C_6H_5NH_2)_2CH_3$
215		125		$NH_2C_6H_4C_6H_5NO_2$
257		17		$C_6H_5NC_6H_4NC_6H_4$
275			66	trimer
366			38	tetramer
457			39	pentamer
548			21	hexamer

3.B.2.1.The Effect of Reaction Period

The samples prepared by electrolysis for 30 and 75 minutes showed significant differences for HNO_3 doped PANI. In Figure 3.12, the TIC curve and the pyrolysis mass spectra recorded at the maxima of the peaks present in the TIC curve of HNO_3 doped PANI prepared by electrolysis for 75 minutes are shown. The nitroanilline peak increased significantly at initial stages. Around 250 ^{0}C, peaks at m/z= 215 Da due to $NO_2C_6H_4NHC_6H_5$ and at m/z=44 Da due to CO_2 was recorded. In the final stage of pyrolysis evolution of CO_2 and benzene and $C_6H_5NHC_6H_5$ was significant. Thus, it can be concluded that NO_3^- reacts with aniline during the electrochemical synthesis. As the reaction period increases NO_2 substitution becomes more effective and polyaniline formation was poisoned. Furthermore, extent of oxidation of the phenyl ring was also increased significantly. Single ion evolution profiles, as shown in Figure 3.12.a, confirms above discussions.

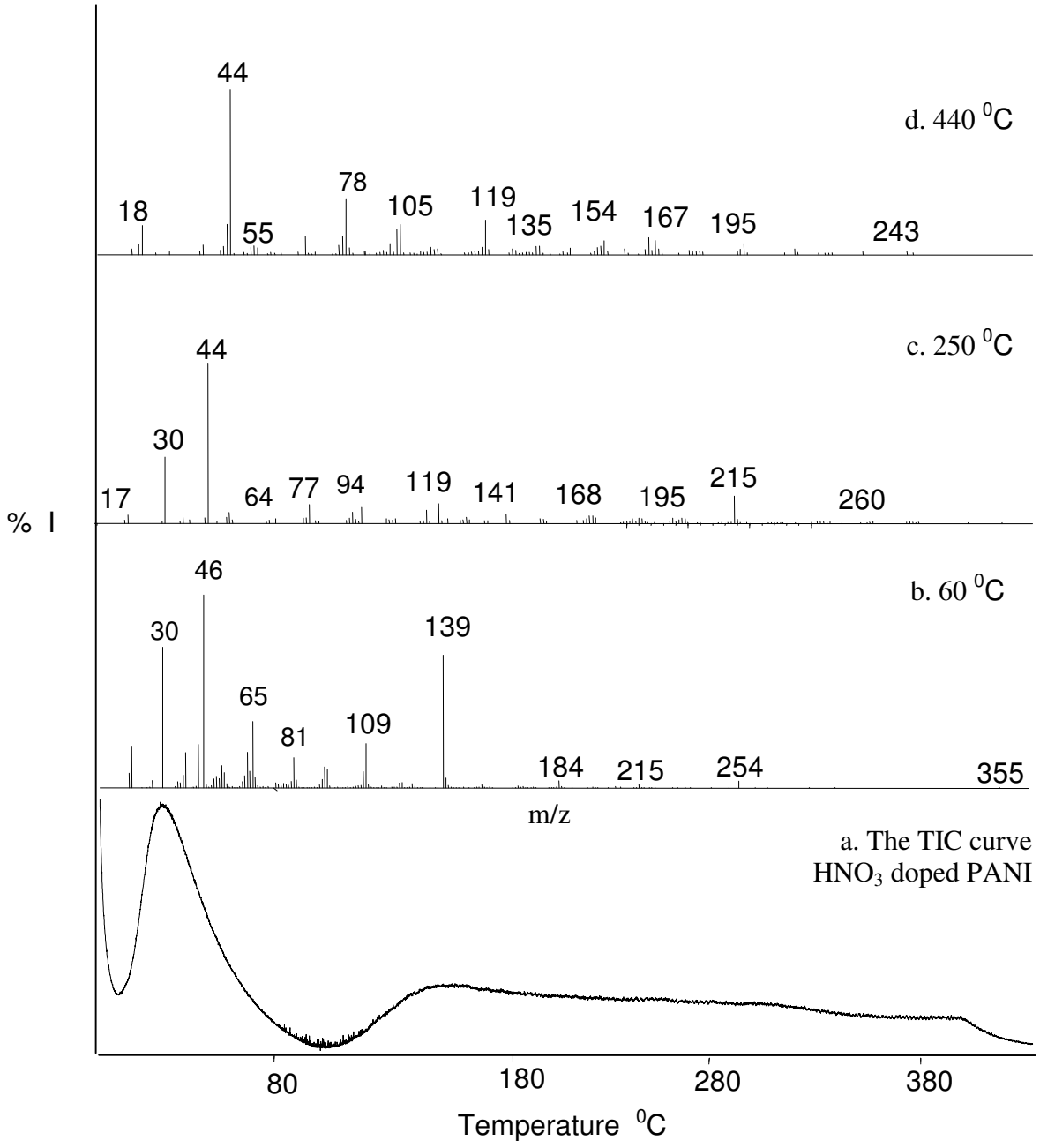

Figure 3.12 Total ion current curve of a. HNO_3 doped PANI prepared by 75 minutes electrolysis and the mass spectra recorded at b.60 ^{0}C, c.250 ^{0}C, d.440 ^{0}C.

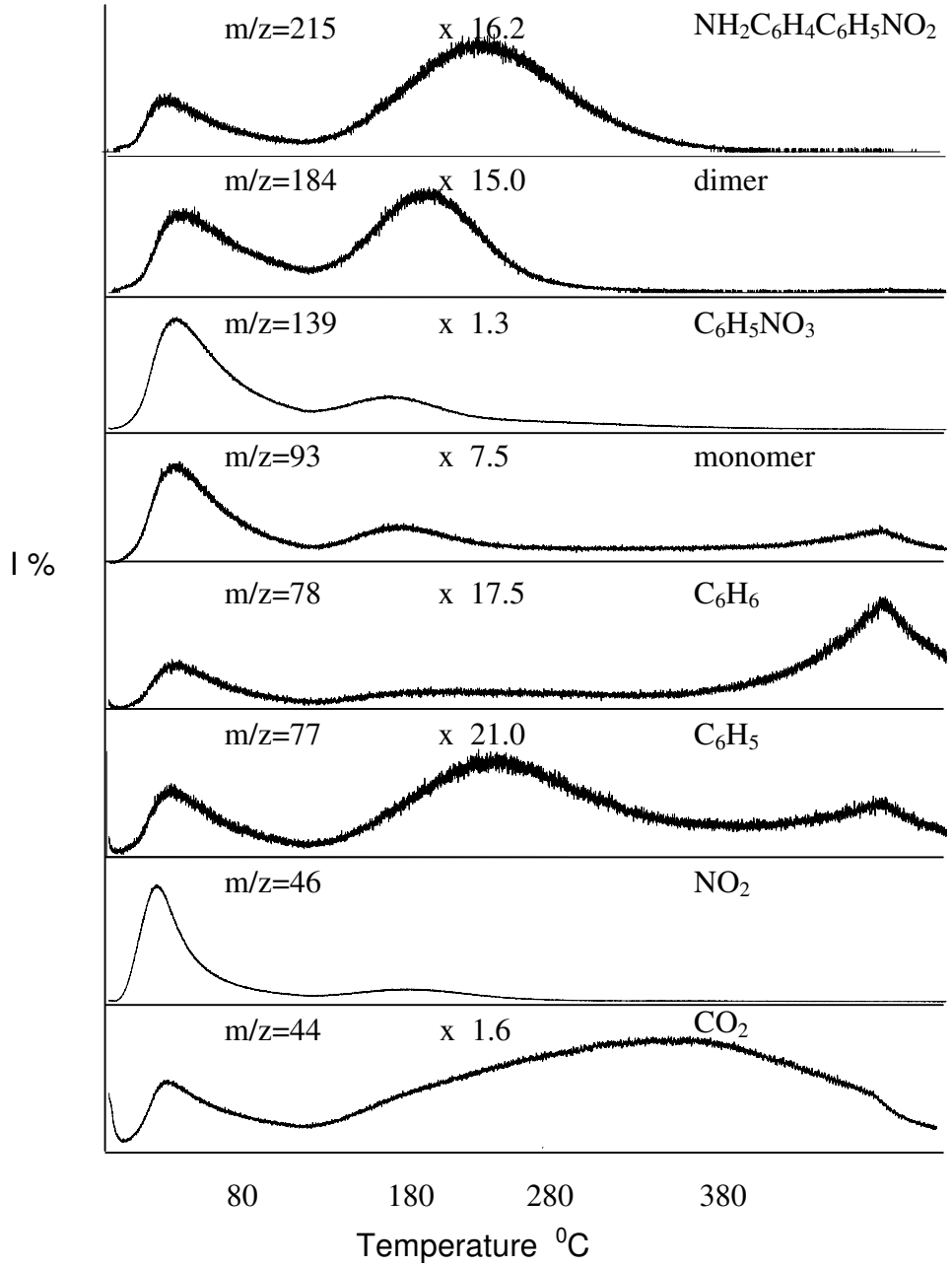

Figure 3.12.a Single ion pyrograms of the ions at m/z 215, 184, 139, 93, 78, 77, 46, 44 Da recorded during pyrolysis of HNO_3 doped polyaniline prepared by pyrolysis for 75 minutes.

3.B.3.Sulfuric Acid Doped PANI

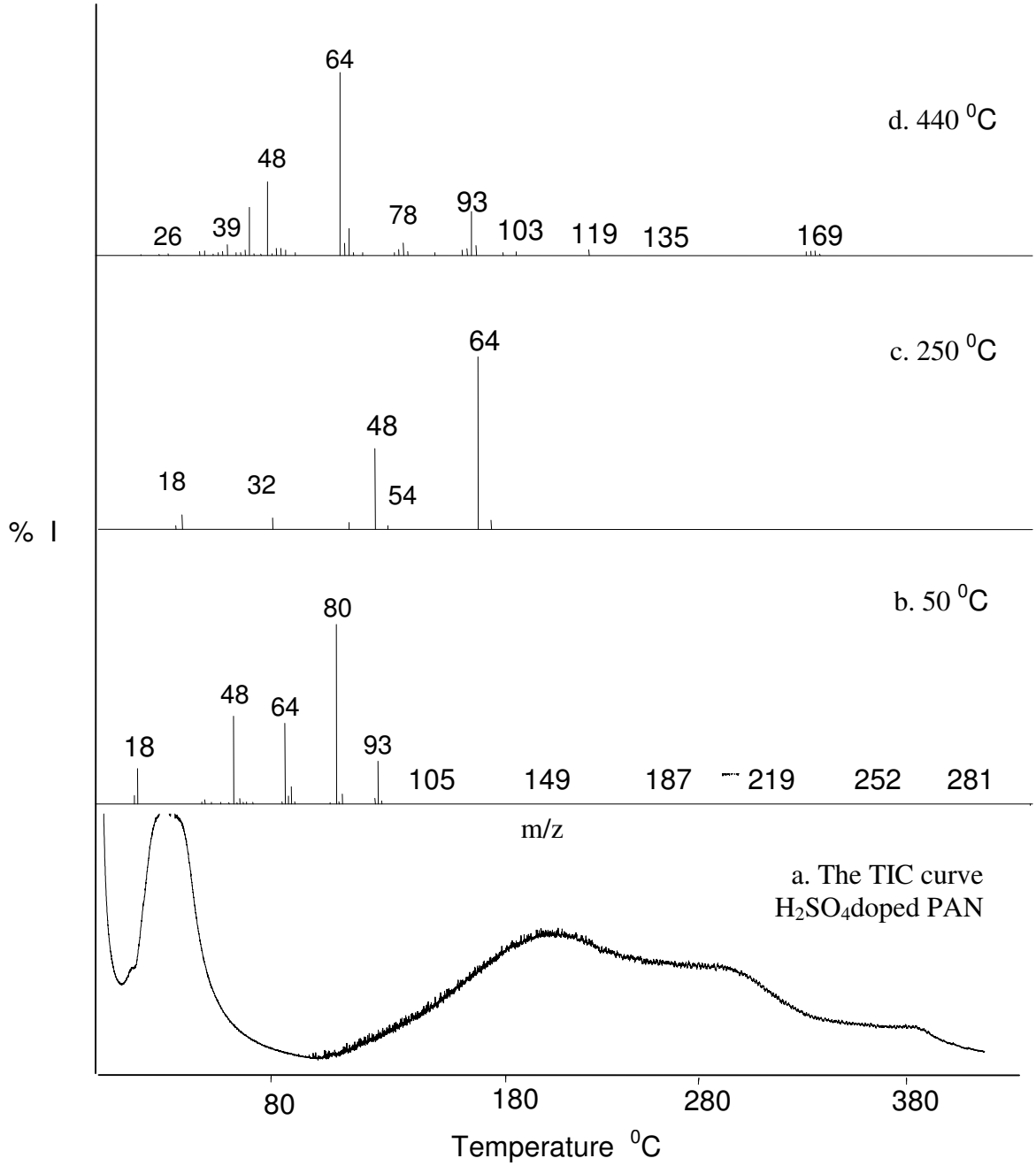

Figure 3.13 Total ion current curve of a. H_2SO_4 doped PANI prepared by 15 minutes electrolysis and the mass spectra recorded at b.50 ^{0}C, c.250 ^{0}C, d.440 ^{0}C.

The total ion current (TIC) curve recorded during the pyrolysis of H_2SO_4 doped PANI prepared by 15 minutes electrolysisis shown in Figure 3.13 together with the mass spectra at the maxima of the TIC curve.

Dopant based peaks were much more abundant for this sample compared to HCl and HNO_3 doped PANI's. Futhermore, although the evolution of SO and SO_2 showed similar trends, SO_3 followed quite a different path. Unlike Cl^- and NO_3^- doped polymer samples, the evolution of monomer, aniline was recorded even at elevated temperatures. Another point that should be noticed was the very low oligomer yield.

Evolution profiles of some products, namely $C_6H_5NHC_6H_5$ (m/z=169 Da), C_6H_6 (m/z=78 Da), C_6H_5 (m/z=77 Da), monomer (m/z=93 Da), SO_3 (m/z=80 Da), SO (m/z=48 Da) are shown in Figure 3.13.a and in Table 3.10 the relative intensities of intense and/or characteristic peaks present in the pyrolysis mass spectra are summarized.

Evolution of SO_2 and CO_2 at elevated temperatures can also be attributed to reactions of dopant with the phenyl ring as in case of HNO_3 doped polyaniline.

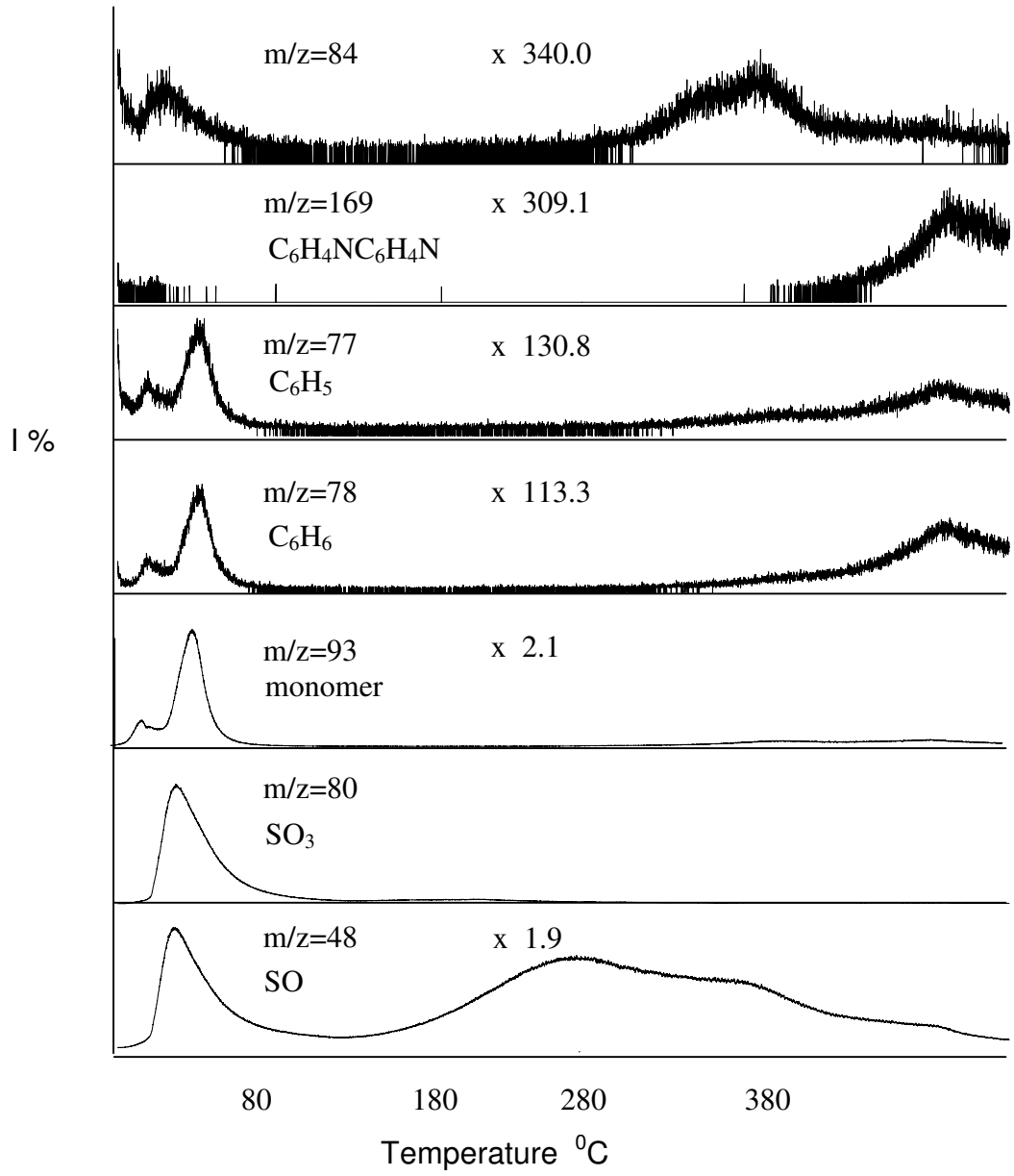

Figure 3.13.a Single ion pyrograms of the ions at m/z 84, 169, 78, 77, 93, 80, 48 Da recorded during pyrolysis of H_2SO_4 doped polyaniline .

Table 3.10 The characteristics and/or intense peaks present in the pyrolysis mass spectra at the maxima of the TIC curves of H_2SO_4 doped polyaniline.

m/z	Relative Yield			Assigment
	60 ^{0}C	200 ^{0}C	440 ^{0}C	
44	9	39	208	CO_2
48	496	472	395	SO
64	444	1000	1000	SO_2
66	50	50	98	S_2H_2
77			22	C_6H_5
78			42	C_6H_6
80	1000			C_5H_6N
91			18	C_6H_5N
92			26	C_6H_5NH
93	251		165	monomer
169			12	$C_6H_4NC_6H_4NH$
207			6	

III.B.3.1.The Effect of Reaction Period

The samples prepared by electrolysis for 30 and 75 minutes showed no significant differences for H_2SO_4doped PANI. In Figure 3.14 the TIC curve and the pyrolysis mass spectra recorded at the maxima of the peaks present in the TIC curve of the sample prepared by electrolysis for 75 minutes are shown. The only difference that can be noted is the increase in relative intensities of dopant based peaks.

Pyrolsis analysis of HCl, HNO_3 and H_2SO_4 doped PANI samples indicated that both NO_3^- and SO_4^{2-} reacted with the monomer and subsutitution and oxidation of aniline have occured.

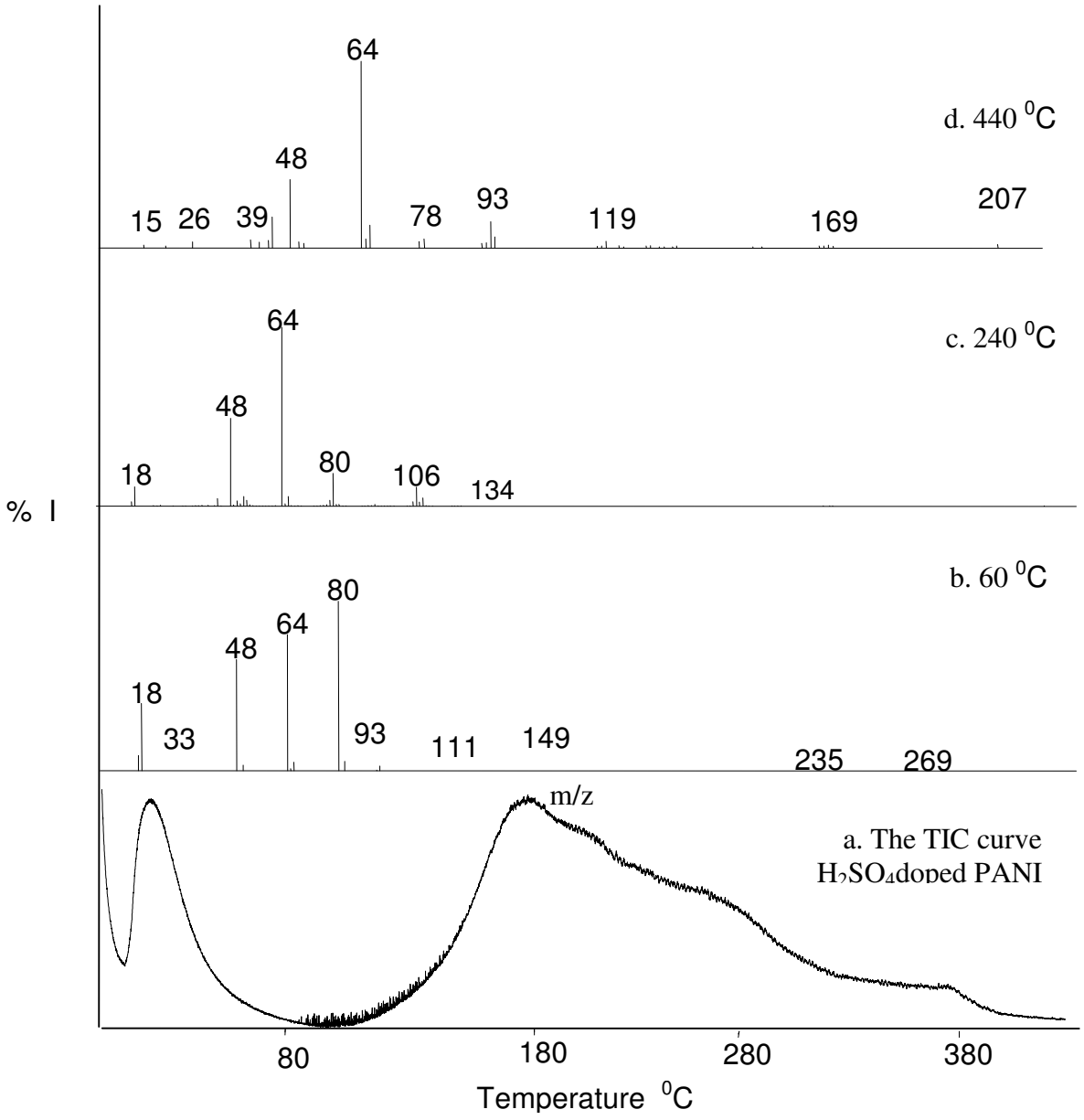

Figure 3.14 Total ion current curve of a. H_2SO_4 doped PANI prepared by 75 minutes electrolysis and the mass spectra recorded at b.60 ^{0}C, c.240 ^{0}C, d.440 ^{0}C.

CHAPTER 4

CONCLUSIONS

In this work, direct insertion probe pyrolysis mass spectrometry technique was used to perform the thermal and the structural characterization of poly(paraphenylene vinylene) and polyaniline.

The poly(paraphenylene vinylene) samples were prepared both electrochemical and chemical polymerization techniques. In order to investigate the reactions taking place and the intermediates, pyrolysis mass spectrometry analysis were repeated for samples obtained at certain periods of both electrochemical and chemical polymerization processes. Thus, pyrolysis of the samples

i.dried at 30 ^{0}C for two hours (EPPV1, CPPV1),
ii.heated further to 245 ^{0}C for 3 hours (EPPV2, CPPV2),
iii. heated further at 245 ^{0}C for 3 more hours (EPPV3, CPPV3).

were carried.

It has been determined that during both the monomer and the polymer preparation processes, the purification of the products from the unreacted starting materials and solvent was impossible. Thus, all the samples under investigation contained significant amounts of low molecular weight unreacted materials. Similar products were recorded for both chemically and electrochemically prepared samples. Yet, pyrolysis studies indicated that during the chemical synthesis a more uniform sample can be obtained.

The impurities observed for electrochemically synthesized sample, mainly the reactants, most propably adsorbed in the bulk during the growth of the polymer on the electrode surface. The multi-step degradation recorded was mainly due to the evolution of species with different thermal stabilities.

In general, for both electrochemically and chemically prepared PPV samples, at initial stages of heating, below 100 ^{0}C, desorption of unreacted monomer, solvent or any other low molecular weight species adsorbed on the polymer film were recorded. Products related to supporting electrolyte were detected in the temperature range of 200-350 ^{0}C for the electrochemically prepared sample. In the temperature range of 280-400 ^{0}C, products due to the thermal degradation of high molecular weight compounds, such as oligomers were observed. In the final step of pyrolysis, decomposition of the polymer backbone was observed. Again for both samples, the pyrolysis mass data indicated the presence of polymer chains with different structures.

In the second part of the study, thermal characteristic, thermal decomposition mechanism and degradations products of polyaniline were investigated. Three diffrent dopant and three different electrolysis periods were used to investigate the effect of dopant and the effect of electrochemical synthesis period.

According to TIC curves and evolution profiles of fragments, three main thermal degradation stages have been recorded; evolution of low molecular weight species, evolution of dopant based products and evolution of degradation products of polymer itself. The low molecular weight oligomers also decomposed around 200 ^{0}C in case of HCl doped PANI. In the final stage of pyrolysis presence of high molecular weight oligomer peaks indicated decomposition of the polymer.

For HNO_3 and H_2SO_4 doped PANI samples significant changes in pyrolysis products have been determined. The trends observed in the single ion pyrograms of oligomer peaks recorded from HNO_3 doped PANI are identical to those recorded from HCl doped polyaniline. Yet, their relative intensities were drastically weak for HNO_3 and

H_2SO_4 doped PANI. In case of H_2SO_4 doped PANI, dopant based peaks were much more abundant while those related to oligomers were even weaker than those recorded for HNO_3 doped PANI. It is clear that for these samples reactions between dopant and monomer/and/or polymer have taken places, yielding oxidized and/or substituted phenyl rings. Under these conditions polymerization reactions were poisened.

HCl doped PANI samples prepared by 30 and 75 minutes electrolysis showed quite similar pyrolysis behavior. On the other hand, the film thickness increases the amount of unreacted monomer adsorbed in the bulk of the polymer also increases.

HNO_3 doped PANI.samples prepared by 30 and 75 minutes electrolysis showed more significant differences. Pyrolysis study showed that dopant reacts with aniline during electrochemical synthesis as the reaction period increases NO_2 substitution of the phenyl ring became more effective and polyaniline formation was poisened as the electrolysis was continued for longer time periods.

H_2SO_4 doped PANI samples prepared by different electrolysis time showed more similar behavior as HCl doped PANI. No significant change in thermal and structural charectistics of polymer was noted for H_2SO_4 doped PANI when electrolysis time was increased from 15 to 75 minutes.

REFERENCES

1. G.Inzelt, M.Pineri, J.W.Schultze, M.A.Vorotyntsev,Electrochimica Acta 45, **2000**, 2403-2421.

2. C. K. Chiang, C. R. Fincher, Jr., Y. W. Park, A. J. Heeger, and H. Shirakawa, E. J. Louis ,S. C. Gau, Alan G. Macdiarmid, Phys. Rev. Letters, 39, **1977**, 17.

3. J.Jagur-Grodzinski,Polym.Adv.Technol. 13, **2002** , 615-625.

4. J.L. Bredas, G.B.Street, Acc. Chem. Res., 18, **1985** , 309-315.

5. Y. Furukawa, J. Phys. Chem, 100, **1996**, 15644-15653.

6. J. A. Chilton, M. T. Goosey, Special Polymers for Electronics and Optoelectronics, UK. Chapman and Hall, **1995.**

7. M. Kabasakaloglu, T. Kiyak, H. Toprak, M.L. Aksu, Applied Surface Science, 152, **1999**, 115-125.

8. Y.Takenaka, T. Koike, T. Oka, M. Tanahashi, Synthetic Metals, 18, **1987**, 207-212.

9. K.Yoshino, R.Hayashi, R.Sugimoto, Jpn. J.Appl.Phys. 23, **1984**, 899.

10. N.Toshima, S.Hara. Prog. Polym.Sci. 20,**1995**, 155.

11. A.F.Diaz, K.K.Kanazawa, in: Extended Linear Chain Compounds 3 J.S.Miller (Eds) Plenum Press : New York, **1982.**

12. L. Toppare, Ency. Eng. Mat., A. Polym. Sci. Techn., New York: Marcel Dekker, 1, **1988** , 8.

13. Electrical and Electronic Properties of Polymers: A State of the Art Compendium, Encyclopedia Reprint Series, John Wiley &Sons, NY.

14. Alan Mc Diarmid, Angew. Chem. Int. Ed. 40, **2001**, 2581-2590.

15. B.Bingöl,Msc.,Middle East Technical Universty,**2003.**

16. Srenger-Smith John D., Polym. Sci., vol 23,**1998**, 57-59.

17. D. Kumar , R. C. Sharma, Eur.Polym.J., 34 (8), **1998 ,**1053-1060.

18. Conjugated polymers The Novel Science and Thecnology of Highly Conducting and Nonlinear Optically Active Materials J.L.Brdas, R.Silbey Kluwer Academic Publishers **1991**.

19. K.D.Gourley, C.D.Lillya, J.R. Raynolds, J.C.W. Chien, Macromolecules, 17**, 1984,** 1025.

20. D.R.Gagnon, J.D.Capistran, F.E.Karasz, R.W.Lenz, S.Antoun, Polymer, 28, **1987**, 567.

21. R.W.Lenz , C.C.Han, F.E.Karasz, J.Polym.Sci.(A),Polym.Chem, 26, **1988**, 3241.

22. Xing-Rong Zeng and Tze-Man Ko ,Polymer Vol.39 No 5,**1998** , 1187-1195.

23. LiZ.F.,Kang E.T.,Neoh K.G.,Tan K.L., Synthetic matels, Vol.87,**1997**, 45-52

24. Matveeva E.S., Callja R.D., Parkhutik V.P., Electrochimica Acta, Vol. 41, No.7/8, **1996,** 1351-1357.

25. Kitani A.,Izumi J.,Yano J.,HiromotoT.,Sasaki K.,Bull.Chem.Soc.Jpn.,Vol 57,**1984**, 2254-2257.

26. Xing-Rong Zeng and Tze-Man Ko, Polymer Vol.39 No 5,**1998** ,1187-1195.

27. Akira Kıtanı, Jinko Izumi, Jun Yano, Yusuyuki Hıromoto and Kazuo Sasakı Bull.Chem.Soc.Jpn.,57, **1984**, 2254-2257.

28. Focke W.F., wnek G.E., Wei Y., J.Phys.Chem.,Vol91,**1987**, 5813-5818.

29. James Y.Shimano , Alan G.MacDiarmid, Synthetic Metals 123 , **2001**, 251-262.

30. J.D.Stenger-Smıth, Prog. Polym. Sci.Vol.23, **1998**, 57-79.

31. Uyar, T., Toppare, L., and Hacaloglu, J. Synth. Met., 119, **2001**, 307-308.

32. Uyar, T., Toppare, L., and Hacaloglu, J. J.Anal. Appl Pyrol. 64, **2002**, 1-13.

33. H.Schulten,N.Simmleit and R.Muller,Anal.Chem.,221, **1989**, 1

33. W.Cecchetti, R.polloni, G.Bergasmasco, R.Seraglia, F.Cecchinato and P.Traldi, J.Anal.Appl.Pyrolysis,230,**1992**,165.

35. T.Ersen,Msc.,Middle East Technical Universty,**1996.**

36. M.Erdoğan, T.Yalçın, T.Tinçer and Ş.Süzer, Eur.Poly.J.,27,**1991**,413.

37. M.M.Fares, J.Hacaloğlu, and Ş.Süzer, Eur.Polym. J.,30,**1994**,845.

38. A.F.Diaz and J.A.Logan ,J.Electroanal.Chem., 111,**1980** ,111.

39. L.H.C.Mattoso, R.M.Faria, L.O.S.Bulhoes, A.G.MacDiarmid, Polymer Volume 35, **1994**, 23.

40. AÇırpan, Z.Küçükyavuz, S.Küçükyavuz, Turk J Chem 27, **2003**, 135-143.